UNIVERSITY OF Hull

Identification of Audio Evoked Response Potentials in Ambulatory EEG Data

being a thesis submitted for the Degree of Doctor of Philosophy in Medical Engineering in the University of Hull

by

Othman Abdulaziz Alfahad

Bachelor of Applied Medical Science, King Saud University, Saudi Arabia (2006)

Master of Science (Medical Engineering), Hull University, United Kingdom (2013)

September 2018

Acknowledgements

I would like to thank Dr Kevin Paulson, who gave me a golden opportunity to work on this project. He has been an inspiration and provided advice and encouragement from an early stage in the project. I would like to commend him for the huge amount of effort that he has invested in me. Without his guidance, patience and work, I would have gained nothing.

I am grateful to Dr Aziz Asghar for his ideas, support, valuable help and guidance. He enabled me to reinforce my understanding of the project. I would like also to thank Mr Anthony Bateson, for his ideas and help during my research project. I am grateful to all the members of the engineering department for their co-operation during my degree. My thanks go to my all friends including Dr. Yaser Alnaam, Dr Khaled Alogaili, Dr. Mohammed Alajmi, Dr. Rahul Saurabh, Mr Saeed Alqarni, Mr Ibrahim Alharthee, and Mr Usman Bamji for their friendship and help.

I am deeply grateful to my parents for their constant support and motivation, which have encouraged me throughout my life. I would also like to express my gratitude to my wife, who supported me while I strove to complete this project. I cannot thank her enough for her tremendous support, sacrifices, and immense patience. Most importantly, I would like to give my heartiest thanks to my children (Lamis, Almas, and Abdulaziz) as well as my precious brothers, cherished sisters and my family and for their love, support, advice and encouragement.

I would also like to express my gratitude to my sponsor, Medical Management at the Ministry of Defence, Saudi Arabia, for their financial and logistic support during my degree.

Last but not least, I offer my regards to all the staff members of the university and my friends and colleagues for their encouragement and support.

This thesis is dedicated to

my parents

Mr. Abdulaziz Alfahad, Mrs. Nourah Alfarhood

&

my beloved wife

Mrs. Sarah Albader

for their endless love, support and encouragement

Abstract

Electroencephalography (EEG) is commonly used for observing brain function over a period of time. It employs a set of invasive electrodes on the scalp to measure the electrical activity of the brain. EEG is mainly used by researchers and clinicians to study the brain's responses to a specific stimulus - the event-related potentials (ERPs). Different types of undesirable signals, which are known as artefacts, contaminate the EEG signal. EEG and ERP signals are very small (in the order of microvolts); they are often obscured by artefacts with much larger amplitudes in the order of millivolts. This greatly increases the difficulty of interpreting EEG and ERP signals.

Typically, ERPs are observed by averaging EEG measurements made with many repetitions of the stimulus. The average may require many tens of repetitions before the ERP signal can be observed with any confidence. This greatly limits the study and use of ERPs. This project explores more sophisticated methods of ERP estimation from measured EEGs. An Optimal Weighted Mean (OWM) method is developed that forms a weighted average to maximise the signal to noise ratio in the mean. This is developed further into a Bayesian Optimal Combining (BOC) method where the information in repetitions of ERP measures is combined to provide a sequence of ERP estimations with monotonically decreasing uncertainty. A Principal Component Analysis (PCA) is performed to identify the basis of signals that explains the greatest amount of ERP variation. Projecting measured EEG signals onto this basis greatly reduces the noise in measured ERPs. The PCA filtering can be followed by OWM or BOC. Finally, cross channel information can be used. The ERP signal is measured on many electrodes simultaneously and an improved estimate can be formed by combining electrode measurements. A MAP estimate, phrased in terms of Kalman Filtering, is developed using all electrode measurements.

The methods developed in this project have been evaluated using both synthetic and measured EEG data. A synthetic, multi-channel ERP simulator has been developed specifically for this project.

Numerical experiments on synthetic ERP data showed that Bayesian Optimal Combining of trial data filtered using a combination of PCA projection and Kalman Filtering, yielded the best estimates of the underlying ERP signal. This method has been applied to subsets of real Ambulatory Electroencephalography (AEEG) data, recorded while participants performed a range of activities in different environments. From this analysis, the number of trials that need to be collected to observe the P300 amplitude and delay has been calculated for a range of scenarios.

Table of Contents

List of Figures

List of Tables

List of Abbreviations

AEEG	Ambulatory Electroencephalography.
AEP	Auditory Evoked Potentials.
AP	Action Potential.
APGN	Additive Pink Gaussian Noise.
AWGN	Additive White Gaussian Noise.
BCI	Brain Computer Interfacing.
BOC	Bayesian Optimal Combining.
BSS	Blind Source Separation.
dB	Decibel.
ECG	Electrocardiography.
EEG	Electroencephalography.
EMG	Electromyogram.
EOG	Electrooculogram.
EP	Evoked Potential.
EPSP	Excitatory Postsynaptic Potential.
ERPs	Event-related potentials.
FA	Frontal Area.
GDSF	Generic Discontinuities Spatial Feature.
HEOG	Horizontal Electrooculogram (Eye Movements).
IC	Independent Component.
ICA	Independent Component Analysis.
IID	Independent and identically distributed.
IPSP	Inhibitory Postsynaptic Potential.
K	Potassium.

KF	Kalman Filter.
LE	Left Eye.
M	Mean.
MAP	Maximum Posteriori Probability.
MEV	Maximum Epoch Variance.
Ms	Millisecond.
N100	Negative Peaks Values.
Na	Sodium.
OWM	Optimal Weighted Mean.
P300	Positive Peaks Values.
PA	Posterior Area.
PCA	Principal Component Analysis.
PCAKF	Principal Component Analysis and Kalman filter.
PDF	Probability density function.
RE	Right Eye.
SAD	Spatial Average Difference.
SED	Spatial Eye Difference.
SNR	Signal to Noise Ratio.
SSEP	Somatosensory Evoked Potentials.
SSVEP	Steady State Visual Evoked Potentials.
TK	Temporal Kurtosis.
TVEPs	Transient visual evoked potentials.
VEOG	Vertical Electrooculogram (Eye Movements).
VEP	Visual Evoked Potentials.

Chapter 1 Introduction

1.1 Introduction

1.1.1 EEG: what is it and why do it?

Researchers, clinicians and neurologists make extensive use of electroencephalography (EEG), a technique for scientifically logging the electrical activity of the brain, in order to monitor and assess brain function and in the diagnosis and management of brain disorders and mental problems, (Nunez & Srinivasan, 2006). Niedermeyer defines electroencephalography as the logging of brain activity via a set of electrodes which are placed on the scalp. The firing of neurons generates a flow of current within the brain which creates a variation in voltage (electric potential) which is measured by the EEG (Niedermeyer, 2005). When the measured brain activity is occurring in response to a sensory, motor or cognitive stimulus, the measured EEG potential is termed the event-related potential (ERP). An individual's brain can create EEG signals that appear to vary in terms of amplitude and frequency, for example, according to various states of consciousness such as waking, sleeping, etc (Luck, 2014).

A key task in the analysis of brain data is the extraction of the ERP responses concealed within the EEG information. For instance, a common ERP stimulus used clinically is a flashing checkerboard, used to gauge the response of the visual cortex, (Odom et al., 2004). Further studies, (Nicolas-Alonso & Gomez-Gil, 2012; Kaplan et al., 2013) have noted increasing application of EEG-ERP measurements in clinical setting, and also in building an understanding of brain function. According to Sanei & Chambers (2013), this interest has led to a focus on the issues surrounding the weakening and corruption of EEG recordings due to unwanted electrical signals

derived from physiological and external sources. It would be beneficial to enhance the signal-to-noise ratio (SNR) of the EEG data by reducing EEG artefacts in order to avoid the erroneous interpretation of EEG data or of the response of the brain to various stimuli. External (non-physiological) artefacts are generally removed by means of linear filtering, or data preparation protocols implemented according to the particular experimental data. However, since physiological artefacts overlap the EEG frequency bands, these cannot be effectively eliminated by basic filtering. Hence, various methods have been suggested for reducing physiological artefacts in EEG signals. According to (Papadelis et al., 2007; Jung et al., 2000a), initial efforts resulted in a significant loss of data as the artefacts were eliminated by rejecting the contaminated temporal segments of multichannel EEG recordings. More sophisticated methods have been developed in order to reduce EEG data loss. Independent Component Analysis (ICA), an example of the Blind Source Separation technique, is effective and widely used. These methods rely upon the use of prior information or assumptions. For example, ICA assumes that brain and non-brain signals are statistically independent. The success of these methods depends upon the validity of the underlying assumptions or prior knowledge (Hyvärinen et al., 2001).

1.1.2 Ambulatory EEG: what is it and why do it?

According to Mauguière (1987), increasing use of electroencephalography is being made in a wide range of applications, including the clinical diagnosis and management of brain function defects, where the use of fixed EEG facilities limits the ability to address clinical or research questions . Hence, the need exists to develop and enable the transfer of EEG from the laboratory into the outside world e.g. by the development of portable battery-powered EEG systems. The recorded data can either be saved to a portable memory device for subsequent off-line study and analysis, or transmitted in

real-time to a PC or handheld device for online viewing. At the present time, commercially available technology includes wearable headsets developed mainly for Brain Computer Interface uses, as well as smaller devices incorporating a limited number of electrodes which can be worn as a headband, with a waist mounted EEG system, and developed mainly for psychophysiological examination and neurofeedback applications. Fully ambulatory EEG (AEEG) systems for research is in development, with favourable early indications (Park et al., 2015).

The majority of investigations aimed at verifying AEEG technology have concentrated on the P300 ERP response. Due to progress in both AEEG technology and signal processing, it is presently feasible to record brain activity during sporting activity. Indeed, Park et al. (2015) noted the recent commercial release of ambulatory EEG equipment designed specifically for sporting applications with the capacity to log up to 64-channels of high resolution EEG, a recording capability previously found only in laboratory-based equipment.

Figure 1.1 A montage of images illustrating the developments in EEG systems (Sanei & Chambers, 2013; Park et al., 2015).

The AEEG equipment used in this thesis was developed at the University of Hull. The core of the system is a waist mounted control system capable of measuring 24 channel voltages, with 24 bit resolution and a 250 Hz sampling frequency. This is sufficient to be compatible with the international 10/20 system, and also provides five additional channels available for ECG, EOG or EMG recordings. The data are sent via WiFi in real time to a partnered laptop or smartphone. An app running on the smartphone allows recording and plotting of live data, whereas a PC provides greater processing capability for algorithms applied to online data. Use of the smartphone allows electrode attachment problems to be identified immediately and greatly reduces the weight and size of the data recording equipment.

For the experiments described in this thesis, 19 EEG channels were monitored with the 20th channel being the reference electrode connected to an ear lobe. Eyes blinks were monitored using electrodes around the eyes. Two electrodes, one above and one below the left eye, measured the electric field generated by vertical eye movements (VEOG). The signal due to horizontal eye movements (HEOG) were measured using two electrodes, one each side of the head at eye-level.

1.1.3 ERP: what is it, why measure it, how is it measured?

(Blackwood & Muir, 1990) define event-related potentials (ERPs) as very small voltage fluctuations which are produced in brain structures in response to specific present-time events or stimuli. ERPs can be prompted by a wide variety of cognitive, motor or sensory events and can be measured at the scalp. Therefore, these time-specific EEG responses can furnish a non-invasive and secure methodology for examining the psychophysiological consequences of mental processes (Sur & Sinha, 2009). Since the amplitude of an ERP is generally less than that of the background

EEG, an accurate ERP is acquired by taking the average of EEG fragments from numerous repeated trials.

According to (Kropotov, 2016), each ERP results from the aggregation of potentials from numerous disparately located and functionally distinct cortical sources, termed components, which are theoretically linked to discrete psychological operations. (Kropotov, 2016; Waryasz, 2017) both described a method for separating the components by observing a difference between two ERPs, e.g. standard and deviant, target and non-target, or oddball and non-oddball.

In humans, ERP signals fall into two groups. The initial sensory or exogenous wave components peak within ~100 milliseconds of the stimulus and depend primarily upon the physical characteristics of the stimulus. However, ERPs arising later relate to the individual's approach to evaluating the stimulus and therefore provide an insight into the processing of information; these are referred to as cognitive or endogenous ERPs. This distinction provides a description of the waveforms in terms of amplitude and latency. (Sur & Sinha, 2009) described various forms of ERP waves including P50, N100, P200, P300, N400, P600, etc. These labels indicate (P) positive or (N) negative excursions and the number is the delay in milliseconds between the stimulus and the response. According to Luck (2005), researchers often present graphs of ERP components with the potential becoming more negative upward, as shown in Figure 1.2, although this is not a universal practice.

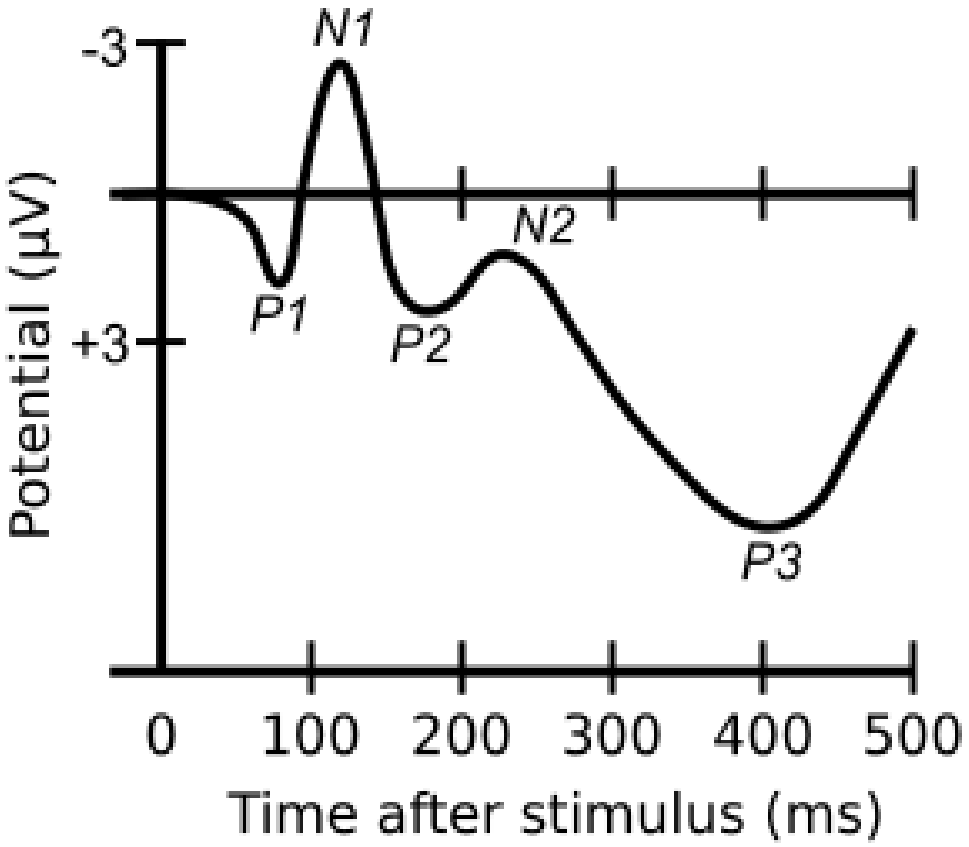

Figure 1.2 An EEG waveform consisting of ERP components N100 (labelled N1), P300 (labelled P3), etc. (Luck, 2005).

1.2 Clinical Uses of EEG and ERP Signals

Electroencephalogram (EEG) and evoked potentials techniques have been widely used clinically to examine brain and sensory function (Polich, 2007; Polich, 2004). The P300 potential is elicited by variants of the 'oddball' paradigm, either auditory or visual ERPs. The subject is required to respond physically or mentally to the target or the 'oddball' stimuli that are presented (Johnson, 1993). This section describes possible correlation of EEG and ERP signals with externalizing spectrum disorders, schizophrenia, bipolar affective disorder, depression, phobia, panic disorder, generalised anxiety disorder, obsessive compulsive disorder, dissociative disorder, personality disorder, seizures and epilepsy, sleep disorder, Alzheimer's and dementia.

Externalizing spectrum disorders

It has been suggested that the general neurobiological vulnerability characteristic of externalizing spectrum disorders such as adult antisocial behaviour, alcoholism, drug addiction and nicotine dependence can be indicated by a decreased P300 amplitude (Patrick et al., 2006). However, although acute ethanol intake is observed to reduce the P300 amplitude, (Patrick et al., 2006) noted that wave anomalies are also observed in abstinent individuals and in patients' immediate relatives.

Schizophrenia

Reduced P300 amplitude is one of the most compelling neurophysiological observations in schizophrenia, becoming increasingly smaller in amplitude and increasingly delayed with increasing duration of the illness. Moreover, (Simlai & Nizamie (1998) noted that the P300 was increasingly delayed in schizophrenic patients but not in their immediate relatives. The P300 amplitude has been observed to decline over time in schizophrenia subjects but not in control subjects (Doege et al., 2009). Observation of differences in P300 amplitudes have shown a high test–retest reliability in schizophrenia patients and control subjects (Poulsen & Jørgensen, 2008). According to Mathalon et al. (2000), longitudinal studies have indicated that P300 amplitude is independent of medication and is responsive to variations in the acuteness of positive symptoms and the persistence of severe negative symptoms. Although (Bramon et al., 2004) noted reduced levels of P50 suppression in schizophrenia patients, (Clementz et al., 1998) noted that this indicator is also observed in non-psychotic relatives. According to O'Donnell et al. (2004), individuals with schizophrenia have also displayed decreased N100, P200 and N200 amplitudes. Meanwhile, (Sur & Sinha, 2009) noted increased delays in N400 and P600 in schizophrenic patients.

Bipolar Affective disorder

(Schulze et al., 2007) have reported reductions in P50 suppression in patients with bipolar disorder involving psychotic symptoms and in their unaffected immediate relatives; which implies that P50 is an endophenotypic indicator for this disorder. Reduction in P300 has been observed by (Salisbury et al., 1999) in manic psychosis. Moreover, (O'Donnell et al., 2004) reported prolonged delay and decrease in amplitude in chronic bipolar patients.

Depression

(Hansenne et al., 1996) have reported decreased P300 amplitude in depressed patients, primarily in cases with psychotic aspects, suicidal thoughts or extreme depression. Observation of changes in P300 have been associated with psychiatric disorders such as depression, bipolar disorder, personality disorders etc. (Sahoo, 2016).

Phobia

According to Miltner et al. (2000), significantly enhanced P300 amplitudes, relative to those of healthy controls, have been demonstrated in individuals with snake and spider phobias when presented with images of the feared objects. This demonstrates increased stimulus processing indicative of fear of danger.

Panic disorder

According to Turan et al. (2002), the dysfunctional prefrontal-limbic pathway hypothesis of panic disorder is supported by an increased P3a (frontal P300) response to distracting stimuli during a three-tone discrimination task. Increased delay in P3b was also observed in drug-free patients, relative to unaffected controls, which may indicate dysfunction of the amygdala and hippocampus.

Generalized anxiety disorder

(De Pascalis et al., 2004) observed that ERPs provoked by threat-related stimuli such as fear-related pictures or words, substantiate the existence of attention bias in patients with high-trait anxiety or anxiety disorders, demonstrated by increased P300 amplitude and protracted waves in comparison with those of healthy controls.

Obsessive compulsive disorder

Significantly reduced delays in P300 and N200, along with increased N200 negativity, have been observed in response to target stimuli for patients with obsessive compulsive disorder relative to healthy controls. There is, however, no significant correlation between these ERP anomalies and the type or severity of obsessive compulsive symptoms. By contrast, (Sur & Sinha, 2009) observed increased P300 delays along with no change in amplitude for individuals with obsessive compulsive disorder.

Dissociative disorder

According to (Sur & Sinha, 2009), the P300 amplitude may be a state-dependent biological indicator of dissociative disorders. Indeed, patients suffering from dissociative disorders displayed significantly reduced P300 amplitudes in comparison with their levels upon remission, although the P300 latency was unaltered.

Personality disorders

A number of investigations have noted certain correlations between N200, P300 and personality in healthy individuals. For example, introverted people consistently display enhanced amplitude P300 in comparison to those of extroverts. The P300 amplitude shows a moderate positive correlation with self-directedness, while the contingent negative variation amplitude is similarly correlated with cooperativeness.

(Sur & Sinha, 2009) assert that an increased delay in N200 may be linked with an enhanced harm avoidance score, while the N200 amplitude is negatively correlated with persistence (hence a decreased N200 amplitude may be associated with a higher persistence score).

Seizure and Epilepsy

Electrical activity of the brain varies from one second to the next and standard EEGs obtain only a brief sample of this activity. Consequently, if epilepsy waves occur in the brain only once every few hours, or only after an hour of sleep, a standard EEG will generally not detect the relevant brain activity. Hence, it becomes essential to obtain extensive records covering significant periods of time when the patients are asleep and awake. According to (Jeong, 2004), a number of extensive studies have employed ambulatory EEG for various recording periods of up to 96 hours in the diagnosis of epilepsy. The study by (Faulkner et al., 2012) indicated that a 48-hour acquisition period was adequate for the diagnosis of most patients with interictal epileptiform discharges on surface EEG.

In a study by (Wang et al., 2012) , the features of AEEG system were examined prior to making the decision to withdraw anti-epileptic drugs, indicating that most anomalous EEGs were due to an inappropriate dose or to patient non-compliance. According to (Askamp & van Putten, 2014), most neurologists believe that ambulatory EEG can have further benefits in the investigation of paroxysms of uncertain cause, but not in the initial diagnosis following a first seizure.

Sleep disorders

In spite of the prevalence of sleep disorders, their diagnosis is challenging and resources are inadequate, so that total waiting times between referral and sleep study in the UK can be as much as three years (Flemons et al., 2004). Diagnosis is usually

by polysomnography involving brain monitoring by EEG along with heart rate and rhythm monitoring by ECG during sleep. In view of the need to have as little effect as possible upon the sleeping patient, the devices employed have to be even less burdensome than in other contexts. (Bruyneel et al., 2013) have suggested the use of home-polysomnography as an economical option for the diagnosis of obstructive sleep apnoea, indicating that this is topic with potential for further research.

Alzheimer and Dementia

The most prevalent neurodegenerative disorder, Alzheimer's disease (AD), is typified by behavioural disruption and loss of cognitive and intellectual capacity. The diagnosis of AD has involved the use of EEG for a number of decades and, in view of its minimal cost, is continuing to develop (Kanda et al., 2014). According to (Jeong, 2004), the primary indicators are a shift in the power spectrum towards lower frequencies and a reduction in the consistency of fast rhythms. In addition, (Wu et al., 2014) noted that the EEG technique has found frequent application in distinguishing between AD and vascular dementia. No published studies have been found dealing with the use of home or ambulatory EEG for dementia cases, even though these techniques could potentially be used to monitor the progression of the condition.

1.3 Research Questions

The major research questions addressed in this thesis focus on the measurement of ERPs from experiments performed using AEEG systems while the participant engages in a range of activities and in a range of environments. The research questions are:

- In environments presenting a person with a range of stimuli, how many repetitions of the ERP measurement are required to reliably identify the ERPs and to separate it from other signals and noise?

- In what range of different activities and environments can ERPs be reliably measured?
- What is the best way of using repeated ERP measurements to estimate ERPs i.e. to separate ERPs from noise and artefacts?

Each ERP measurement trial involves the recording of EEG signals during a trial that starts just before the stimulus and ends when the associated brain response has become too small to measure. Historically, ERP responses are estimated by averaging trial time-series across tens of trials, sometimes from more than one individual. The number of trials needed to obtain the signal-to-noise ratio (SNR) necessary to observe features in the ERP, depends upon the SNR in each trial. The noise level depends on the nature of the experiment and the characteristics of the subject (Luck & Todd, 2004). Assuming the trial noises are statistically independent, the SNR in the averaged evoked response is proportional to the number of trials (Luck, 2005; Goldenholz et al., 2009). The number of trials typically required in the average to be able to observe clinically important features, such as P300, has been reported to be around 36 usable trials (after artefact rejection or correction) in each stimulus category (Polich, 2004), although there is evidence that 20 trials may suffice (Cohen & Polich, 1997). Woodman reported around 35-60 trials for each condition from each subject (Woodman, 2010). The much smaller P100 and N100, can require between 300 to 1000 trials for each condition to measure consistently. These are for EEG recordings in ideal conditions. It is far more challenging to observe ERP responses in AEEG data collected in stimulating environments and while the participant engages in activity.

In practice, individual trials vary considerably in SNR. Artefacts such as eye-blink signals, are high amplitude and intermittent. Therefore, some trials have very low SNRs and including these in an average reduces the SNR in the ERP estimate. A two stage approach is required where the uncertainty in trials is estimated and then trials

are combined in an optimised way. Some trials may contain so little ERP information that they are not worth using. Pre-processing of trial time-series may identify these trials or reduce the noise artefacts before optimal combining. The latter part of this thesis looks at the quantification of uncertainty in trial data and methods of combining trial data that yields an estimate of the ERP and its uncertainty. This can be calculated during an ERP experiment so data acquisition can be terminated when the uncertainty is low enough. There are many clinical applications that could be made faster and less intrusive on the participant if these processes were used.

1.4 Thesis Outline

The research carried out in this thesis can be outlined as follows:

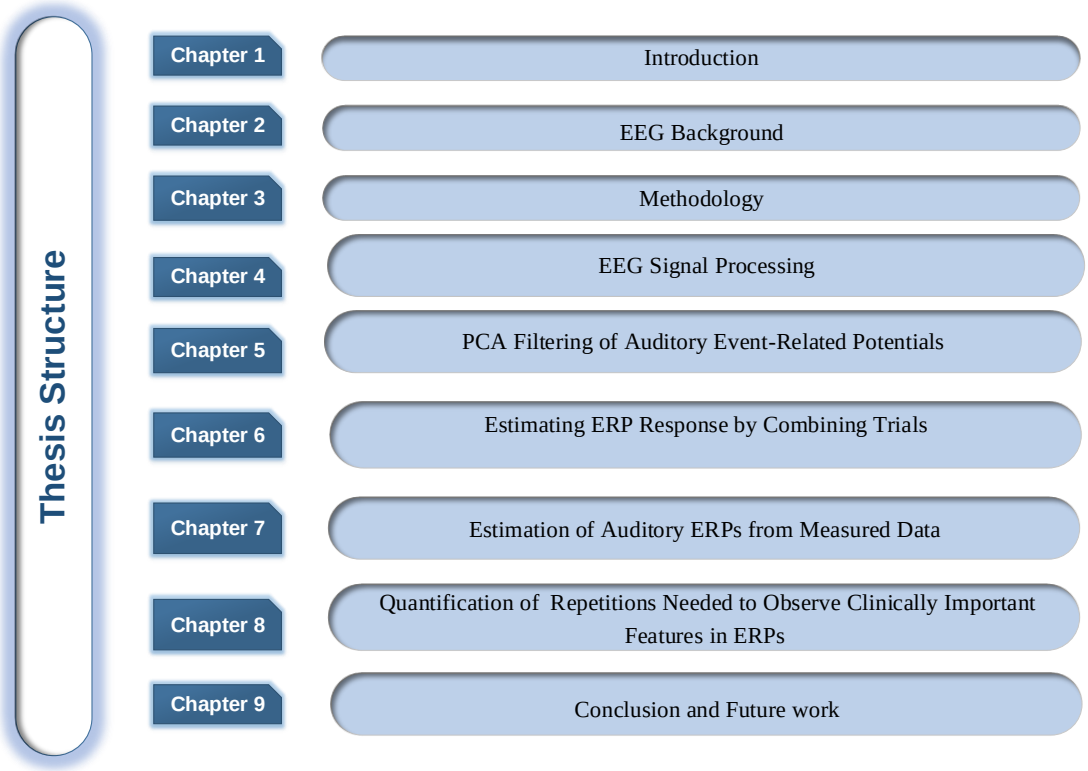

Figure 1.3 Block diagram of the thesis structure.

Chapter 1: Introduction

This chapter provides a brief introduction to EEG, ERPs, and clinical uses of EEG. It focusses on applications of AEEG systems and states the research questions of this project.

Chapter 2: EEG Background

This chapter expands on the topic of EEG signals. It begins with a brief historical background of EEG. The anatomy and physiology of the brain are presented from neuron activities to action potentials. The process of EEG generation, brain waves and the basic concepts of EEG recording are presented.

Chapter 3: Methodology

The protocol followed in this project, when making ERP measurements, is detailed. This includes preparing the EEG experiment, connecting the participant to the EEG, experimental procedures, collecting data and pre-processing data.

Chapter 4: EEG Signal processing

This chapter looks at the signal to noise ratio (SNR) in ERP measurements. It presents the detection and reduction of artefacts using standard ICA and ADJUST in the EEGLAB toolbox.

Chapter 5: PCA Filtering of Auditory Event-Related Potentials

ERP filtering by projection onto subspaces spanned by Principal Component (PCA) basis signals, is developed and evaluated. The PCA filtered ERPs are further filtered by optimal fusing with the apriori expected ERP signal. This MAP estimate is presented in terms of Kalman Filtering. Much of the power of the proposed algorithm comes from exploiting apriori cross-channel information in the form of a PCA weight covariance matrix. The performance of the method is quantified using synthetic multi-channel ERP signals with known amounts of synthetic noise added to all the channels.

Chapter 6: Estimating ERP Response by Combining Trials

In this chapter different methods for combining filtered trial ERPs are investigated. Traditionally, unweighted averages have been used. However, as the noise varies considerable across trials, other methods such as optimal weighted mean and Bayesian optimal combining, promise to yield better estimates of the underlying ERP. These methods are evaluated using synthetic data and a new processing protocol is chosen that combines PCA filtering of trails with optimal combining.

Chapter 7: Estimation of Auditory ERPs from Measured Data

Chapter 7 explicitly states the proposed processing protocol in steps that can be applied in a clinical situation. In previous chapters, some processing parameters were chosen using knowledge of the underlying ERP. New methods are tested for estimating the noise power in measured ERPs.

Chapter 8: Quantification of Repetitions Needed to Observe Clinically Important Features in ERPs.

A dataset of measured AEEG data collected in a range of environments and while the participant is standing or walking, is used to evaluate the proposed processing protocol. The number of trials that need to be filtered and combined, to estimate clinically important P300 parameters, is calculated for standard processing and the proposed processing protocol.

Chapter 9: Conclusion and future work.

The final chapter presents a summary of the results and achievements along with suggestions for future work.

1.5 Thesis Aims

The major research questions addressed in this thesis focuses on the measurement of ERPs from experiments performed using AEEG systems while the participant engages in a range of activities and in a range of environments. As seen in thesis outline there are 9 chapter of this thesis. To address research questions, there are many steps were developed in chapters 5,6,7 and 8. In flowchart 1.4 summarize each chapter.

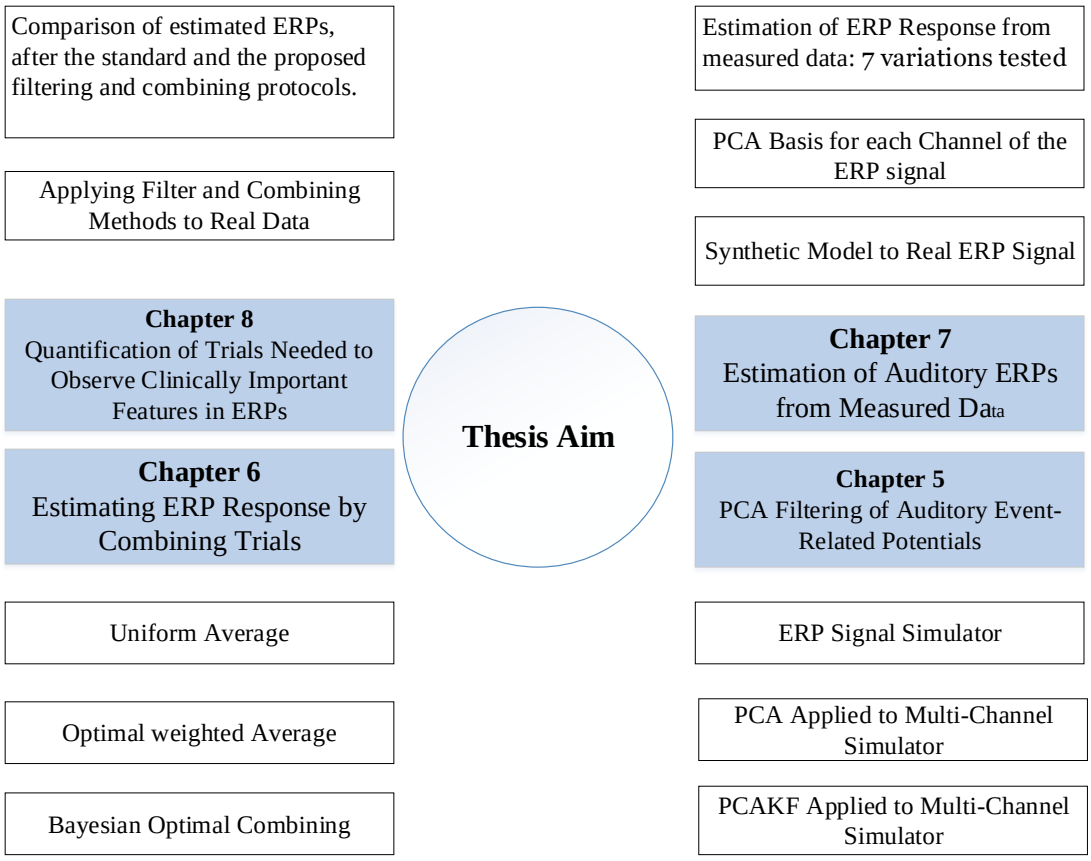

Figure 1.4 Thesis Aim flowchart.

1.6 List of Publications

The following publications by the author have resulted from this project

- Paulson, K. S. & Alfahad, O. A. (2018) Estimation of auditory event-related potentials using a combination of principal component analysis and Kalman filtering. Proceedings of the 4th World Congress on Electrical Engineering and Computer Systems and Science (EECSS'18). Madrid, Spain.

- Paulson, K. S. & Alfahad, O. A. (2018) Identification of auditory event-related potentials using a combination of principal component analysis and Kalman filtering. 3rd International Conference on Biomedical Imaging, Signal Processing (ICBSP 2018) Bari, Italy.

1.7 Summary

The measurement of brain signals by EEG has been introduced, with an emphasis on the estimation of ERP signals using AEEG systems. Clinical applications have been reviewed and research questions developed. This project will focus on the estimation of ERPs from repeated AEEG measurements in stimulating environments or while the participant is active. It will focus on the signal processing aspects of EEG filtering and ERP combining.

Chapter 2 EEG Background

2.1 Introduction

Electroencephalography is a health diagnostic imaging method which measures electrical signals produced by brain function on a set of electrodes connected to the scalp. The electroencephalogram (EEG) is the set of electrical signals, often decomposed into different frequency bands. The electrodes are often metallic and electrically conected to the scalp using a conductive media (Teplan, 2002). When EEG signals are acquired on the skin the output is known as an electrocardiogram, whereas measurements from inside the head are known as an electrogram.

Brain function requires activation of neurons (brain cells). The activation of many neurons in a region of the brain produces a small current and electric field which leads to the electrical signals on the scalp measured by the EEG. Generally, EEG measures only those currents which are produced during synaptic excitations of cerebral cortex neurons. Neuronal current or impulses are associated with Na^{+}, K^{+}, Ca^{++}, and Cl^{-} ions which are propelled through channels and regulated by the neuronal membrane potential (Teplan, 2002; Tortora & Derrickson, 2011). Enormous populations of active neurons are required to generate electrical impulses that are recordable on the scalp (Teplan, 2002; Nunez & Cutillo, 1995). Weak neuronal impulses may be also recorded by EEG after amplifying and other computational processes, but controlling noise is essential in these processes. Measurable electrical neuronal signals start in the foetus during the 17th to 23rd week and at birth the full number of neural cells is developed, approximately 10^{11} neurons (Nunez & Cutillo, 1995; Akaishi et al., 2013).

Normal EEG patterns are observable across the bulk of the population. However, abnormal patterns are consistently associated with neural problems. Therefore, EEG

is considered as a very powerful tool in the field of neurology and neurophysiology (Dubey & Pathak, 2010). For example, abnormal EEG potentials are associated with some abnormalities such as a seizure (induced by pentylenetetrazol), hypercapnia, and asphyxia (Caspers et al., 1987).

2.1.1 Neuron Activity

Neurons are made of three major parts; axons, dendrites, and cell bodies; as shown in Figure 2.1. Generally, neurons respond to stimuli and transmit information (Tortora & Derrickson, 2011). Axons are long cylinders that transmit electrical impulses. Dendrites are linked to either the axons or dendrites of other neurons and thus receive impulses from other neurons. In the human brain, one neuron is linked to around 10,000 other neurons, through dendritic linkage (Tortora & Derrickson, 2011).

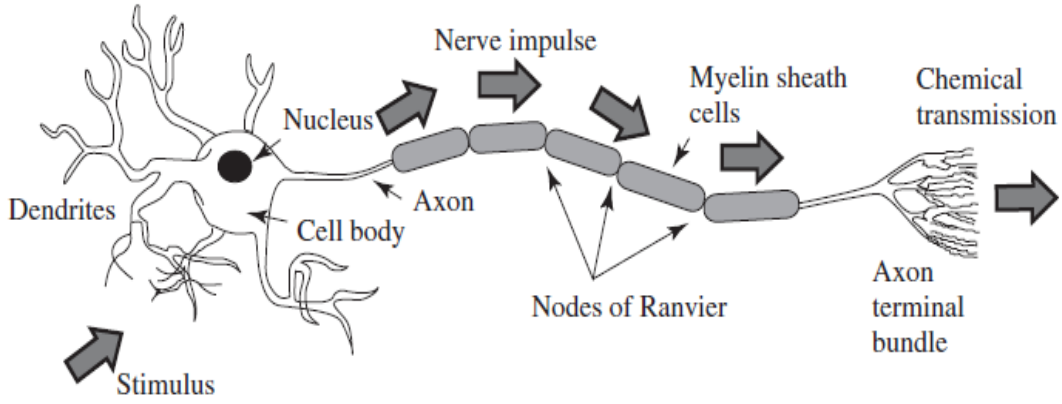

Figure 2.1 Structure of neuron which consist of three major parts; axons, dendrites, and cell bodies (Sanei & Chambers, 2013).

The activities or impulses of neurons are primarily associated with the synaptic currents which are transferred between the connections (synapses) of axons and dendrites, or dendrites and dendrites, of neurons. A potential of 60-70 mV exists across the neural membrane and a reversal of polarity is linked with synaptic activities (Sanei & Chambers, 2007). When the potential travels along the fibre that ends in an

excitatory synapse, an excitatory postsynaptic potential (EPSP) arises in the neuron. When the fibre ends in an inhibitory synapse, hyperpolarization will occur, indicating an inhibitory postsynaptic potential (IPSP) as shown in Figure 2.2 (Speckmann, 1993; Shepherd, 2003).

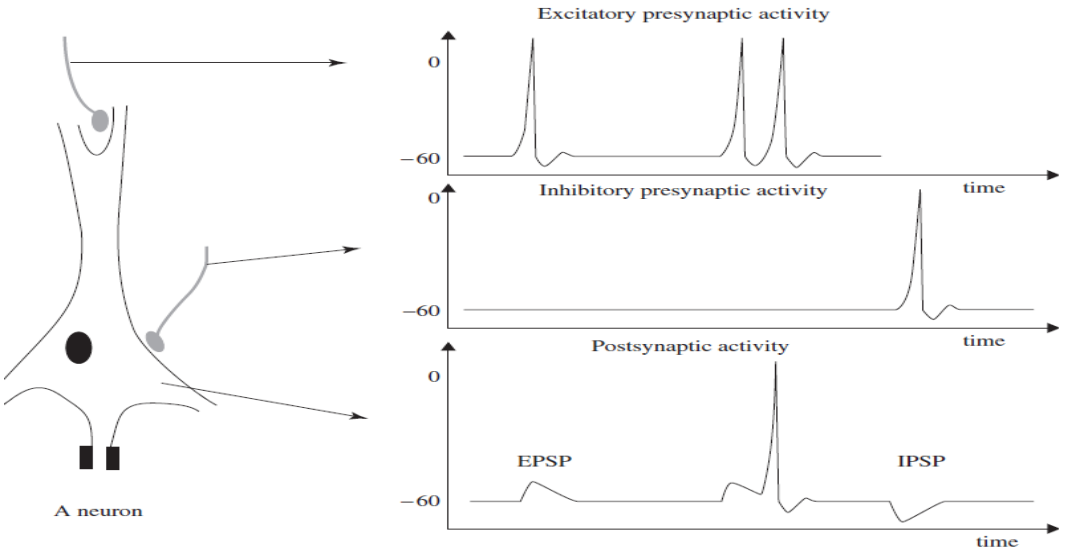

Figure 2.2 Action potentials in the excitatory and inhibitory presynaptic fibre respectively lead to EPSP and IPSP in the postsynaptic neuron (Sanei & Chambers, 2007).

Primary currents from the membrane generate secondary currents (inonal) alongside the neuronal membranes in the intra- and extracellular space. The extracellular space currents are mainly responsible for the field potentials at frequencies less than 100 Hz. It is variation in these signals that are commonly measured using EEG.

2.1.2 Action Potentials

The information communicated by a neuron is known as an action potential (AP). AP is initiated by an exchange of ions through the neuronal membrane. AP is a brief alteration in neuronal membrane potential, which is communicated throughout the axon. It is typically introduced in the neuron cell body and moves in one direction

(Sanei & Chambers, 2013). The neuronal membrane potential depolarizes, i.e. reverses polarity for a short time. After the depolarisation peak, the neuronal membrane repolarizes relatively slowly while being negative for about 4 millisecond (ms), as shown in Figure 2.3. Generally, APs of most neurons last between 5 and 10 milliseconds (Sanei & Chambers, 2007).

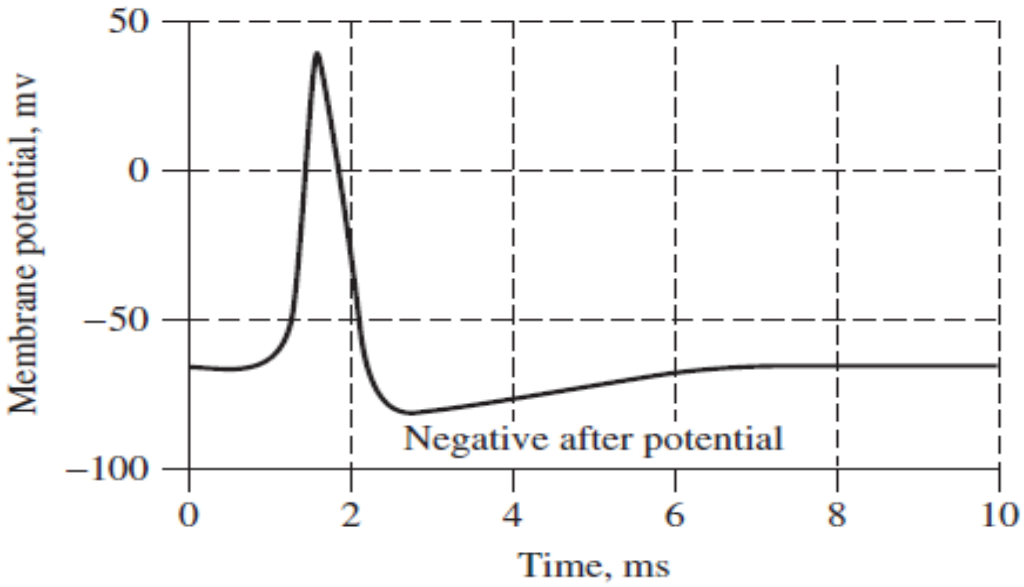

Figure 2.3 Schematic plot of action potential (Sanei & Chambers, 2007).

The stimuli must surpass a threshold point to initiate an AP. weak stimuli may trigger a tiny native electrical disruption, but they are not able to generate a transmitted AP. Once the stimuli exceeds the threshold point, an AP is generated and travels down the neurons (Sanei & Chambers, 2013).

The AP spikes are generally instigated by the opening of sodium (Na) ion channels. The Na^+ pump yields a gradient of sodium and potassium (K) ions, which are important to the generation of APs. After opening, the Na channel allows a rush of Na^+ ions into the neuronal cell (Fridlyand et al., 2013; Kim et al., 2010). This event causes the neuronal membrane potential to become positive i.e. depolarized, and thus

generating the spikes. In humans, the APs amplitude ranges may vary between -60 mV and 10 mV (Testa-Silva et al., 2014; Moore et al., 2014).

2.1.3 EEG Signal Generation

When neurons are stimulated, synaptic currents are generated inside the neuronal dendrites. These currents may further produce a magnetic field which may be measured by electromyogram (EMG) and a subsequent secondary electrical field over the scalp measurable by EEG (Nicolas-Alonso & Gomez-Gil, 2012; Rossini et al., 2015). In the brain, the current is mainly generated due to the pumping of positive ion gradients (Na^+, K^+, Ca^{++}) and negative ion gradients (Cl^-), throughout the neuronal membrane in the same direction that is directed by the membrane potential (Atwood & MacKay, 1989).

The human head may be anatomically divided into three major components: the scalp, skull and brain; and many thin layers between (Acar & Makeig, 2013; Sadleir & Argibay, 2007). The skull reduces the intensity of the electrical signals about one hundred times more than the other soft tissues. Hence, only huge populations of active neurons can produce sufficient potential to be recordable using the electrodes on the scalp. These signals may be amplified significantly for display (Sanei & Chambers, 2007). The noise in measured electrical signals may be internal, due to other biological functions, or external due to the measurement system and other non-biological sources (Sanei & Chambers, 2013).

2.1.4 Brain Rhythms

Many neuro-disorders may be diagnosed by the visual introspection of EEG signals. The five main brain signals are differentiated by frequency ranges. The EEG bands,

from low to high frequencies, are commonly known as alpha (α), theta (θ), beta (β), delta (δ), and gamma (γ) as shown in Figure 2.4.

Delta waves range from 0.5 to 4 Hz and are mainly associated with deep sleep and the waking state. Sometimes, delta frequencies are very close to artefact signals generated by neck muscles. These muscles are near the skin surface and therefore produce large signals, particularly at the back of the head. Usually neck muscle artefacts are easily separated from brain generated EEG signals unless the movements are excessive (Ashwal & Rust, 2003).

Theta waves are found between 4 and 7.5 Hz. The term theta may acknowledge the origin of these signals in the thalamic origin. Theta waves appear during drowsiness and deep meditation. Theta waves often occur simultaneously with other waves and appear to be associated with the level of stimulus. They are particularly strong during infancy and childhood. The rhythmic changes in theta waves are examined mainly for emotional analysis (Ashwal & Rust, 2003).

Alpha waves lie between 8 and 13 Hz as round or sinusoidal shaped signals and are mostly observed in the posterior lobes and occipital region of the brain. The alpha frequencies are often the highest amplitude waves but their origin and physiological significance are still unknown (Niedermeyer, 2005).

Beta waves range between 14–26 Hz and are associated with activities such as thinking, attention, focus or solving concrete problems. They appear in normal adults but high-amplitude beta waves are also found in people of all ages in states of panic and around the temporal regions (Sterman et al., 1974; Chapman, 1999).

Gamma waves are found above 30 Hz and are sometimes also called fast beta frequencies. The amplitudes of gamma are low and they are relatively rare. They may be observed to confirm certain brain diseases and are a good indicator in event-related

studies. It can be used to demonstrate the locus for right and left index finger movement, right toes, and the rather broad and bilateral area of tongue movement (Pfurtscheller et al., 1994; Kornmeier & Bach, 2012).

Frequencies higher than the EEG activity range, generally 200 to 300 Hz, may be found in the cerebellar region of the brain and they do not have any role in clinical diagnostic neurophysiology (Javitt et al., 2008; Dalal et al., 2013).

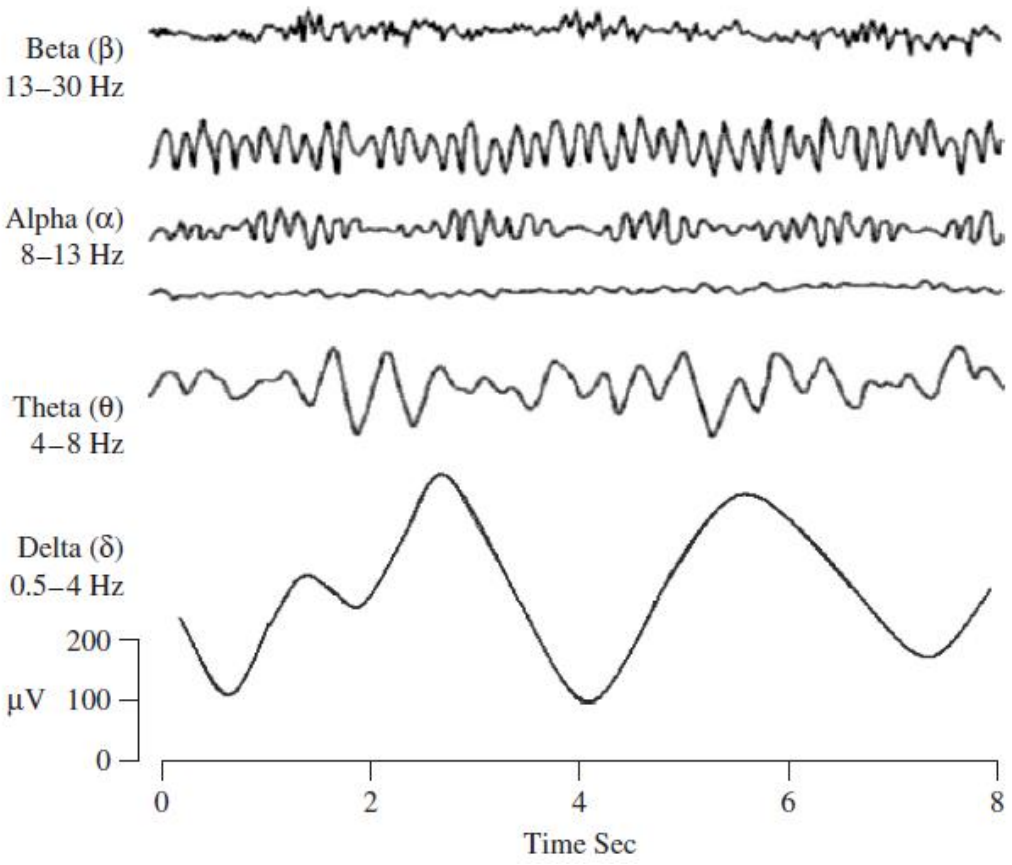

Figure 2.4 Typical waves of brain rhythm from high to low frequencies (Sanei & Chambers, 2007).

2.1.5 EEG Recording and Measurement

EEG systems have three major components: a set of electrodes on the surface of the head connected to electronics which amplify and condition the measured scalp voltages, and some sort of data recording device; historically, needle or moving pen recorders traced the multichannel EEG signals onto paper (Sanei & Chambers, 2013). For the last 50 years or so computer based systems have been used to digitize and store the signals. Digital systems permit variable settings, stimulations, and sampling frequencies, and may be paired with simple or advanced signal processing devices for processing the signals. The transformation from analogue to digital EEG is performed by means of multichannel analogue-to-digital converters. The bandwidth of EEG signals is relatively small, limited to approximately 100 Hz (Sanei & Chambers, 2007). The EEG recording electrodes are very important for obtaining reliable data. A wide range of electrodes are used in the EEG recording systems, such as disposable (gel-less, and pre-gelled types), reusable disc electrodes (gold, silver, stainless steel, or tin), headbands and electrode caps, saline-based electrodes, and needle electrodes (Sanei, 2013).

2.1.6 Conventional Electrode Positioning

The International Federation of Societies for Electroencephalography and Clinical Neurophysiology has suggested the conventional electrode setting for 21 electrode systems (without the earlobe electrodes), commonly known as 10-20 system, as shown in Figure 2.5 (Sanei & Chambers, 2013). The earlobe electrodes are commonly referred to as A1 and A2 and are attached to the left and right earlobes respectively. They are used as the reference electrodes for the voltage measurements. The 10–20 system yields reproducible and comparable measurements by locating electrodes relative to particular anatomical locations. Distances are measured relative to an ear-

to-ear measurement across the top of the scalp. The odd electrodes are placed on the left side and the even are on the right side. (Sanei & Chambers, 2007).

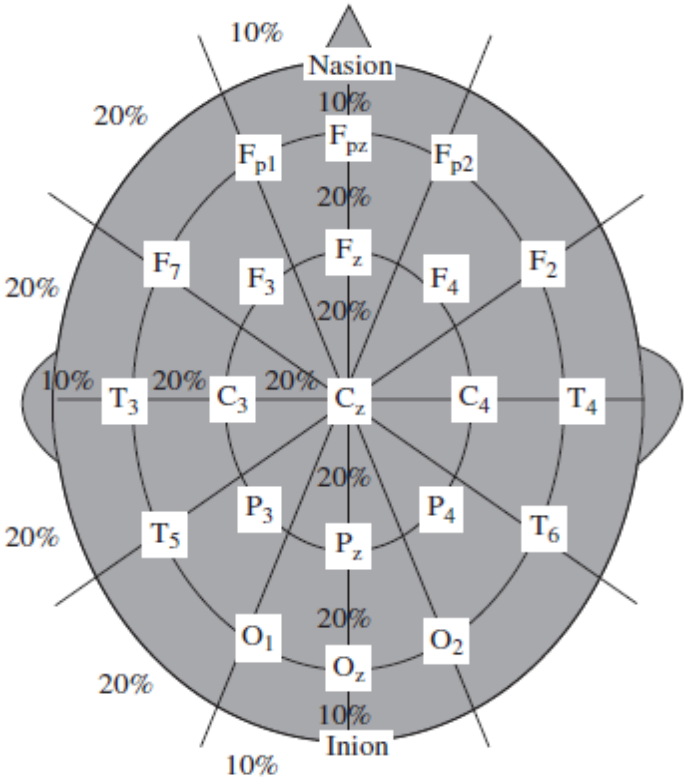

Figure 2.5 Conventional 10-20 EEG electrodes position and placement. 20% are the distance between each electrodes or 10% between Inion or Nasion and electrode. (Sanei & Chambers, 2013).

Further electrodes may be placed equi-distant between two standard locations. For example, C1 may be positioned between C3 and Cz. About 75 electrodes together with reference electrodes may be placed according to the American EEG Society standard, as shown in Figure 2.6. Occasionally, extra electrodes are employed to measure the eye blink and surrounding muscles. In ERP analysis and brain computer interfacing, a single channel might be used in a standard location. Electrodes C3 and C4 may be placed to measure signals related to right and left finger movement respectively, for brain-computer interfacing applications. Electrodes F3, F4, P3, and P4 are particularly sensitive to ERP P300 signals (Sanei & Chambers, 2013). Physical references can be

used such as vertex (Cz), linked-ears, linked-mastoids, ipsilateral ear, contralateral ear, C7, bipolar references, and tip of the nose (Sanei & Chambers, 2013).

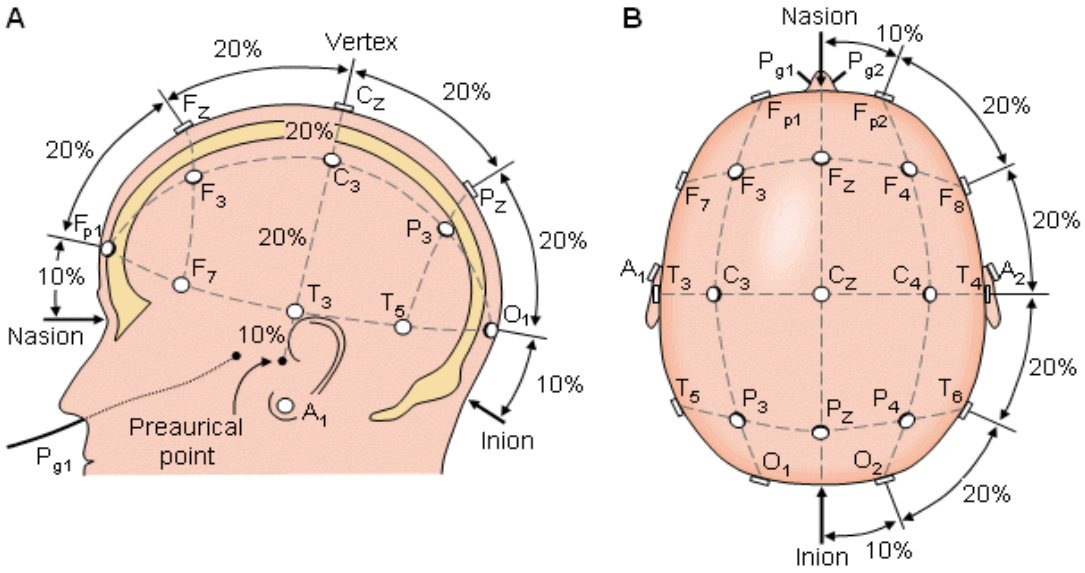

Figure 2.6 The international 10-20 system seen from (A) left and (B) above the head. The letters refer to electrode placement frontal (F), parietal (P), occipital (O), and temporal (T). The odd electrodes are placed on the left side while the even are on the right side. (Sanei & Chambers, 2013).

2.2 Event-Related Potentials

Event-related potentials (ERPs) are very small signals produced in the brain in response to particular events or stimuli (Woodman, 2010). They indicate a change in the EEG dependent upon sensory or cognitive events. Measurement of ERPs is a non-invasive and harmless method to examine the psychological and physiological connection of mental progressions (Peterson et al., 1995). ERP experiments yield a temporal resolution which allows the measurement of brain responses from one millisecond to the next. This compares to aspects of attention and perception that develop over tens of milliseconds (de Haan, 2013). Since the brain is fundamentally a wet electrical device, these electrophysiological measurements deliver a direct measure of the frequency of the system (Woodman, 2010). For the human brain, ERP

may be classified into two categories. The early components, collected within 100 milliseconds of the stimulus, are commonly referred to as ‘sensory’ or ‘exogenous’. These are determined by the physical parameters of stimuli. The later ERP signal is produced while the participant assesses the stimuli, and are generally known as ‘cognitive’ or ‘endogenous’ ERPs (Csibra et al., 2008).

2.2.1 Common ERP Forms

P50

The most positive peak between 40 and 75 (ms) after the conditioning stimulus is the P50 (Olincy & Martin, 2005). The P50 amplitude is the absolute difference between the P50 peak and the preceding negative trough (Clementz et al., 1997). The P50 amplitude change between the first and second repetition of a stimulus is related to the potency of the inhibitory pathway. This pattern is used when investigating sensory gating. Sensory gating is very important to an individual’s capability to carefully attend to salient stimuli and ignore repetitive information, which may protect the brain from information overload (Light & Braff, 2003).

P 300

The P300 wave is a positive deflection and it is usually stimulated in an "oddball" pattern once a subject notices a special "target" stimulus in a steady sequence of typical stimuli. The name P300 refers to a positive signal that reaches a peak about 300 ms after the stimulus (Sutton et al., 1965). The P300 wave signal is most pronounced when the participant is actively involved in the task of spotting unusual targets. Its amplitude and time of peak depend upon the distinguishability and type of common and oddball stimuli. A typical adult peak latency is 300 ms. In people with reduced mental aptitude, the P300 is less significant and later than in age-matched normal

subjects. The origin of the P300 wave is unknown and its role not fully understood. The P300 may possess numerous intracerebral generators, with the hippocampus and various association areas of the neocortex all contributing to the scalp-recorded potential. The P300 wave can characterise the transmission of information to cognizance, a process that utilises several specific areas of the brain. P300a originates from stimulus-driven frontal attention mechanisms during task processing, whereas P300b originates from temporal-parietal activity associated with attention and appears related to subsequent memory processing (Picton, 1992). P300 can be seen between 200- 500 ms (Doege et al., 2009) while (Luck, 2005) said P300 peaks between 350 to 600 ms post stimulus.

P600

The P600 is an ERP normally related to the processing of wave pattern irregularities or incompatibilities, which raises the question whether these ERP responses reflect common essential progressions, and what might be the precise procedures which are combined during successful parsing of well-formed sentences and the detection and repair of syntactic anomalies (Gouvea et al., 2010).

N100 or N1 wave

The negative peak (N100) contains several different subcomponents that have peaks between 80 to 150 ms after the stimulus (Luck, 2005). A negative excursion may be measured between 90-20 (ms) after the stimulus begins. It is a positioning or matching response and occurs on every occasion a stimulus is compared with earlier stimuli, particularly when the brain has been trained to respond to the particular stimulus. It produces highest amplitude at Cz and so is also known as a vertex potential (Sur & Sinha, 2009).

2.2.2 Evoked Potential

Evoked potentials (EPs) are neural electrical events in response to external stimulation factors such as light, sound, taste or smell. EEG EP signals are due to polyphasic waves ranging between 0.1-20 μA within 2-500 ms of the stimulation. The signals may be synaptic discharges or post-synaptic potentials along neural pathways (Akay, 2012).

The clinical uses of EPs are mainly due to their ability to investigate abnormalities of the sensory system. This is particularly useful when the neurological examination is difficult, i.e. when the participant cannot or will not cooperate. Furthermore EP measurements provide information on the temporal and anatomical distribution of brain activity pattern and aid the understanding of the pathophysiology of disease processes.

The three main types of EPs used in routine clinical studies are (Akay, 2012; Walsh et al., 2005):

1. Somatosensory evoked potentials (SSEPs),
2. Auditory evoked potentials (AEPs),
3. Visually evoked potentials (VEPs).

2.2.2.1 Somatosensory Evoked Potentials

Somatosensory evoked potentials (SSEPs) are measured EEG responses due to touch stimulus. The stimulus may be based on vibration, position, or epicritic tactile senses (Akay, 2012). In some cases the peripheral sense is stimulated by delivering an electric current. SSEPs are primarily measured in the region of the cortex.

Components of SSEPs

SSEPs are broadly divided into early, middle and late components as shown in Figure 2.7 (Akay, 2012).

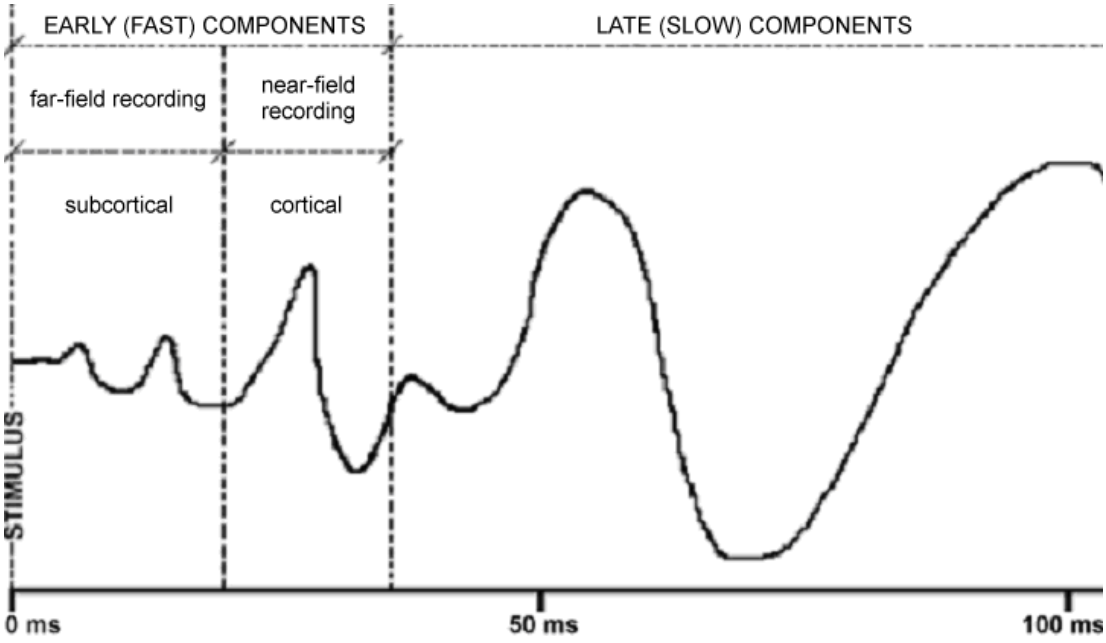

Figure 2.7 Schematic diagram of SSEPs divided into early, middle and late components. potentials with very small amplitude for 10-15 ms before the occurrence of components with a large amplitude that start nearly 20 ms after stimulus (Akay, 2012).

In the above Figure, the late components are non-specific waves that may differ for the same person depending on the attention-consciousness of that person at the time. It is not only associated with the primary cortex region but it is also related to the cortical association, activities of the components, and effects of the Ascending Reticular Activating System. Those component potentials having large amplitude are cortical activities which are recorded under and around the active electrodes; known as near-field recording or middle components. The small amplitude before the near-field potentials arises from the subcortical regions, commonly known as far-field recording or early components of SSEPs (Akay, 2012).

The shape of the measured SSEPs response depends strongly on the location of the reference electrode. The responses of subcortical structure are detected first. The amplitude and polarity may differ due to the location of the electrode and some components may be missing or not appear. For example, if the reference electrode is fixed on the forehead region the components of subcortical regions may become weak.

Effective recording of the subcortical components requires that the electrodes should be placed near the source. Generally SSEPs are used to examine the spinal cord, somesthetic cortex and peripheral sensory fibres (Akay, 2012).

2.2.2.2 Auditory evoked potentials

Auditory evoked potentials (AEPs) are used to examine the auditory channels up to the primary cortex regions, by applying auditory stimulus through a classic audiometric earphone above the hearing threshold to the external auditory canal. The auditory stimulus device typically generates square waves of 100 - 200μs, 10 times per second, known as a "click" sound. Generally, the intensity of the sound applied to generate stimulus is 65-70db and so well above hearing threshold. It is increased in patients having hearing problems (Akay, 2012).

When the stimulus rate is greater than 10 per second, the absolute latencies and inter-peak latencies are extended and the amplitudes are decreased. If the sound intensity is reduced, the morphology of waves change. In an AEP examination, a minimum of 2000 samples of 10 ms duration each, must be acquired for each ear, and the examination should recur at least twice (Akay, 2012).

2.2.2.3 Visual evoked potentials

Visual evoked potentials (VEPs) are produced by retinal stimulations. These stimuli may be generated by various sources, such as (a) stroboscopic flashing light with continuous flashing intervals - mainly used for babies and uncooperative patients, (b) a flashing LED - used for special designed lenses, (c) alternating checkerboard pattern stimulation – this is a commonly used technique due to its highly sensitive and stable nature. This method is also known as pattern-shift visual evoked potential (Akay, 2012).

VEPs caused by short-term stimuli are generally transient responses of the visual system. Transient visual evoked potentials (TVEPS) are responses to speedy alterations in the input (Basar et al., 1999). Long-term stimuli are generally sinusoidally modulated monochromatic light. These EEG waves are commonly known as steady-state visually evoked potentials (Regan & Regan, 1988). SSVEPs yield EEG measurements with distinct frequency components that remain similar in amplitude and phase over a long period, and so may be identified by temporal averaging (Nakayama & Mackeben, 1982; Wandell et al., 2007). SSVEPs may be found in both in humans and animals (Nakayama & Mackeben, 1982; Rager & Singer, 1998).

Transient VEPs are used to estimate the time required for a visual stimulus to travel from the eye to occipital cortex. This value may be used to diagnose ophthalmological diseases, multiple sclerosis and abnormalities of the brain's visual function area.

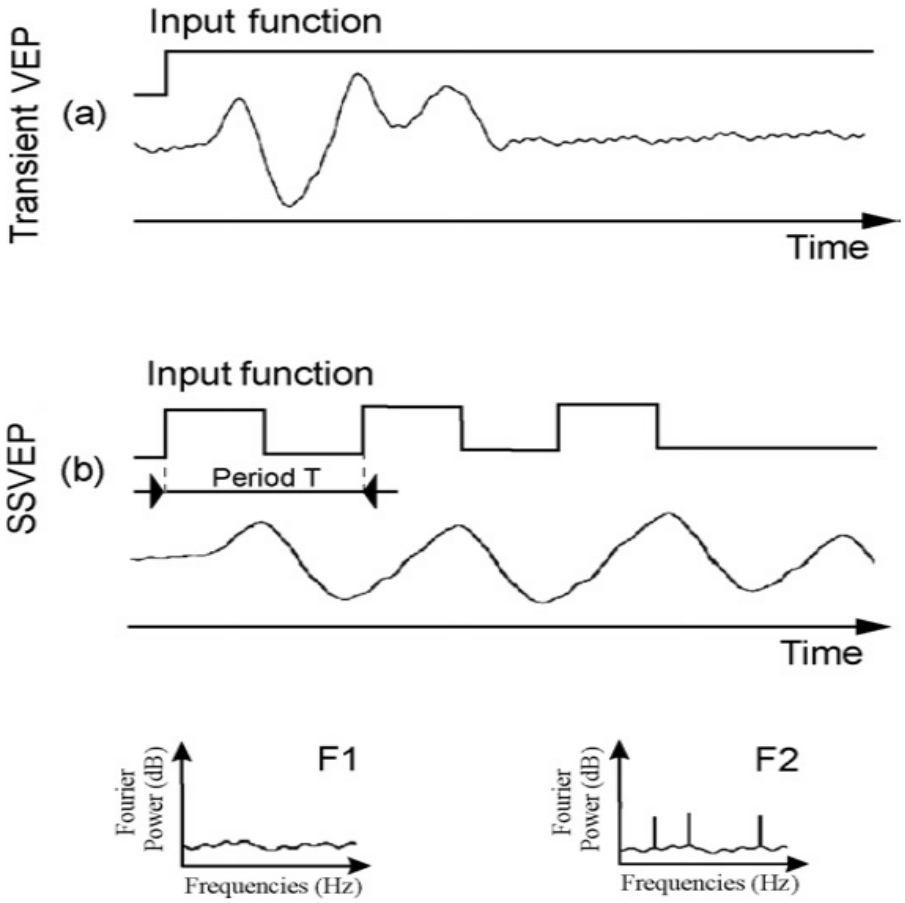

Figure 2.8 Schematic diagram of TVEPs and SSVEPs. (a) Input function with a square stimulation transient and measured TVEP. (b) Steady state input and SSVEP. Lower left and right are the power spectral density for TVEPs and SSVEP respectively.

In Figure 2.8, the shape of the response over one input cycle is not enough to differentiate the SSVEPs from TVEPs. However, the spectral response contains distinct peaks for the SSVEP associated with the input pulse rate. If the stimulus is repeated then this response complex may be similarly repeated, and the collective response will be structured i.e. with stationary periodic oscillations. The power spectral density highlights the difference between TVEPs and SSVEPs (Vialatte et al., 2010).

2.3 EEG and Artefacts

EEG measures the electrical potential on the scalp using several electrodes (Nunez & Srinivasan, 2006). The changes in potential are principally due to brain activity. It is not possible to measure the activity of a single cortical neuron on the scalp, due to the very weak electrical field produced by a single neuron. On the other hand, many cortical neurons acting together do generate a small but measurable electrical field that is detected on the scalp (Nunez & Srinivasan, 2006; Delorme et al., 2012). The measured activity has a broad spectrum, similar to pink noise, but with peaks in particular frequency bands, related to EEG rhythms (Sörnmo & Laguna, 2005). Other neurological activities can also be measured, such as changes in brain rhythms and evoked potentials (Fatourechi et al., 2007).

Artefacts are unwanted signals that may obscure or distort the brain signals of interest (Anderer et al., 1999). EEG artefacts are often non-cerebral in origin. They may be broadly classified into physiological and non-physiological artefacts as seen in figure 2.9.

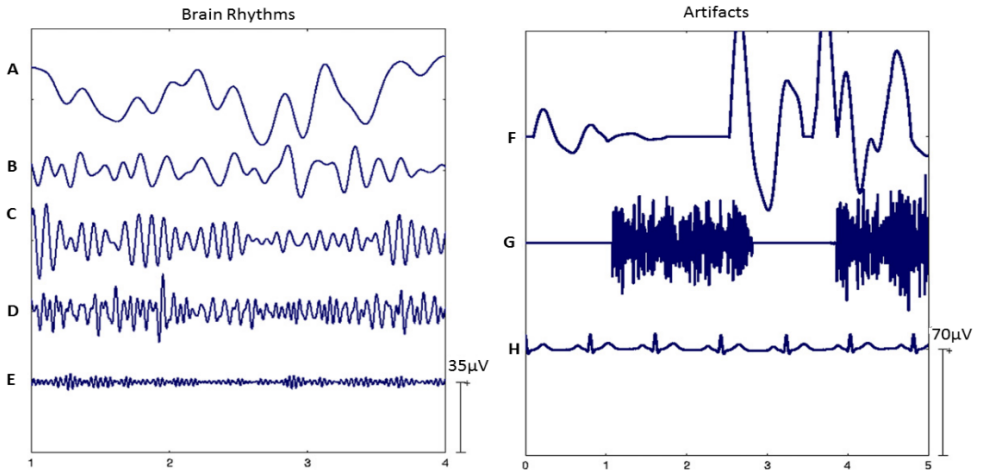

Figure 2.9 Normal brain rhythms and artefacts. Left figure is brain: (A) Delta (B) Theta (C) Alpha (D) Beta (E) Gamma comprise the typical EEG spectrum from low to high frequencies. Right figure is Artefacts: (F) Ocular (G) Muscular (H) Cardiac are the common contaminants in the EEG recording.

2.3.1 Physiological Artefacts

Physiological artefacts are generated by the body. Muscles produce electrical fields when they contract and so eye-blinks and neck support can cause large artefact signals in EEG. The pumping of blood through the head by the heart causes rhythmic shape and conductivity changes in the head. These can be seen in EEG measurements (Urigüen & Garcia-Zapirain, 2015; Fisch & Spehlmann, 1999).

2.3.1.1 Ocular Artefacts

Ocular artefacts arise due to eye movement and blinks. Normally, electrooculogram (EOG) determines the electrical activities produced by eye movements. The EOG signals are large enough to be measured by the EEG (Croft & Barry, 2000). The eye movement signals are mainly collected by the frontal electrodes (Romero et al., 2008; Fisch & Spehlmann, 1999). The signal intensities of eye movement may depend on the closeness of the electrodes position to the eyes as well as the direction of eye movement. Eye blinking may also cause artefacts on the EEG recording. Generally, the amplitude of artefacts due to blinking is much larger than the EEG signals (Urigüen & Garcia-Zapirain, 2015; Croft & Barry, 2000), especially for electrodes near the front of the head as seen in figure 2.10. EOG reference signals may be measured at the same time as the EEG recording, and may be partially cancelled (Urigüen & Garcia-Zapirain, 2015). Usually the vertical (VEOG), horizontal (HEOG) and radial (REOG) signals are recorded independently as these signals propagate differently across the scalp (Urigüen & Garcia-Zapirain, 2015).

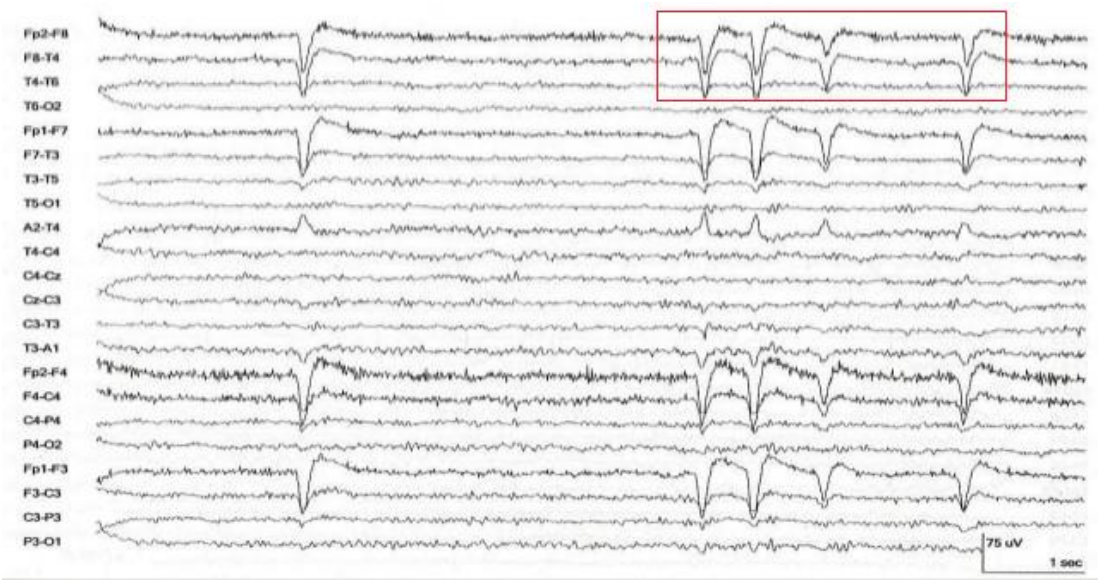

Figure 2.10 Medium amplitude and low frequency signals confined to the frontal electrodes may be recognized as an ocular artefact (red) due to their signal morphology (Marella, 2012)

2.3.1.2 Muscle Artefacts

Muscle artefacts are linked to muscular movement during EEG recording. An electromyogram (EMG) measures electrical signals on the body during muscular movements. The muscular artefacts may be associated with swallowing, walking and talking (Sörnmo & Laguna, 2005). The EMG spectral shape and intensities may depend on the types of muscles and their contraction strength. EMG has large amplitudes and frequency range, and so disturbs all EEG bands; although particularly in the beta and alpha bands. EMG is often measured across the entire scalp due to myogenic activity of the head, face and neck (Goncharova et al., 2003). Other EMG artefacts are more common or stronger in the frontal and temporal electrodes. EMG artefacts can be reduced by low-pass frequency filtering below 35 Hz (Reis et al., 2014). It can be seen in figure 2.11 EEG recording shows the EMG artefacts in electrodes T3 and T5.

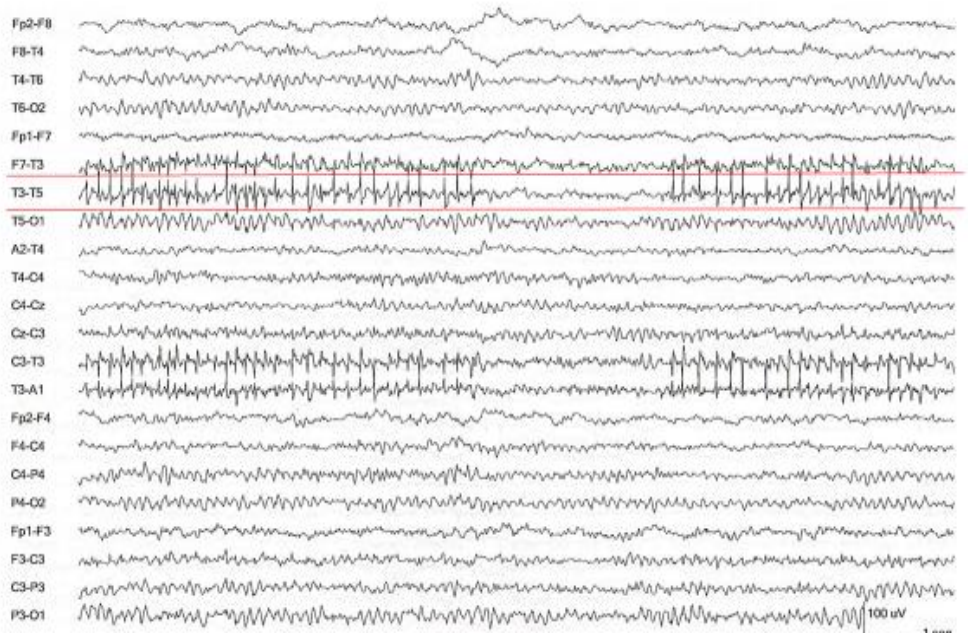

Figure 2.11 EEG recording shows the EMG artefacts appearing in T3-T5 electrodes (between red lines) (Marella, 2012).

2.3.1.3 Cardiac Artefacts

The heart generates two distinct types of artefacts: i) electrical and ii) mechanical. Both types of cardiac artefacts are time locked to cardiac contractions and identified by their synchronization with complexes in the ECG channel (Fisch & Spehlmann, 1999; Urigüen & Garcia-Zapirain, 2015). The electrical cardiac artefact is the ECG signal, as recorded from head electrodes. The P and T waves commonly do not appear, due to the distance from the heart and the orientation of the associated electrical field vector in the heart. The artefact is a distorted QRS complex cardiac mechanical artefacts arise via the circulatory pulse and are sometimes classified as electrode artefacts. They arise when an electrode rests over a vessel. The cardiac signal appears as a periodic slow wave with a consistent interval that follows the ECG artefact's peak by about 200 ms. It occurs over the frontal and temporal regions but it may present over other regions of the brain (Fisch & Spehlmann, 1999) as seen in figure 2.12.

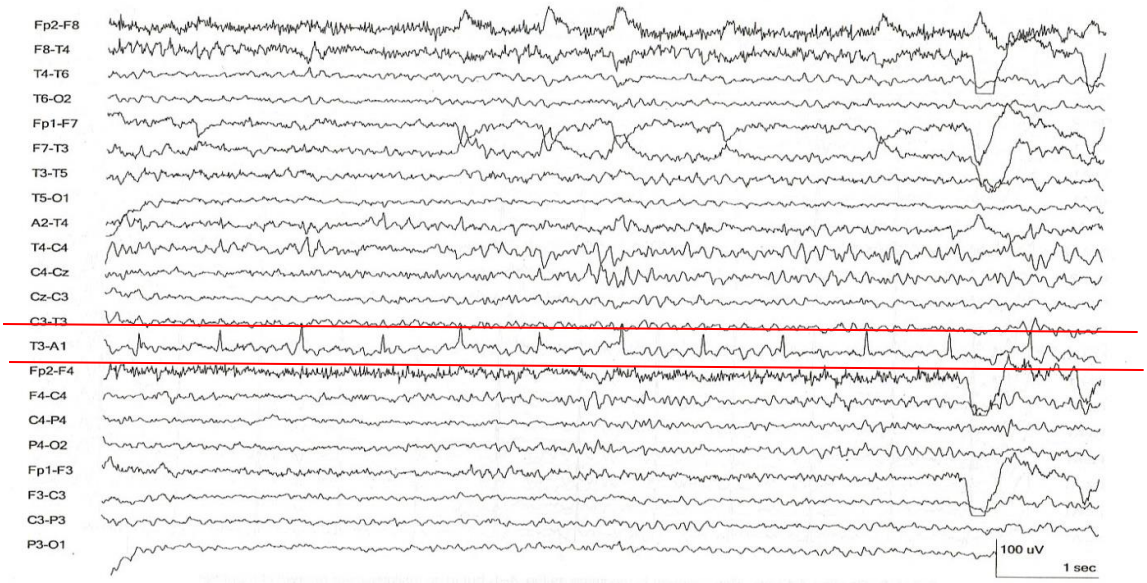

Figure 2.12 EEG recording shows the ECG artefacts appearing at T3-A1 electrodes (between red lines) (Marella, 2012).

2.3.2 Non- physiological Artefacts

Various types of external devices generate EEG artefacts. The most common external artefacts are due to the alternating current through an electrical power supply (Fisch & Spehlmann, 1999) . The noise is usually of medium to low amplitude and having single component at mains frequency, 60 Hz in the USA and 50 Hz in the rest of the world. Mains artefacts may appear in all or some channels and may include electrodes that may have inadequately coordinated impedances (Urigüen & Garcia-Zapirain, 2015; Fisch & Spehlmann, 1999). The signal can be due to poor isolation within the EEG instrument, voltage induced on electrodes by nearby electrical equipment, or by coupling between the EEG and poorly isolated electrical equipment.

Artefacts in the EEG signal can also be caused by changes in the electrode attachment to the scalp. Attachment is sometimes problematical due to hair. Sometimes electrodes adhere directly to the scalp and sometimes a conductive jelly is introduced into the space between the electrode and the scalp. Electrode detachment or loss of electrical connection due to movement or drying of the conductive jelly, means that

the measured voltage no longer tracks the potential on the scalp. Physical movement of the electrodes can lead to signals due to changes in location, electrical effects due to rubbing or rapid changes due to intermittent attachment.

Chapter 3 Methodology

3.1 Introduction

This chapter details the processes involved in recording and processing EEG to estimate ERPs during a range of activities and in a range of environments. These initial experiments were performed to trial the complete measurement process and to produce data on which to develop and test ERP estimation algorithms. The steps in the experiment are described, as well as the initial quality control processing of the EEG data.

3.2 Experimental Procedure

The ERP task consisted of a number of tests while the subjects were in environments with different levels of stimuli and while participating at different levels of activity. The smartphone based AEEG system used was developed at the University of Hull and is specified in (Bateson et al., 2017). The core of the system is a waist mounted control system capable of measuring 24 channel voltages, with 24 bit resolution and a 250 Hz sampling frequency. This is sufficient to be compatible with the international 10/20 system, and also provides five additional channels available for ECG, EOG or EMG recordings. The data are sent via WiFi in real time to a partnered laptop or smartphone. An app running on the smartphone allows recording and plotting of live data, whereas a PC provides greater processing capability for algorithms applied to online data. Use of the smartphone allows electrode attachment problems to be identified immediately and greatly reduces the weight and size of the data recording equipment.

For the experiments described in this thesis, 19 EEG channels were monitored with the 20th channel being the reference electrode connected to an ear lobe. Eyes blinks were monitored using electrodes around the eyes. Two electrodes, one above and one below the left eye, measured the electric field generated by vertical eye movements (VEOG). The signal due to horizontal eye movements (HEOG) were measured using two electrodes, one each side of the head at eye-level. Each experiment consisted of a 10 minutes period during which the participant listened to a series of tones through earphones controlled by the smartphone. All the tones were 64 ms in duration and three-quarters of the tones were at the common frequency of 600 Hz while one quarter were at the oddball frequency of 1200 Hz. The tones were presented to the participant in a pseudo-random sequence and the participant was asked to count the number of oddball tones. In each test, participants would listen to 340 tones, of which about 25% would be oddball. The AEEG system recorded a marker on the EEG data at the time of each tone (Bateson et al., 2017).

Experiments were performed in a range of situations:

1. Sitting in a shielded room;
2. Walking in a shielded room;
3. Sitting in a laboratory;
4. Walking in a laboratory;

The shielded room is a large metal lined room designed to eliminate external electromagnetic interference. It is considered to be a very low-stimulus environment. The laboratory contains a lot of equipment and is visually stimulating.

For the sitting shielded room and laboratory experiments, the participants were encouraged to keep their heads as still as they could. However, for the walking experiment, more head and eye movements were expected as the participants navigated around obstacles. These experiments were designed to highlight the difference between movement artefacts and brain signals due to sensory stimulation.

3.3 Participants

Ten healthy participants (aged 20–45) two females and eights males were selected from a group of volunteers. To be selected the applicants needed to match a set of inclusion and exclusion criteria to match the ethical approval. These were designed to eliminate people with health conditions that may affect the measurements, and individuals who could be disturbed by the measurement process. The full procedure and instructions of the protocol were explained to all participants. This study was conducted under ethical approval from the Faculty of Science and Engineering Ethics Review Board and written informed consent was obtained from each participant.

Figure 3.1 AEEG data recorded in during sitting inside shielded room.

3.4 Initialising EEG Equipment

Ambient electromagnetic noise may cause problems during the recoding of EEG. The EEG equipment (stimulus generating devices and data collections instruments) is switched on 10 minutes before use for stabilizing and warming up the equipment. A check is then performed to minimise any mains noise (between 50-60Hz) or any other frequency peaks (Light et al., 2010).

The participant's hair must be washed without using any conditioners or gel products, as these can affect the electrical connection between the electrodes and the scalp. Participants were asked to do this before they came for measurements.

The electrode cap must be selected according to the participant's head size and electrodes should already be snapped into white plastic adaptors on the cap (Light et al., 2010).

Via a lead, electrodes should be connected to the EEG measurement and recording equipment. As more than 20 electrodes are used, it is important that the cap electrode agrees with the electrode position built into the equipment.

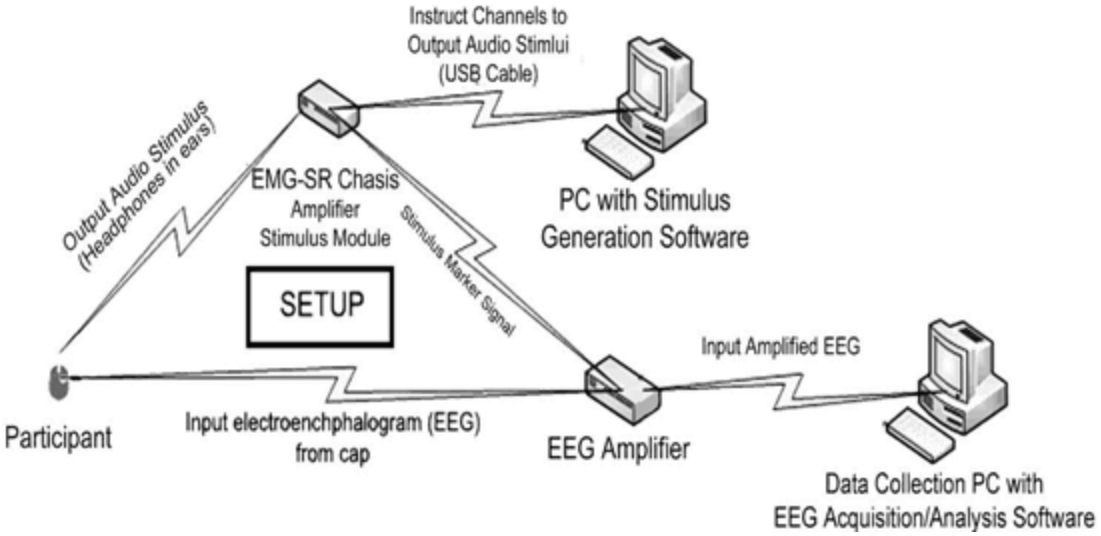

Figure 3.2 Schematic diagram of a typical EEG setup. Stimulus generation computer outputs stimuli to the subject via the stimulus amplifier. EEG data collected by

electrode cap on participant's head is relayed to EEG amplifier and integrated with information about timing. Amplified EEG data with stimulus markers is then relayed to acquisition computer for data analysis (Light et al., 2010).

3.5 Mounting the Caps on the Participant

Before fixing the cap on the participant's head, the distance between nasion (nose-bridge) and inion (bump on the lower base of skull) must be measured as this distance sets the position of all the electrodes. The cap should be tight and is placed on the head and centred by ensuring that the distance from the central electrode, Cz, to the ears is the same on both sides as well as the distance between nasion (nose-bridge) and inion should be equal. When in the correct position, the cap should be secured with a chin strap.

Additional electrodes may be placed on the cap or directly on the skin to measure eye movement. Electro-oculographic electrodes (EOGs) may be placed around the eyes to monitor vertical and horizontal eye movements as well as reference and ground electrodes (Light et al., 2010).

The impedance of electrical connection between electrodes and the scalp must be minimized by applying electrolyte gel. The gel also reduces noise due to electrode movement. However, too much gel can weaken the electrical connection by interference between electrodes. Impedance can be controlled by filling electrodes with gel or by gently scrubbing the scalp with gel before placing electrodes. Impedance can also be lowered by continuously twisting a Q-tip on the scalp (Light et al., 2010). For these experiments, a small amount of gel was injected through the electrode to fill the space between the electrode and the scalp. Electrical connection was tested by observing the signals through all electrodes before the experimental measurements were started.

3.6 Data Collection

For data collection, the EEG acquisition software was initiated and a participant file is created. It is necessary to observe the resting activity of all electrodes. In the ideal conditions, electrode signals exhibit low amplitude and correlated variation. If any faulty channels are suspected then more electrolyte gel should be applied. Initial data are filtered and compared with the reference or control values (Light et al., 2010).

When the operation of the equipment has been verified, the experimental measurements are performed following the sequence specified in Section 3.2.

3.7 Post EEG Experiment

After the experiment, the cap and electrodes are removed gently from the participant's head. Gel should be cleaned from the hair and all electrodes should be cleaned and safely stored to prevent corrosion or damage to the electrodes or cables.

3.8 EEG Data Pre-processing

The recorded EEG signals were collected and analysed using the Matrix Laboratory (MATLAB) and EEGLAB toolbox (Delorme & Makeig, 2004) . A frequency filter was first used to remove noise outside the EEG frequency range, and to remove any 50 Hz mains hum. High pass filters were used for low frequency, baseline wander removal (0.1-1 Hz) whereas low pass filters were used remove high frequency noise, such as EMG activity (45-60Hz). Then 19 electrode channels were selected for signal observation, with the 20th used as a reference which put on the right ear. The filtered EEG data were segmented into individual trials from 200 ms before the stimulus to 800 ms after. ERPs trials were calculated using averaging over each category of recording i.e. common or oddball as seen in figure 3.2, sitting or walking, shielded

room or lab as seen in figure 3.3. There are differences in ERP signal before and after eye blinks filters as seen in the figures 3.4. There are variations in ERP signals during different activities, tasks etc. (Heinrich & Bach, 2008; Debener et al., 2012). Moreover, the signal to noise ratio for each task was estimated.

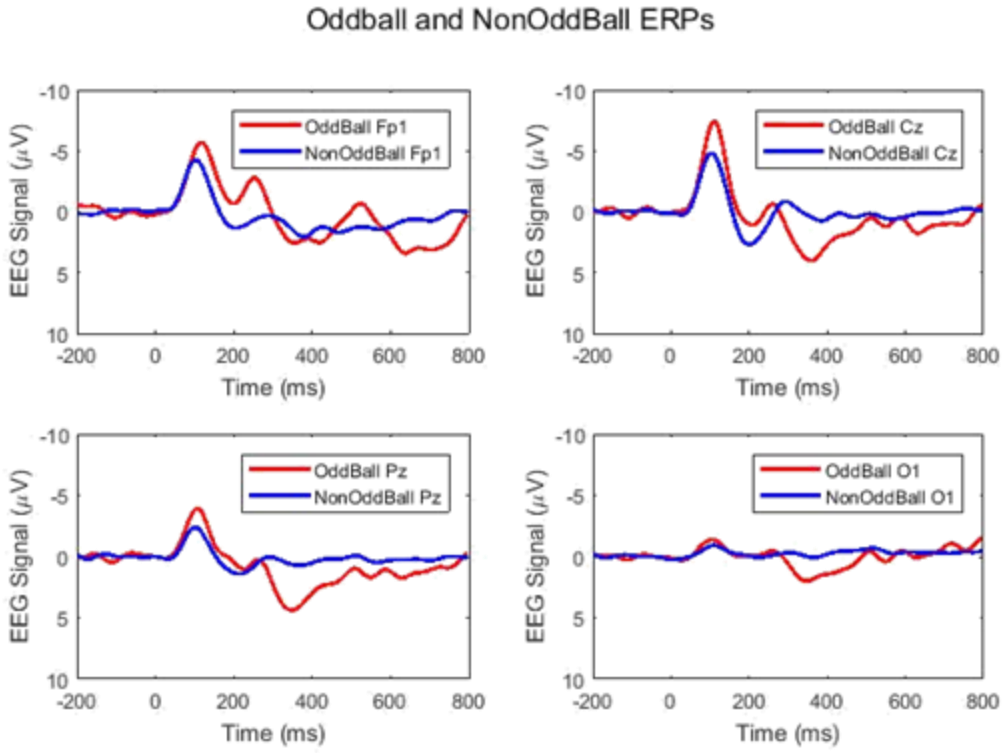

Figure 3.3 Oddball and Non oddball ERPs for different channels. It can be seen variations of ERP Oddball and standard signal in different electrodes.

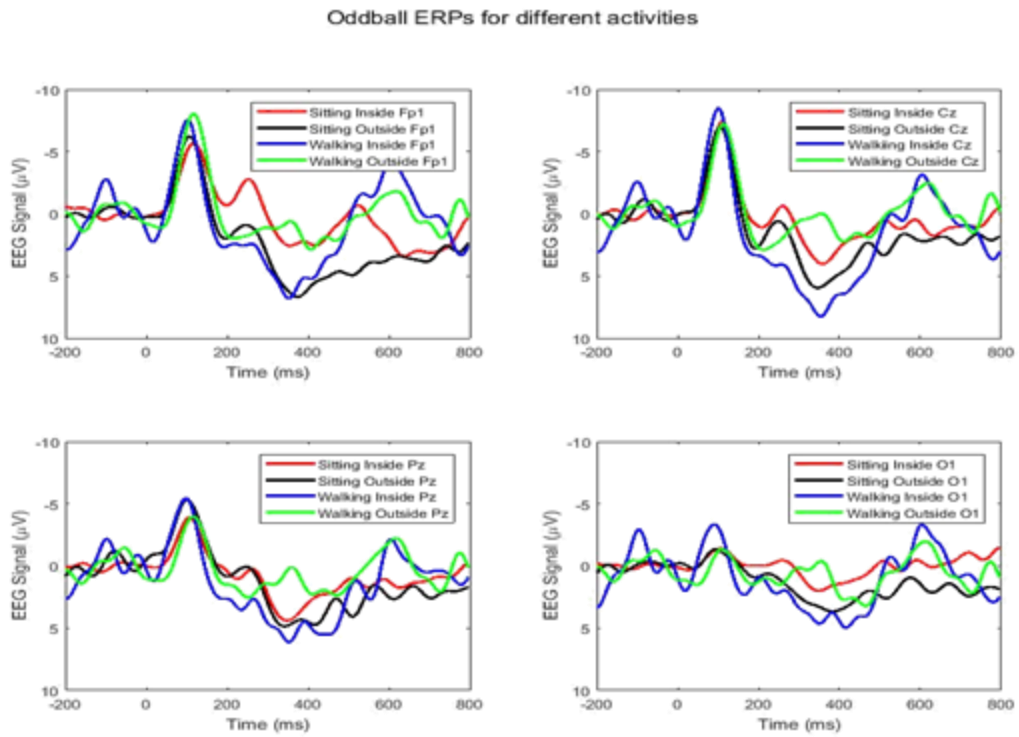

Figure 3.4 Oddball ERPs during sitting and walking inside & outside shielded room. It can be seen variations of ERP Oddball signal in different environments and electrodes also Oddball ERP can be seen in Cz and Pz electrodes much better than O1 and O2 electrodes.

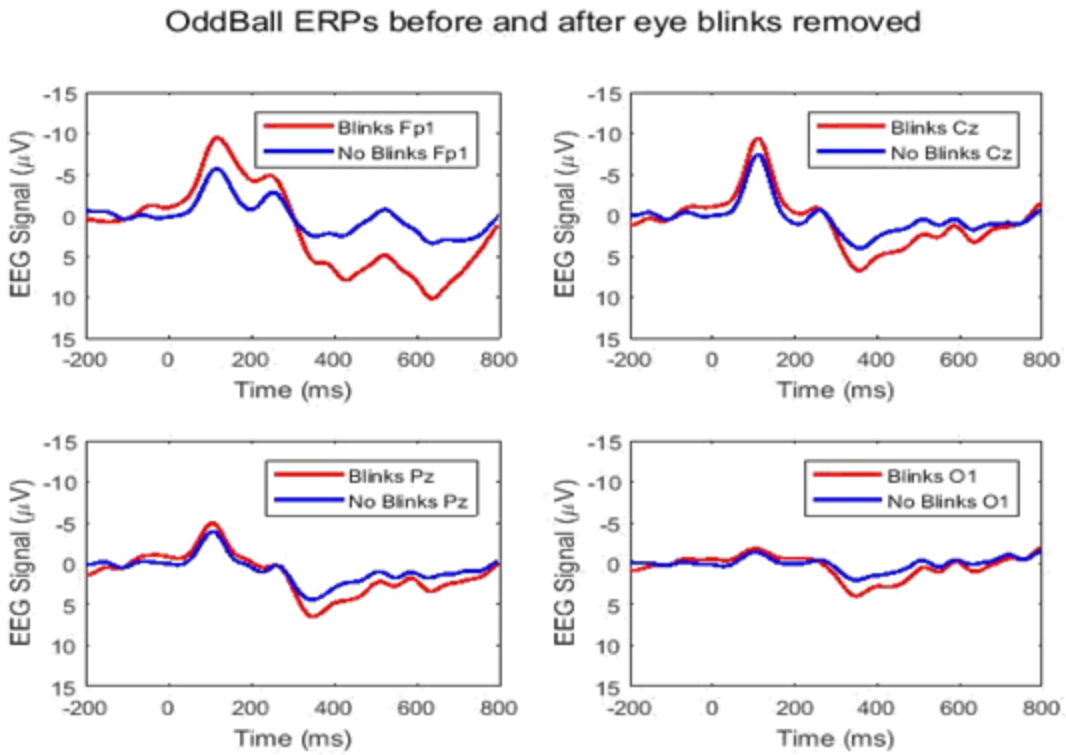

Figure 3.5 Oddball ERPs before & after Eye blinks removal. It can be seen variations of Oddball ERP in different electrodes when eye blink filtered.

3.9 Conclusions

An experimental protocol has been defined and an initial set of data acquired from ten healthy participants. The following chapter describes the processing of these data to estimate the ERP.

Chapter 4 EEG Signal Processing

4.1 Introduction

This chapter introduces the signal to noise ratio as a measure of EEG signal quality. Sources of noise are presented along with their spatial and temporal characteristics. The most contemporary and commonly used EEG denoising algorithm is presented. This is known as ADJUST and is a plug-in to the widely used EEGLAB toolbox within MATLAB software. ADJUST uses Independent Component Analysis (ICA) to separate eye-blink and other artefact signals from brain signals. ICA is presented in some detail along with the heuristics applied, along with statistical independence, to separate the signal and artefact time series. This work introduces a weak form of spatial filtering that leads to the more robust spatial averaging developed in Chapter 6, based on Principal Component Analysis.

4.2 Signal to Noise Ratio

4.2.1 Theoretical Overview of SNR

Signal to noise ratio (SNR) is the ratio of signal power to noise power (Ahlfors et al., 1993):

$$P = \frac{\mathrm{P_{Signal}}}{P_{Noise}} \qquad PdB = 10\log_{10}(P)$$

At low SNR it is difficult to observe features of the signal as they are obscured by variation due to the noise. Therefore, the SNR indicates whether clinically important features will be observable in the processed signal. For individual ERP measurements, the SNR is often low due to the high amplitude noise signals caused by electrode movement and other bio-signals. Many repetitions of the ERP measurement are

averaged in an attempt to increase the SNR. The SNR of the average indicates whether the required quality has been achieved.

4.2.2 EEG Signal Noise

The SNR depends upon the number of individual ERP time-series in the average, the SNR of each time-series, and time between stimuli (Ahlfors et al., 1993). When designing an ERP experiment, it is necessary to determine the number of trials to be performed. Averaging tends to maintain the power of the coherent signal while reducing the power of the incoherent noise. Therefore the SNR of the average increases as the number of trials is increased. The noise power in ERP time-series will depend on the nature of the experiment and the characteristics of the subjects (Luck & Todd, 2004). If each ERP time series is contaminated by independent and stationary noise, then the noise power decreases as one over the number of time-series in the average, and the noise amplitude decreases as one over the square root of the number in the average (Ahlfors et al., 1993; Luck, 2005). This has been stated to be approximately the case for EEG signals (Stecker, 2000). However, noise in ERP time-series is not stationary or independent. Non-stationary noise comes from intermittent artefacts such as eye-blink artefacts. When an eye-blink occurs, the noise can have an amplitude of an order-of-magnitude larger than the ERP signal, but each blink typically affects a single ERP trial. Dependent noise can come from non-brain signals produced by responses to the ERP stimulus, e.g. the subject may flex a muscle each time a stimulus is received. For these reasons, the SNR in the average may not reduce as expected by the number in the average, and may not reduce at all. For example, if one more trial time-series is included in the average but it includes a very large eye-blink noise artefact, then the SNR in the average could increase (Farwell & Donchin, 1988).

The following sections explore the SNR in ERP signals collected to determine the presence or absence of a P300.

4.3 Reduction of EEG Artefacts

Contamination of EEG signals by artefacts due to eye movements, blinks, muscle, heart and lead noise is a serious problem for EEG interpretation and analysis. Eye movement and blink artefacts are the largest biological sources of noise in EEG measurements. Many methods have been proposed to reduce the amplitude of these artefacts in EEG recordings, such as fixation, rejection and correction (Pham et al., 2011; Croft et al., 2005) .

Typically EEG signals due to neural sources have much less amplitude than those due to artefacts. Artefacts can be generated by physiological sources or sources external to the body. Eye movements can affect the electrical field over the entire scalp but particularly near the eyes (Croft & Barry, 2000).

4.3.1 Identification of Artefacts in EEG using ICA

Independent Component Analysis (ICA) is a blind source separation method that divides complex signals into sets of maximally statistically independent signals (Hyvarinen et al., 2000). ICA can be used for identifying the information sources mixed in the EEG data (Lee et al., 1999). ICA has been proven to be successful in attenuating several types of artefacts such as eye movements, eye blinks, muscle and cardiac artefacts (Hoffmann & Falkenstein, 2008).

Many sources of noise artefacts are independent of the brain response to stimuli, and so ICA can separate multi-channel ERP time-series into brain response and artefact signals. The ICA-based artefact reduction approach has the advantage of avoiding the rejection of trials contaminated with ocular artefacts. This can be of particular

importance when recording sessions need to be short and the amount of EEG data collected is minimal, as for instance is the case when testing clinical populations or children (McMenamin et al., 2011)

Many ICA based EEG denoising algorithms have been developed for visual stimuli, as well as muscle activity, cardiac signals, electrode noise, etc. Regressing out muscle artefacts is most difficult as muscle signals derive from numerous muscle groups which require different reference channels.

ICA procedures are based on the expectation that the signals recorded on the scalp are mixtures of temporally independent cerebral and artefact signals. These arise from different parts of the brain, scalp, and body; and are summed linearly at the electrodes (Lee, 1998). Jung et al developed a numerical tool that decomposes EEG data in blocks of sources with maximally independent time series, and so have suggested an automatic ICA-based algorithm to identify EEG artefacts (Jung et al., 1998). Makeig et al. (Makeig et al., 1996) found that ICA could be used to automatically separate neural activity from muscle and blink artefacts in multichannel recordings (Makeig et al., 1997; Vigário, 1997). Bell and Sejnowski, have created a technique to remove and isolate most EEG artefacts by linear decomposition using an extension of the ICA algorithm (Bell & Sejnowski, 1995).

ICA does not need reference channels for each artefact source because it uses spatial filtering. When the independent time series of artefact sources are separated, these can be subtracted from the measured EEG data to remove the contributions of the artefact sources (Jung et al., 2000b).

In the 1996, Jung said that regression in the time and frequency domains were applied to remove eye movement's artefacts (Jung et al., 2000a).

Multichannel EEG activity is recorded at many places on the scalp and so includes some redundant information, i.e. the same brain activity is recorded at multiple electrodes. The same is true for artefact signals. When the triggers for brain activity and artefacts are independent, then ICA can be used to both separate brain signal and artefacts, and to perform some level of spatial averaging (Jung et al., 2000b; Makeig et al., 1996).

4.3.2 Identification of Artefacts in EEG using ADJUST plugin

Artefacts in EEG signals due to eye movements can be identified and eliminated using the ADJUST plug-in to the EEGLAB toolbox in Matlab, where ADJUST stands for Automatic EEG Artefact Detection Based on the Joint Use of Spatial and Temporal information. This tool isolates the artefact-specific temporal and spatial elements by automatically tuning the parameters of the EEG data. It is essential also to examine the separate component classification in the absence of any other information e.g. electrooculography (EOG) channels. The ADJUST plug-in performs the three key steps shown schematically in Figure 4.1 and described in the following paragraphs (Mognon et al., 2011).

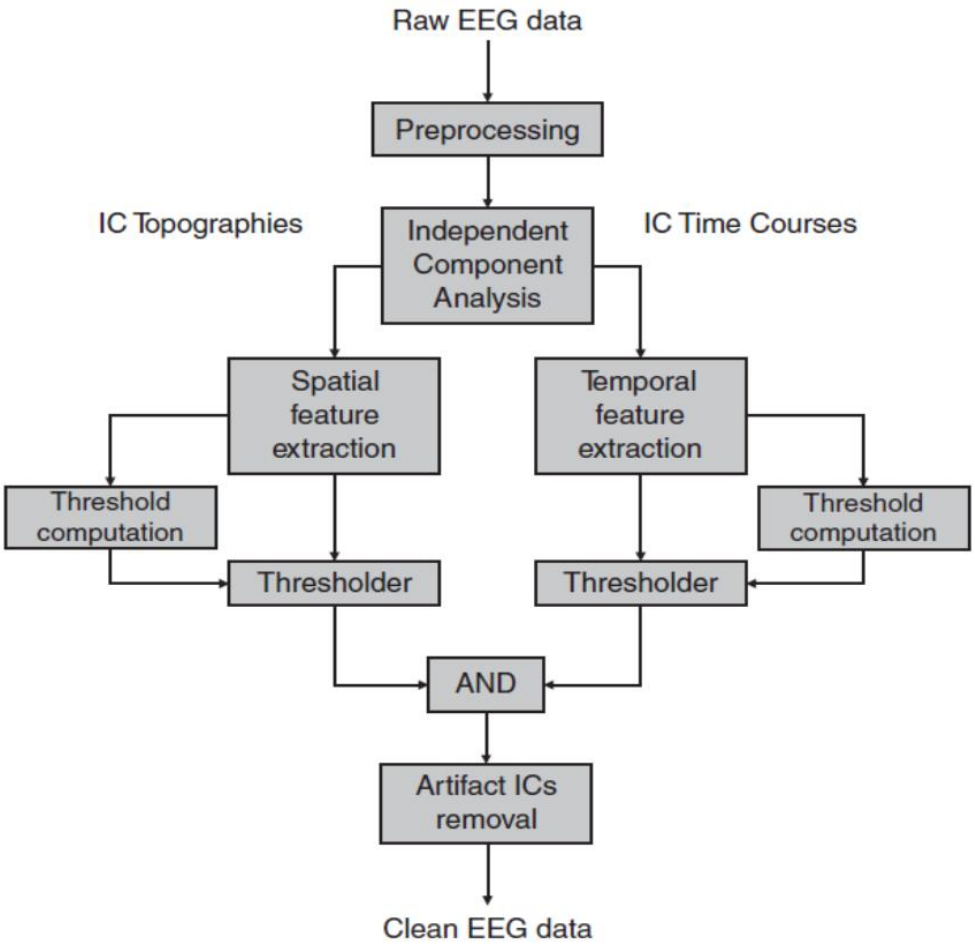

Figure 4.1 The architecture of the ADJUST algorithm a generic detector with one spatial and one temporal feature (Mognon et al., 2011).

It is assumed that a sequence of q measured time series random variables described by the function $\mathbf{G}(t) = \left[g_1(t), \ldots., g_q(t) \right]^T$ is obtained by linear combination of p independent source signal time series $\mathbf{S}(t) = \left[S_1, \ldots, \ldots S_p(t) \right]^T$. In order to obtain a unique independent decomposition, the number of observations q must be greater than the number of independent source signals (i.e. $p \leq q$). The source signals can be non-Gaussian or non-white in time (Lee et al., 1999; Belouchrani et al., 1997).

The ICA model can be described by equation (4.1):

$$\mathbf{G}(t) = \mathbf{AS}(t) + \boldsymbol{N}(t) \tag{4.1}$$

where the observations $\mathbf{G}(t)$ can be obtained by combining the source signals $\mathbf{S}(t)$ using a constant $[q \times p]$ matrix $\mathbf{A}$, termed the mixing matrix, with addition of the white noise vector $\mathbf{N}(t)$, which is ignored in some implementations. The mixing matrix is full column-rank $(r(\mathbf{A}) = p)$.

On the basis of these assumptions, a solution to the problem of isolating the ICA components can be realised, and the independent components (ICs) approximated, by determining a $[p \times q]$ matrix $\mathbf{W}$, termed the unmixing matrix. The product of $\mathbf{W}$ and the function $\mathbf{G}(t)$ gives the source signal time series $\mathbf{S}(t)$ as stated in equation (4.2):

$$\mathbf{S}(\boldsymbol{t}) = \mathbf{W}\mathbf{G}(\boldsymbol{t}) \tag{4.2}$$

In contrast to Principal Component Analysis, ICA is non-linear and, hence, its solution requires non-linear optimisation.

The INFOMAX algorithm is based on a learning rule which minimizes the mutual information between source signal estimates. This algorithm has been used by (Bell & Sejnowski, 1995) to implement ICA within the ADJUST plug-in in EEGLAB.

4.3.2.1 ADJUST Features Computation

With respect to spatial and temporal features, Figure 4.2 indicates the most suitable acquired behaviour of the ICs associated with four types of artefacts, namely: eye-blinks, horizontal eye movements, vertical eye movements and generic discontinuities. These are described in the following sections.

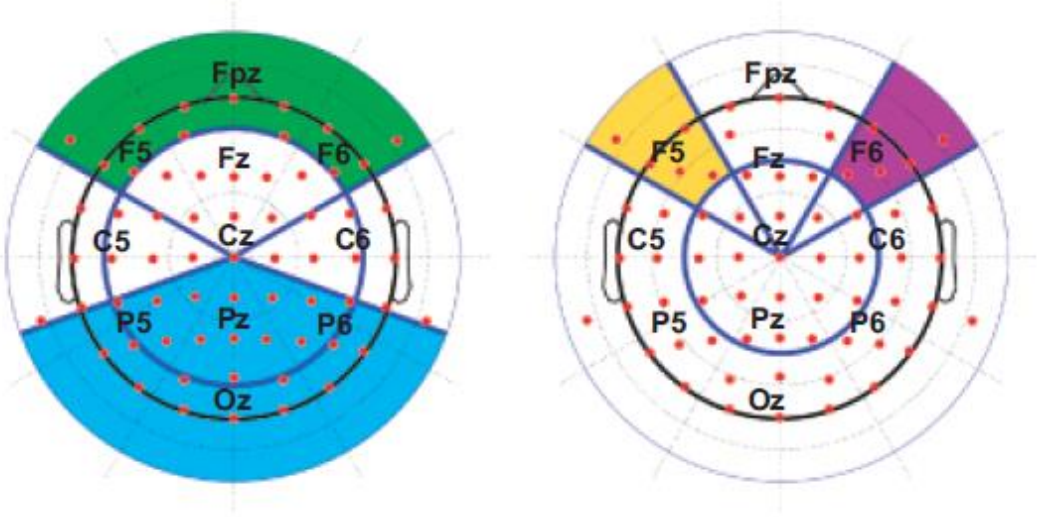

Figure 4.2 The areas of scalp used in the ADJUST computation of spatial features for the automatic detection of spatial-temporal EEG artefact. Left: Frontal area (green) and posterior area (blue). Right: Left eye area (yellow) and right eye area (purple). The red dots indicate channel positions in the validation dataset (Mognon et al., 2011).

4.3.2.1.1 Eye Blinks

Eye blinks generally create sudden jumps in the signal amplitude in frontal electrodes. Since the kurtosis (the third statistical moment) is highly sensitive to outliers in the amplitude distribution, this measure satisfactorily encapsulates the time period of eye blinks ((Barbati et al., 2004; Delorme et al., 2007). Because the presence of slow drifts in amplitude would impede its sensitivity to sudden jumps, the kurtosis is first calculated within individual trial epochs after subtracting the epoch mean, and subsequently averaged over epochs: such that their average is very low, resulting in a spuriously high value of the spatial average difference (SAD), as indicated in equation (4.3):

$$Temporal\ Kurtosis = \ trim\_and\_mean \left\langle \frac{\langle \mathbf{S_i}\,(t)^4 \rangle_{ep}}{\langle \mathbf{S_i}\,(t)^2 \rangle_{ep}^2} - 3 \right\rangle_{\mathbf{i}} \qquad (4.3)$$

where $S_i(t)$ is the IC time series given by equation (4.2) within the *i*th epoch, the brackets $\langle \dots \rangle_{ep}$ indicate the average within an epoch, and $trim\_and_{mean}\langle \dots \rangle_i$

indicates the average across epochs calculated after removal of up to 1% of the samples. According to (Mognon et al., 2011), this measure is preferable to the simple average because the latter would be too sensitive to bogus outliers.

The spatial topography of blink ICs is described by the SAD, a measure which is particularly sensitive to epochs in which the frontal areas display higher amplitudes than the posterior areas. It is given by equation (4.4):

$$Spatial\ Average\ Difference\ =\ |\langle \boldsymbol{a} \rangle_{\boldsymbol{FA}}| - |\langle \boldsymbol{a} \rangle_{\boldsymbol{PA}}| \qquad (4.4)$$

where $\boldsymbol{a}$ is the vector of IC topography normalised across the scalp, $\langle \dots \rangle_{FA}$ is the average over all channels in the frontal area (FA) and $\langle \boldsymbol{a} \rangle_{PA}$ is the average over all channels in the posterior area (PA) as indicated in Figure 4.2 (Mognon et al., 2011). Two further controls are applied, as follows:

1) In order to distinguish between blinks and horizontal eye movements, the average IC topography weights over the left eye (LE) area must have the same sign as those over the right eye (RE).

2) The variance of scalp weights in the FA must be greater than those in the PA. This control is stated computationally in equation (4.5), which should be positive for eye blink components:

$$Spatial\ Variance\ Difference\ =\ \left(\langle \boldsymbol{a^2} \rangle_{\boldsymbol{FA}} - \langle \boldsymbol{a} \rangle^{\boldsymbol{2}}{}_{\boldsymbol{FA}}\right) - \left(\langle \boldsymbol{a^2} \rangle_{\boldsymbol{PA}} - \langle \boldsymbol{a} \rangle^{\boldsymbol{2}}{}_{\boldsymbol{PA}}\right) \qquad (4.5)$$

This control is essential in avoiding false positives; in cases where the IC weights across the PA encompass both positive and negative values, their average would be extremely low and, hence, the SAD would be spuriously high.

4.3.2.1.2 Vertical Eye Movements

Since vertical eye movements give rise to large amplitude fluctuations in the frontal channels that are generally slower than those produced by blinks, they are not readily identifiable by the kurtosis. They are, however, adequately identified via a temporal characteristic based on the signal variance within each epoch. This maximum epoch variance (MEV) is given by equation (4.6):

$$Maximum\ Epoch\ Variance = \frac{trim\ and \max\left(\langle s_i(t)^2\rangle_{ep} - \langle s_i(t)^2\rangle_{ep}\right)_i}{trim\ and\ mean\left(\langle s_i(t)^2\rangle_{ep} - \langle s_i(t)^2\rangle_{ep}\right)_i} \quad (4.6)$$

where $trim\ and\ max\ (\ldots)_i$ is the maximum value of the trimmed vector of variance within the epochs. As with kurtosis, the MEV is preferable to the simple maximum since the latter would be over-sensitive to bogus outliers. In order to more effectively identify the difference from the baseline behaviour of the time series, the MEV is normalised relative to the average of trimmed variance values, $trim\ and\ mean\ (..)_i$, as in the above description of Temporal Kurtosis (TK). Moreover, the similarity between the spatial distributions of artefacts due to vertical eye movement and blink artefacts means that the SAD is again used and the same additional controls are applied. In Figure 4.3, vertical eye movement artefacts are identified by ADJUST via MEV crossing the threshold, while IC is identified as a blink artefact via SAD and TK crossing the threshold.

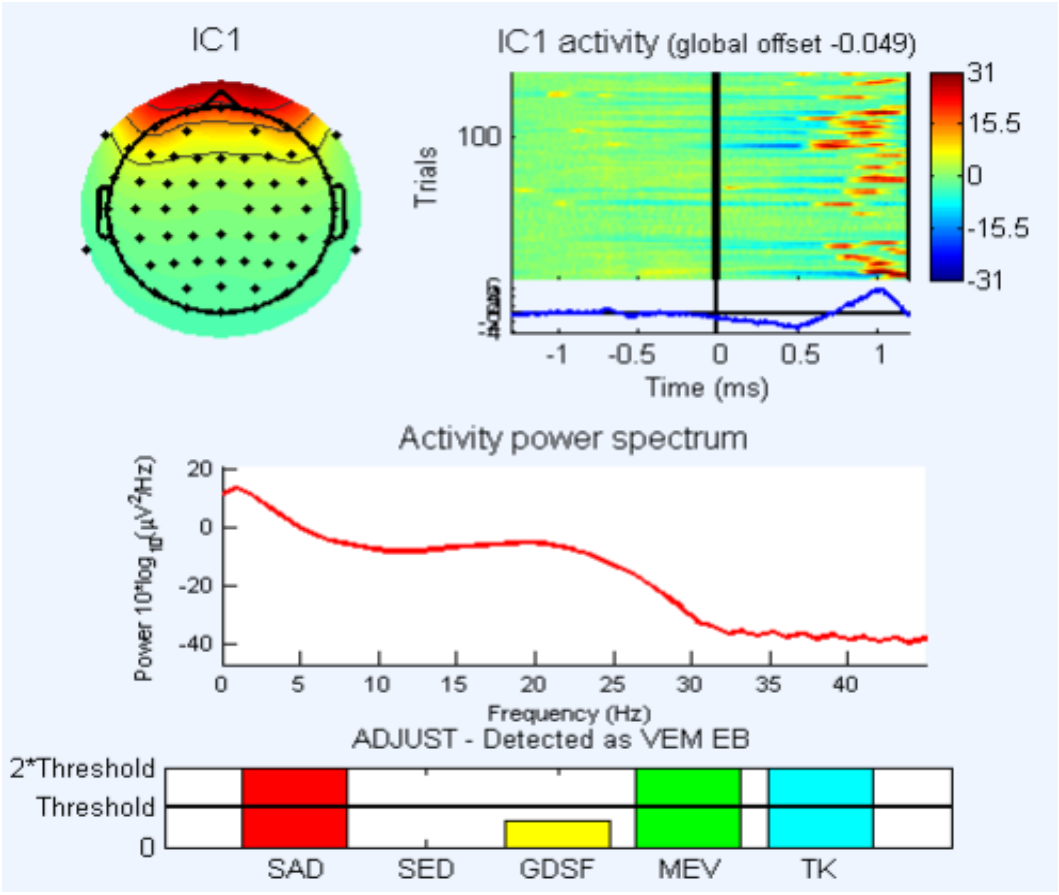

Figure 4.3 Detection of vertical eye movements and eye blinks by ADJUST. The IC were categorized as a vertical eye movement and Eye blinks because of both features associated with SAD, MEV and TK obviously cross threshold (Mognon et al., 2011).

4.3.2.1.3 Horizontal Eye Movements

The time series of artefacts resulting from horizontal eye movement is comparable to that produced by vertical eye movement; hence, the same temporal feature is used, namely the $Maximum\ Epoch\ Variance$ (MEV) in equation (4.6). The spatial distribution is typified by large amplitude signals in the frontal channels close to the eyes, generally in opposite phases (i.e. one positive and one negative). The spatial average difference is sensitive to this pattern and is given by equation (4.7):

$$Spatial\ Average\ Difference = |\langle \mathbf{a} \rangle_{LE}| - |\langle \mathbf{a} \rangle_{RE}| \quad (4.7)$$

where $\langle \dots \rangle_{LE}$ and $\langle \dots \rangle_{RE}$ indicate the average overall channels in the LE and RE areas respectively.

In order to verify that the amplitudes are in opposite phases, the additional control is applied that the average of the IC topographic weights in the LE and RE must differ in sign. In Figure 4.4, artefacts due to horizontal eye movement were identified by ADJUST via SAD and MEV crossing the threshold.

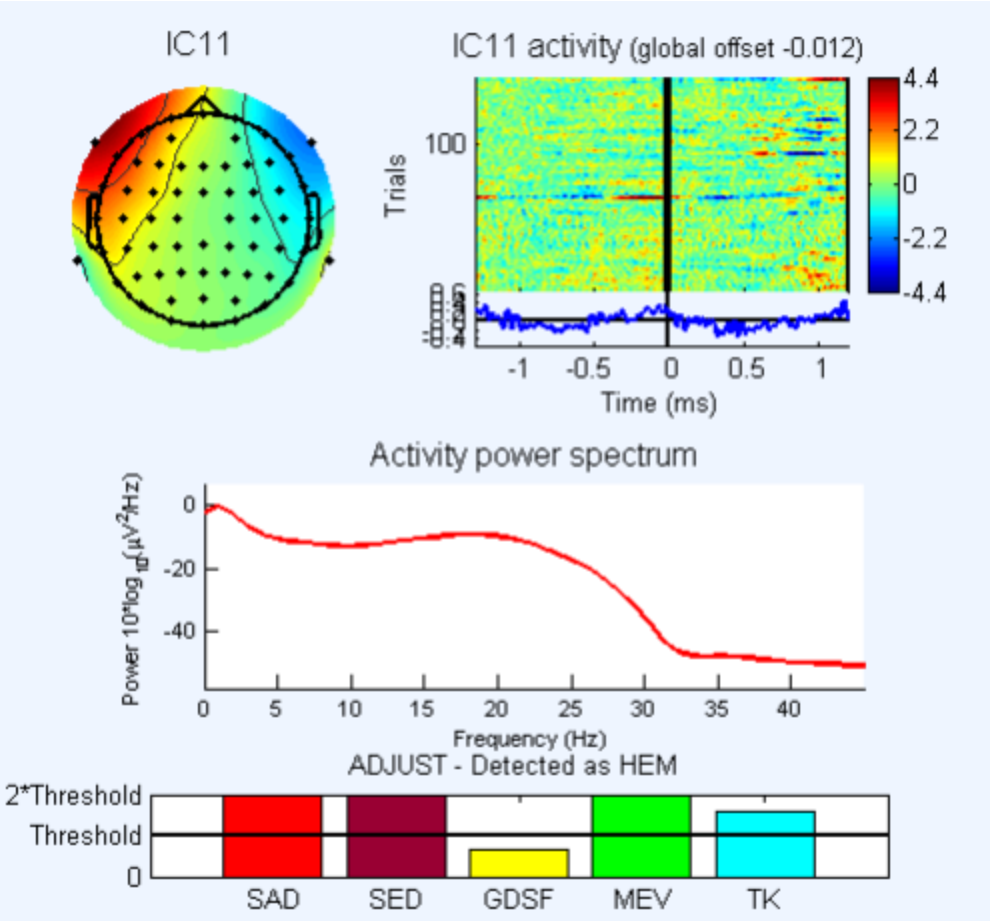

Figure 4.4 Horizontal eye movements detected by ADJUST. The IC were categorized as a horizontal eye movement because both features associated with HEM, SED and MEV obviously cross threshold (Mognon et al., 2011).

4.3.2.1.4 Generic Discontinuities

Variations in impedance or interference from electronic devices generally lead to artefacts characterised by abrupt amplitude variations in one channel, with no spatial bias. The time series of this artefact is encapsulated by $Maximum\ Epoch\ Variance$ (MEV) in equation (4.6), while its spatial distribution is encapsulated by the generic

discontinuities spatial feature in equation (4.8) which is sensitive to local spatial discontinuities:

$$Generic\ Discontinuities\ Spatial\ Feature = \max(\ |\mathbf{a}_n - \langle K_{mn}\mathbf{a}_n \rangle_m|\ )_n \quad (4.8)$$

where $\mathbf{a}_n$ is the nth topography weight, $\max(...)_n$ is the maximum over all channels n of the scalp, and the factor K_{mn} declines exponentially with distance (i.e. $\langle K_{mn} = \exp(-||y_m - y_n||)$, where $||y_m - y_n||$ between channel m and channel n is the average over all channels $m \neq n$).

4.4 Conclusions

ADJUST is state-of-the-art in EEG ERP artefact reduction. It uses some spatial information to identify and reduce artefacts. However, It has been used to produce reasonable spatial heuristics, rather than optimally combining spatial information. ADJUST can greatly reduce some artefacts, and can be used as a pre-processor before more sophisticated artefact reduction.

Chapter 5 PCA Filtering of Auditory Event-Related Potentials

5.1 Introduction

Auditory event-related potentials (ERPs) are contaminated by a variety of artefacts and noises, making it difficult to separate ERPs from other brain signals, biological signals such as muscle (EMG) and eye movements, artefacts due to electrode and equipment movement, and interference from other systems. In measurements from ambulatory EEG (AEEG) systems, the artefacts are often even larger and more frequent than for a static system. However, there is increasing interest in the measurement of ERPs while individuals engage in the physical activities associated with normal living (Bateson et al., 2017).

Typically, individual ERP measurements are too noisy to allow ERPs to be observed. ERP signals may have peaks of several micro-Volts (μV), while noise artefacts can have peaks of tens or hundreds of μV. Often, ERPs from many repeated measurements, on single or multiple individuals, are averaged before clinically important features can be observed. Important features include the positive and negative voltage peaks, often labelled N100, P200, P300 etc. (Luck, 2005). A 20-electrode EEG system provides 19 channels of differential ERP measurement from different standard locations on the scalp (Luck, 2005; Debener et al., 2012). Each electrode measures the same brain reaction, but filtered due to the electrode position and the intervening tissue, plus noise. A method is introduced that allows averaging across channels. Although each channel sees a different view of the ERP response, a priori knowledge of the signal correlations allows the channels to be combined to yield the best estimate of the underlying ERP.

Principal Component Analysis (PCA) has been applied to ERP signals before. PCA was used for reducing ocular artefacts in ERP signal by subtracting the principal component related to eye artefacts such as eye-blinks, horizontal eye movements and vertical eye movements from raw EEG data (Costa et al., 2014; Casarotto et al., 2004). The Electrooculogram (EOG) signal is a large noise artefact in measured EEG data and for frontal electrodes has an amplitude much larger than brain signals. Reducing the EOG component of the measured EEG signal is vital when observing ERPs. The Casarotto et al. PCA method yielded efficient and effective reduction of EOG artefacts (Casarotto et al., 2004). Similarly, Kobayashi and Kuriki employed PCA to increase the signal-to-noise ratio (SNR) in evoked neuromagnetic signals applied to subjects. Using simulated evoked fields they demonstrated SNR improvement compared to the common averaging method (Kobayashi & Kuriki, 1999).

Kalman filtering was developed by Kalman in 1960 for parameter estimation and has been widely applied to parameter tracking applications in many fields. It yields the maximum likelihood estimator given a priori and posteriori estimates of parameter vectors, (Kalman, 1960). Kalman Filters (KF) have been applied to EEG time series. Kalman Smoothing has been applied to EEG signals to identify spikes associated with psychological diseases, (Oikonomou et al., 2009). Oikonomou found that there is a significant enhancement in EEG SNR when using time-varying coefficients for an autoregressive model signal, estimated using Kalman filtering (Oikonomou et al., 2007).

In this chapter, PCA bases are calculated in two different seniarios:

1. PCA basis for each channel of ERP signal;
2. PCA basis for all channels of ERP signal concatenated.

The chapter begins by introducing a method to produce synthetic multi-channel ERP signals in section 5.2. These synthetic signals are used to quantify the performance of the proposed ERP estimation method. Section 5.3 describes the calculation of PCA bases for each channel ERP signal and the calculation of the covariance of channel PCA basis weights. The projection of ERP signals onto PCA bases, and the filtering it provides, are described in Section 5.3.1. Section 5.3.2 introduces Kalman filtering to provide the optimal combination of PCA filtered channel ERPs and the a priori expected multi-channel ERP. Finally, Sections5.3.3 test the algorithms with synthetic signals and noises and this is followed by a discussion section.

Then we have introducing same a method to produce synthetic multi-channel ERP signals in section 5.2. These synthetic signals are used to quantify the performance of the proposed ERP estimation method. Section 5.4.1 describes the calculation of PCA bases for all channel ERP signal and the calculation of the covariance of all channel PCA basis weights. The projection of ERP signals onto PCA bases, and the filtering it provides, is described in Section 5.4.1. Section 5.4.2 introduces Kalman filtering to provide the optimal combination of PCA filtered channel ERPs and the a priori expected multi-channel ERP. Sections 5.4.3 test the algorithms with synthetic signals and noise. Finally, consideration is given to the combining of results from many trials to estimate the underlying ERP.

5.2 Multi-Channel ERP Simulation

When the brain responds to a stimulus, electrical signals move around the part of the brain involved in processing that stimulus. This could be modelled as a movement of charge or the movement, rotation and evolution in strength, of one or more electrical dipoles. Electrodes attached to the scalp measure the electric potential on the surface due to this brain activity. The multi-channel simulator assumes that all channels

measure the same underlying brain process, but filtered by the bone and tissue between the activity and the electrode on the scalp. Therefore, many features of the ERP response will be consistent across channels. For example, the P300 response is assumed to be measured at the same time on all channels. Similarly, the response amplitude is assumed to vary proportionately across all channels. It is the resulting correlation across channels that will be exploited in the proposed algorithm introduced below.

The ERP signal on each channel is approximated by a sum of Gaussian pulses:

$$E_i(t) = \sum_{j=1}^{N_G} A_{ij} f(t; t_j, \sigma_j) \tag{5.1a}$$

$$\text{where } f(t; t_j, \sigma_j) = exp\left(-\frac{1}{2\sigma_j^2}(t - t_j)^2\right) \tag{5.1b}$$

E_i is the pure ERP signal measured on the *i*th channel, for a particular trial. For this project, three pulses were used i.e. $N_G = 3$; corresponding to the N100, P200 and P300 responses. The three parameters for each pulse : A_{ij}, t_j, and σ_j; specify the amplitude, centre time and width of each of the Gaussian pulses respectively. For each trial, these parameters are determined from six independent samples from a Standard Normal distribution: $z_k \leftarrow N(0,1), k = 1, \cdots, 6$.

$$A_{ij} \leftarrow \bar{A}_{ij} \times (1 + 0.1 z_j)\,, j=1,2,3 \tag{5.2a}$$

$$t_j \leftarrow \bar{t}_j + 10 z_{j+3}\,, j=1,2,3 \tag{5.2b}$$

The 2D array $\bar{A}_{ij}$ is preset with amplitudes that reflect the spatial-channel dependence of the responses. Each of the N100, P200 and P300 response amplitudes are assumed to vary independently, from trial to trial and from each other. However, for any trial, the amplitudes are consistent across channels. Similarly, the response peak times are assumed to vary independently but are the same for all channels. The mean peak times are: $\bar{t}_j = \{100,200,350\}\, ms$ and the peak widths are $\sigma_j =$

$\{50,30,75\}\,ms$. These parameters have been chosen to match the ERP responses in (Luck, 2005; Debener et al., 2012) . For 3 Gaussians and 19 differential measurements, the mean peak amplitude array used is:

$$\bar{A}_{ij} = \begin{bmatrix} 18 & 17 & 53 & 85 & 110 & 90 & 55 & 85 & 170 & 190 & 180 & 60 \\ 18 & 17 & 53 & 85 & 110 & 90 & 55 & 85 & 170 & 210 & 180 & 60 \\ 30 & 40 & 53 & 85 & 160 & 130 & 55 & 85 & 190 & 220 & 180 & 60 \end{bmatrix} \cdots$$

$$\begin{bmatrix} 54 & 160 & 100 & 95 & 52 & 12 & 11 \\ 54 & 160 & 120 & 95 & 52 & 12 & 11 \\ 54 & 160 & 200 & 155 & 52 & 20 & 18 \end{bmatrix} \times 10^{-2}\,\mu V$$

Figure 5.1 illustrates a typical synthetic multi-channel ERP response.

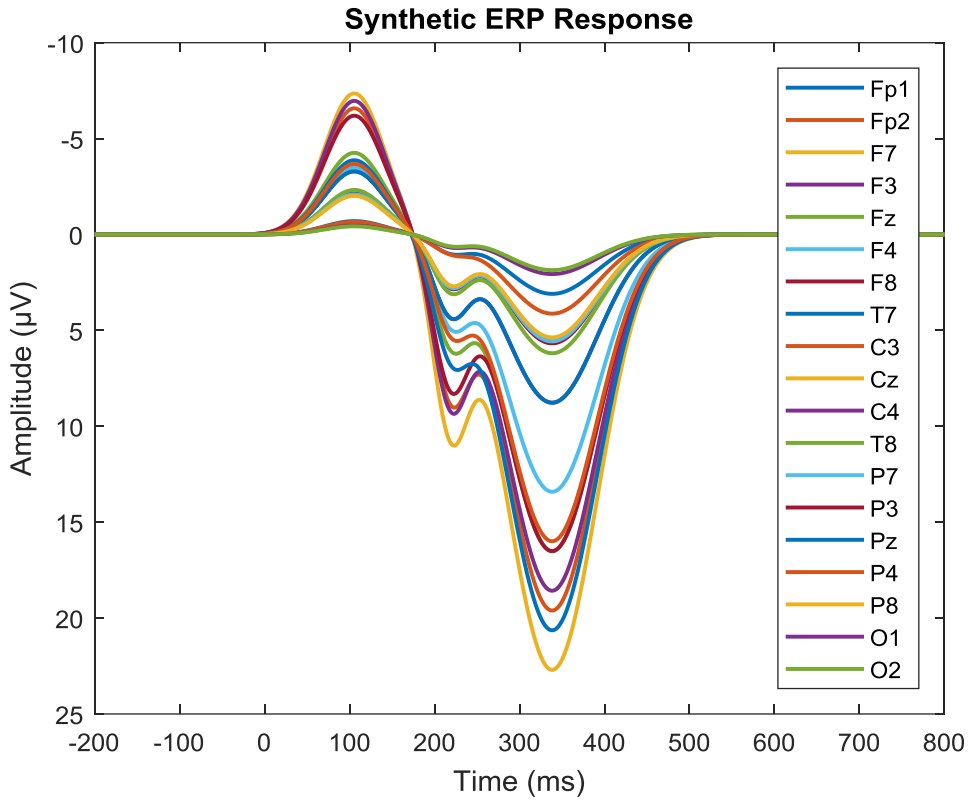

Figure 5.1 Synthetic ERP Signal for 19 channels. Three parameters for N100, P200 and P300 specify the amplitude, centre time and width of each of the Gaussian pulses respectively for 19 channels across the head.

5.3 PCA basis for each Channel of ERP Signal.

The PCA basis is calculated from ERP trial data for each channel. Each channel ERP signal can then be expressed as a weighted sum of PCA basis signals. Finally, the covariance of channel PCA basis weights is calculated. In this section, the multichannel ERP simulator is used to test the use of PCA data to filter noisy ERP data.

5.3.1 Principal Component Basis for Individual Channels

An ERP measurement on a single channel yields a discrete voltage time series $\mathbf{E} \in \mathrm{R}^{N_s}$, of N_s samples. If a set of N_t ERP measurements is available, then an uncentred covariance matrix $\mathbf{C} \in \mathrm{R}^{N_s \times N_s}$ may be estimated. This matrix provides information on the joint probabilities of sample values. The Eigenvectors of the covariance matrix are the principal component (PCA) basis signals. The Eigenvalues indicate how much of the variation between signals comes from components along PCA basis directions. Typically, the first few PCA basis signals span a large majority of the variation in the ERP responses. Later basis signals span the noise. Projecting the ERP signal on the subspace spanned by the first few PCA basis signals will keep many of the features of the ERP signal while greatly reducing the noise. Let $\mathbf{B} \in \mathrm{R}^{N_s \times N_b}$ be a matrix whose N_b columns are the first N_b PCA basis vectors of length N_s samples, for a particular channel. The first PCA basis vector is the mean ERP signal: $\bar{\mathbf{E}}$. Projecting the measurement vector onto the subspace spanned by the PCA basis vectors to get a vector of PCA basis weights $\mathbf{A} \in \mathrm{R}^{N_b}$ can be written in matrix notation as:

$$\mathbf{A} = \mathbf{B^t E} \tag{5.3}$$

and the projected signal is:

$$\mathbf{E}_{pca} = \mathbf{BA} = \mathbf{BB^t E}. \tag{5.4}$$

When the PCA weights are to be filtered, then a diagonal filter matrix $\mathbf{F} \in \mathrm{R}^{N_b \times N_b}$ may be introduced: $\mathbf{F} \equiv diag(f_i)$. The filter weights can be chosen to yield a smooth truncation to avoid Gibbs ringing e.g. $f_i = exp\left(-\left(i - T_{pca}\right)^2/2\right)$ where T_{pca} is the truncation basis number. The PCA filtered ERP signal may be written:

$$\mathbf{E}_{\mathbf{pca}}^{\mathbf{f}} = \mathbf{BFA} = \mathbf{BFB^t E}. \tag{5.5}$$

If $\mathbf{E} \in \mathrm{R}^{N_s \times N_t}$ is a matrix whose N_t columns are ERP measures from N_t trials, then (6.5) yields $\mathbf{E}_{\mathbf{pca}}^{\mathbf{f}} \in \mathrm{R}^{N_s \times N_t}$: a matrix of the results after PCA filtering of each trial ERP measurement. A weighted mean of ERP measurements may be calculated by introducing a weight vector $\mathbf{W} \in \mathrm{R}^{N_t}$ where: $\mathbf{W} \equiv (w_i)$. The weighted mean ERP measurement may be written: $\bar{\mathbf{E}} = \mathbf{EW}$, and the PCA filtered mean measurement is:

$$\bar{\mathbf{E}}_{\mathbf{pca}}^{\mathbf{f}} = \mathbf{BF}\bar{\mathbf{A}} = \mathbf{BFB^t EW}. \tag{5.6}$$

Due to the associative property of matrix multiplication, $\mathbf{BFB^t(EW)} = \mathbf{(BFB^t E)W}$, and so the weighted mean of the PCA filtered ERP responses is the same as the PCA filtered weighted mean ERP response.

Figure 5.2 illustrates the first 5 basis functions for the Fz channel, derived using ERP trial data produced using the multichannel simulator with additive white Gaussian noise.

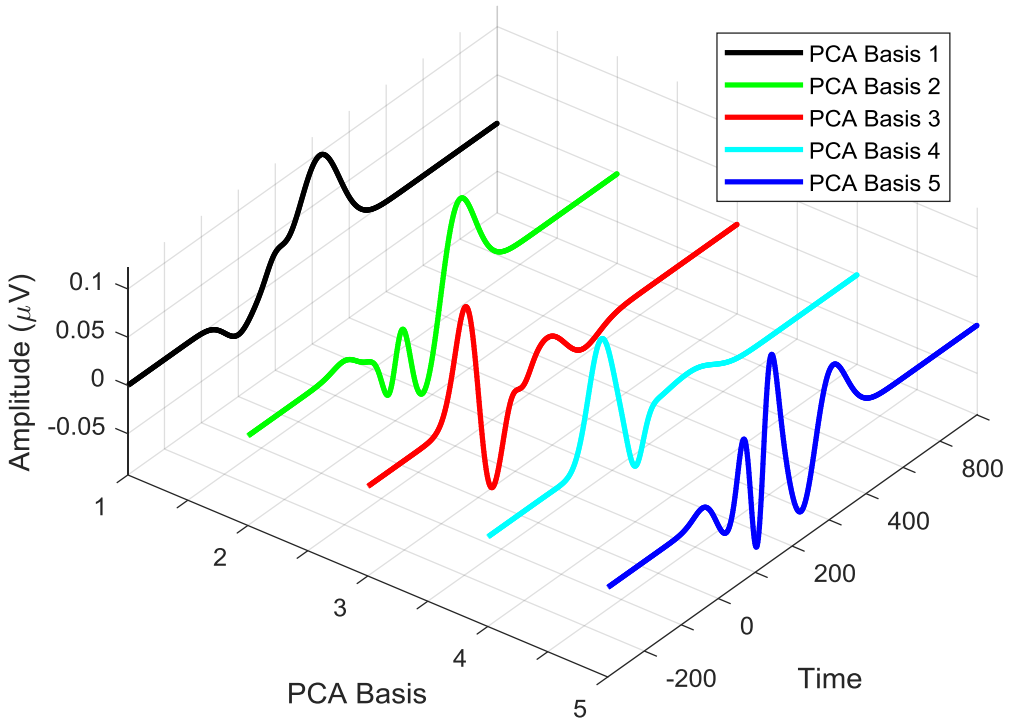

Figure 5.2 Principal Component Basis for channel Fz, derived using ERP trial data produced using the multichannel simulator with additive white Gaussian noise.

5.3.1.1 Multi-Channel Information

Using the multi-channel ERP simulator introduced in Section 5.2, PCA bases can be calculated for each channel using the methods described in Section 5.3.1. As the underlying ERP signals have so much in common, the PCA bases and PCA projection weights $\mathbf{A}$ will also have similarities. For a given trial j, the PCA projection weights for each channel i can be collected into a vector: $\mathbf{X}_j \equiv \left(\mathbf{A}_{ij}\right)$, where $\mathbf{A}_{ij}$ is the vector of N_b PCA basis weights for channel i in trial j. The vector $\mathbf{X}_j \in \mathrm{R}^{N_c N_b \times 1}$, where N_c is the number of channels. The collection of $\mathbf{X}$ vectors for the N_t trials allows a mean and covariance matrix to be estimated:

$$\bar{\mathbf{X}} = \mathrm{mean}\left(\{\mathbf{X}_j\}, j = 1, \cdots N_t\right) \tag{5.7}$$

$$\mathbf{C_X} = \mathrm{cov}\left(\{\mathbf{X}_j\}, j = 1, \cdots N_t\right) \tag{5.8}$$

The covariance matrix encapsulates all knowledge of the correlation between ERP components on all channels. The mean state vector is our a priori best estimate of the multi-channel ERP PCA basis weight vector.

5.3.2 ERP Estimation

This section follows the conventional notation of Kalman Filtering, applied to an individual PCA filtered ERP measurement i.e. an individual subject and trial. All the channels, as described by the state vector **X**, are estimated at the same time using an algorithm we call PCAKF. The estimation forms an optimal weighted sum of two sources of information: the a priori **X** and the measured **X**.

A priori, an ERP state vector is a sample from the multi-dimensional Normal distribution with mean $\overline{\mathbf{X}}$ and covariance $\mathbf{C_X}$. In the absence of any further information, the maximum likelihood estimate of the ERP signal is that given by the mean vector $\overline{\mathbf{X}}$. In terms of Kalman Filters the $\overline{\mathbf{X}}$ and $\mathbf{C_X}$ correspond to $\mathbf{X}_{k/k-1}$ and $\mathbf{P}_{k/k-1}$.

Given an ERP measurement on all channels, for a given subject and trial, a measured vector $\hat{\mathbf{X}}_j$ can be calculated using the processes in Section 5.3. The measurement has an uncertainty covariance matrix $\mathbf{R}_j$ that is estimated from the difference between the filtered PCA estimate and the measurements, see Section 5.3.2.1. Given the a priori knowledge of ERP and the information provided by the measurement process, an estimate of the particular ERP for this subject and trial $\mathbf{X}_j$, can be calculated by solving (5.9) for **K** and then using (5.10):

$$\mathbf{K}\left(\mathbf{C_X} - \mathbf{R}_j\right) = \mathbf{C_X}, \tag{5.9}$$

$$\mathbf{X_j} = \hat{\mathbf{X}}_\mathbf{j} + \mathbf{K}\left(\mathbf{X}_j - \bar{\mathbf{X}}\right) = \mathbf{C_X} \tag{5.10}$$

5.3.2.1 Estimation of Measurement Uncertainty

In order to implement Kalman Filtering, it is necessary to develop an estimate of the PCA filtered measurement uncertainty in a single ERP measurement. If $\mathbf{A^f_{pca}} = \mathbf{FB^tE}$ are the filtered PCA measurement weights, then we need to estimate the measurement uncertainty matrix $\mathbf{C_A} \in \mathrm{R}^{N_b \times N_b}$ such that the probability density function for the actual ERP PCA weight vector, given the measurement, is multi-variate Normal with mean $\mathbf{A^f_{pca}}$ and covariance $\mathbf{C^f_A}$. It will be assumed that the noise in the ERP measurement is uniformly distributed across the unfiltered PCA basis weights, assuming a full PCA basis of rank N_s . Let n_i^2 be the noise power or variance in the *i*th PCA weight. Then, by Parseval's Theorem:

$$N^2 = \sum_{i=1}^{N_s} n_i^2 \tag{5.11}$$

where N^2 is the noise power in the measured ERP signal. This can be estimated by assuming the noise is close to the difference between the measured ERP signal and the PCA filtered signal:

$$N^2 \approx \left\|\mathbf{E^f_{pca}} - \mathbf{E}\right\|^2. \tag{5.12}$$

Given (6.11) and the assumption of uniform distribution of noise, then for all *i*:

$$n_i^2 = \frac{N^2}{N_s} \approx \frac{\left\|\mathbf{E^f_{pca}} - \mathbf{E}\right\|^2}{N_s}. \tag{5.13}$$

The covariance in the unfiltered PCA weights is then:

$$\mathbf{C_A} = n_i^2 \mathbf{I}_{N_b}. \tag{5.14}$$

where $\mathbf{I}_{N_b}$ is the identity matrix of rank N_b , and the covariance of the PCA filtered ERP is:

$$\mathbf{C}_{\mathbf{A}}^{\mathbf{f}} = n_i^2 diag(w_i^2). \quad (5.15)$$

The multi-channel uncertainty matrix $\mathbf{R}_j$ that is the block diagonal matrix formed from the individual channel uncertainty matrices i.e. $\mathbf{R}_j = \text{diag}\left(\mathbf{C}_{\mathbf{A}_1}^{\mathbf{f}}, \mathbf{C}_{\mathbf{A}_2}^{\mathbf{f}} \ldots \mathbf{C}_{\mathbf{A}_{N_c}}^{\mathbf{f}}\right)$

5.3.3 SNR Performance for Individual Channels

A simulated 20 channel AEEG system, with a 1 kHz sample rate, has been used to test the performance of the PCA and PCAKF filters. The channel PCA bases, mean PCA weights vector $\bar{\mathbf{X}}$ and weights covariance matrix $\mathbf{C}_{\mathbf{X}}$ were calculated using 100 simulated multichannel ERP signals. Each channel signal is sampled from 200 ms before the stimulus to 800 ms after. In Monte Carlo tests, synthetic noise was added to the synthetic signals to simulate 100 ERP measurement trials for a range of noise scenarios. The ERP signal and synthetic noise were different for every trial. Three noise scenarios have been tested: additive white Gaussian noise (AWGN), additive pink Gaussian noise (APGN), and AWGN noise with amplitude varying with channel. All noise was band limited to a maximum frequency of 15 Hz before SNR calculations. Signal and noise powers were defined to be the mean square amplitude of the 1000 sample signal sequences.

Figure 5.3 illustrates a single channel with band limited AWGN with an initial SNR=0 dB. The black curve is the synthetic ERP signal produced by the multi-channel simulator, and for these tests can be taken as the true, noise-free ERP signal. The red curve is the measured signal including synthetic noise. PCA filtering reduces the noise in the signal by removing PCA components that are largely noise. In this example the PCA components are smoothly truncated around the 10th basis signal using Gaussian weights. This signal is further combined with the expected signal using a Kalman Factor to yield the green curve. Although only one channel is illustrated, the algorithm

mixes information from all channels. All channels had the same initial SNR although, as the channel ERP signals have different amplitudes, the noise amplitudes will also change between channels. Figure 5.4 shows the SNR improvement with filtering, starting from a range of initial SNRs. PCA filtering (solid lines) yields about a 10 dB SNR improvement just by rejecting components that are predominantly noise. PCAKF (dashed lines) yields a further improvement of about 7 dB for relatively clean signals and the improvement grows linearly for noisy signals where the measured signal is largely disregarded and the a priori expected signal is returned as the most likely response. Note that some of the noise reduction comes from the projection method forcing the ERP signal to be zero before the stimulus and after the expected ERP response. A shorter time span, say from -100 ms to 500 ms, would yield a smaller SNR improvement.

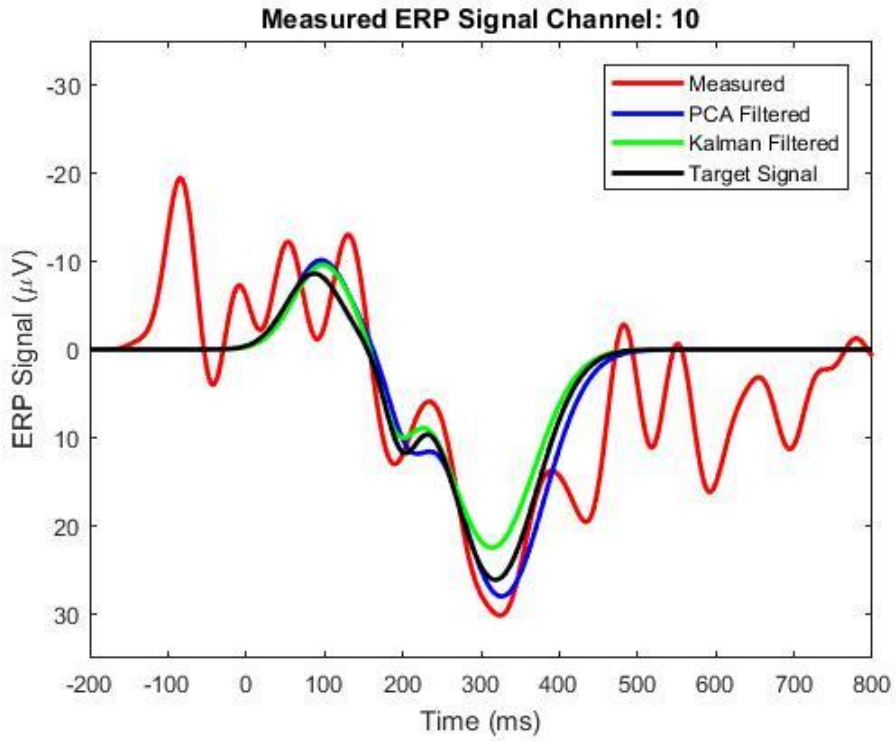

Figure 5.3 Measured, filtered and true channel 10 ERP signal for band limited AWGN, SNR=0 dB. The black curve is the synthetic ERP signal produced by the multi-channel simulator, and for these tests can be taken as the true, noise-free ERP signal. The red curve

is the measured signal including synthetic white noise. PCA filtering reduces the noise in the signal by removing PCA components that are largely noise. This signal is further combined with the expected signal using a Kalman Factor to yield the green curve.

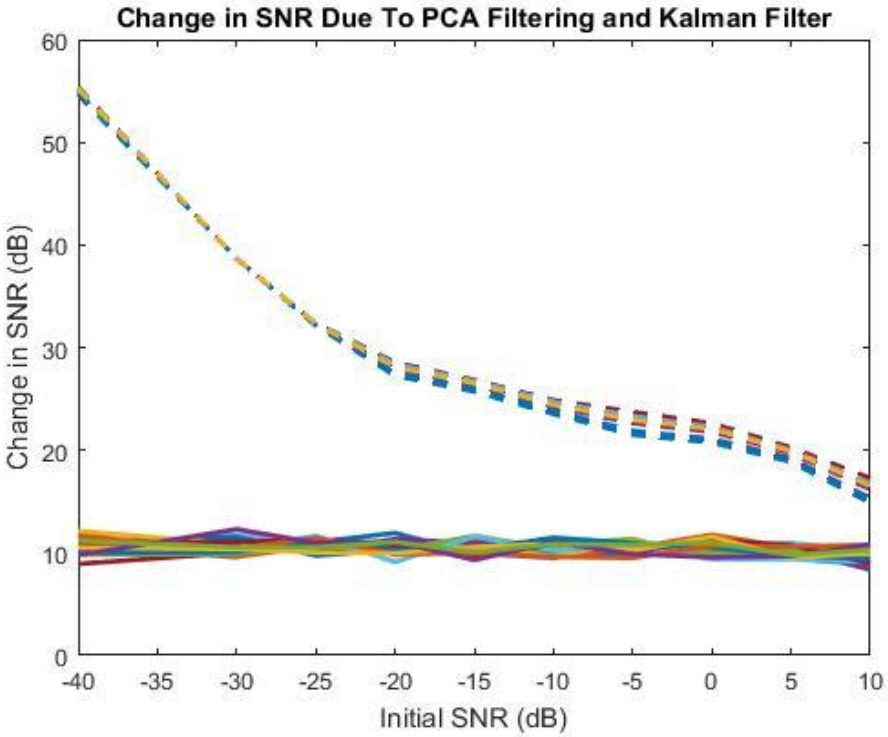

Figure 5.4 Change in SNR Due to PCA and Kalman Filtering for AWGN, for all channels. The SNR improvement with filtering, starting from a range of initial SNRs. PCA filtering (solid lines) yields about a 10 dB SNR improvement just by rejecting components that are predominantly noise. PCAKF (dashed lines) yields a further improvement of about 7 dB.

Figure 5.5 illustrates the results for the same experiment but using pink noise across all channels. Pink noise is much more challenging as it has more power at the lower frequencies, which overlap more with the expected ERP signal. However, both PCA projection and Kalman filtering offer similar SNR improvements as with AWGN.

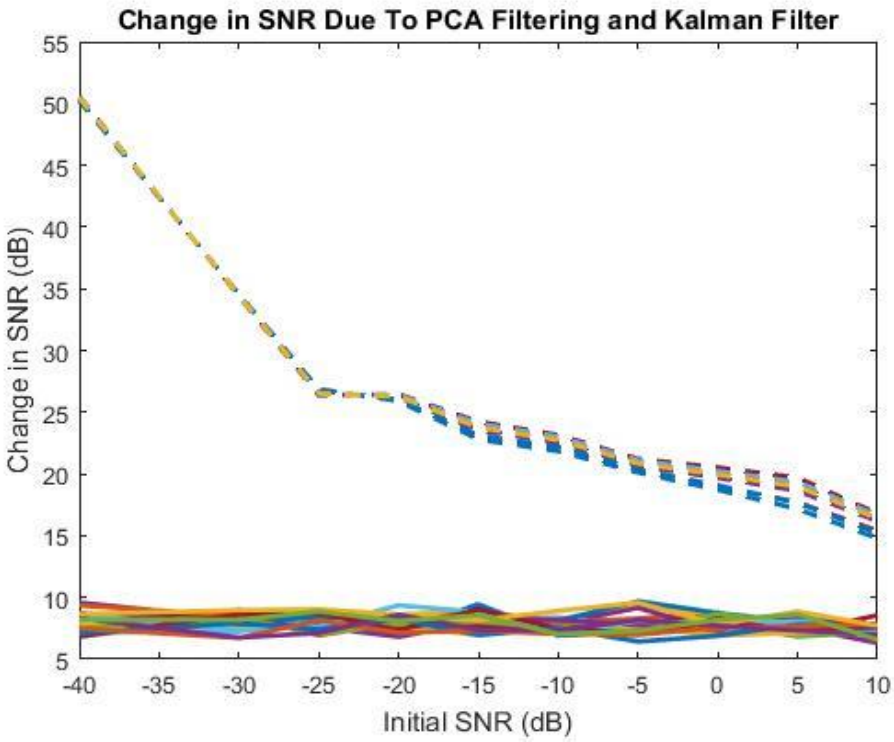

Figure 5.5 Change in SNR Due to PCA and Kalman Filtering for APGN. The SNR improvement with filtering, starting from a range of initial SNRs with APGN. PCA filtering and PCAKF (dashed lines) yields an improvement offer similar SNR improvements as with AWGN.

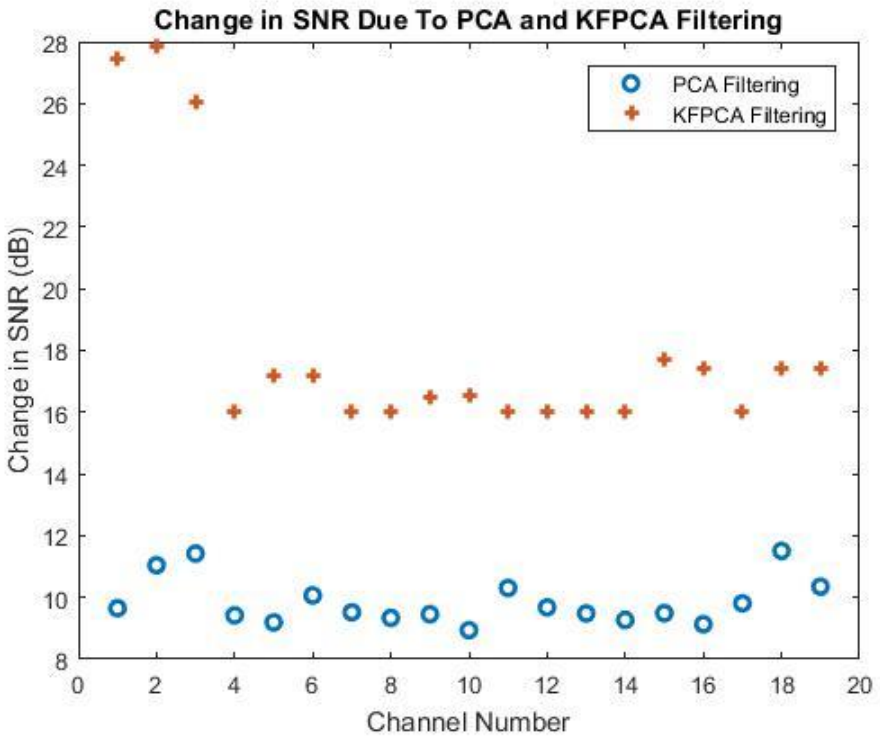

Figure 5.6 Change in SNR Due To PCA and Kalman Filtering where channels 1, 2 and 3 have an initial SNR=0 while the other channels have an SNR=10. PCA filtering yields the same SNR improvement on all channels as the same noise amplitude exists in all the PCA bases. However, Kalman Filtering uses the cross-channel information and yields much higher SNR improvement in the three noisy channels.

Finally we consider the case where the initial SNR is not the same across all channels. This is typically the situation where noise is due to electrode connection problems, electrode movement or for biological signals such as eye-blink artefacts. Eye-blinks, in particular, affect the channels at the front of the head much more strongly than those further back. PCAKF filtering has the large advantage of utilizing expected correlations between all channel signals. Noisy channels are identified as part of the algorithm and the filtered signals on these channels are guided by the signals measured on the less noisy channels. This is illustrated in an example where channels 1, 2 and 3 (Fp1, Fp2 and F7) have initial SNR=0 dB while the other channels have SNR=10 dB. For this test, AWGN was used. PCA filtering yields the same SNR improvement on all channels as the same noise amplitude exists in all the PCA bases. However,

Kalman Filtering uses the cross-channel information and yields much higher SNR improvement in the three noisy channels. In effect the algorithm reconstructs the signals on these channels from the more reliable information measured on the relatively clean channels.

5.3.4 Discussion

There are many methods applied to treat EEG signal from noise and separating signal from artefacts. Principal component analysis (PCA), independent component analysis applied in many biological signals for instant ECG and EMG (ICA) were used in many application of EEG signal. Many ECG applications are revised where PCA procedures have been efficaciously employed for the detection of some abnormality of heart function and heart diseases such as atrial fibrillation, myocardial ischemia and abnormalities in ventricular depolarization. (Castells et al., 2007). PCA were applied successfully for ECG Modelling and QRS Detection (Chawla et al., 2006). PCA were applied in ECG and validated SNR improvements so it has been decided to apply that in ERP measurement to EEG signal. The success of PCA in ECG signal lead us to applied PCA in EEG signal as well.

This chapter presents a synthetic multichannel ERP simulator. The simulator has been used to demonstrate the SNR improvements produced by two denoising filter processes. Initially, PCA bases are calculated for each channel. In practice this would be done using a set of clean ERP signals derived from averages over many trials from many individuals. We have used synthetic ERP signals as these allow SNR improvements to be calculated. PCA filtering reduces artefact noise by projecting measured ERP signals onto low dimensional subspaces spanned by the first 10 principal component signals in each channel. A smooth truncation was used to reduce Gibbs ringing. In these tests, PCA projection increased SNR by about 10 dB for both

white and pink Gaussian noise. In a second stage, the PCA projection weights were optimally combined with a priori weights using knowledge of the estimation uncertainty, the expected covariance of weights and a Kalman factor. In effect, this uses information from all channels to reduce noise in each channel. The method was demonstrated in a scenario where three channels initially had 10 dB more noise than the others, to simulate eye-blink artefacts. After PCAKF filtering, all channels had near the almost SNR. This method provides a new way to interpolate missing channels that is much more sophisticated than methods based on weighted sums of adjacent channels. We propose to use PCAKF filtering on real data as a preprocessor, before combining trial outputs in a statistically optimised way to estimate ERP signals in the minimum number of trials.

5.4 PCA basis for all channels of ERP signal

The previous method calculated a PCA basis for each channel independently. This resulted in a state vector with $N_c N_b$ elements. The matrices that needed to be solved during KF were square and of this size. Here an alternative, more computationally efficient method is presented. The channel time series are concatenated to yield a long measurement vector of length $N_c N_s$. A single PCA basis is calculated for the trial long measurement vectors. The number of significant basis vectors is much less than the $N_c N_b$ required in the previous method. As matrix manipulations often require $O\left(n^3\right)$ calculations, large computational savings are made during KF. In the development that follows, many of the equations and symbols are unchanged, but need to be interpreted given the new definition of measurement vector. In particular, the number of basis vectors, N_b, will be larger as the basis vectors now span all the channel measurements.

5.4.1 Principal Component Basis for ERP Measurements for all Channels

As previously, an ERP measurement on a single channel, for the kth trial, yields a discrete voltage time series $\mathbf{E}_{ik} \in \mathrm{R}^{N_s}$, of N_s samples. The measurement vector $\mathbf{E}_k \in \mathrm{R}^{N_c N_s \times 1}$ from the kth trial can be formed from stacking the ERP measurements from N_c channels. If a set of N_t ERP measurement vectors is available, then a mean vector and uncentred covariance matrix $\mathrm{C}_{\mathrm{E}} \in \mathrm{R}^{N_c N_s \times N_c N_s}$ may be estimated:

$$\bar{\mathbf{E}} = \mathrm{mean}(\{\mathbf{E}_k\}, \boldsymbol{k} = \mathbf{1}, \cdots \boldsymbol{N_t}) \tag{5.16}$$

$$\mathbf{C}_{\mathbf{E}} = \mathrm{cov}(\{\mathbf{E}_k\}, \boldsymbol{k} = \mathbf{1}, \cdots \boldsymbol{N_t}) \tag{5.17}$$

As before, the covariance matrix encapsulates all knowledge of the correlation between ERP samples on all channels. The mean state vector is our a priori best estimate of the multi-channel ERP measurement vector.

The PCA basis may be calculated from the covariance matrix of the concatenated channel measurement vectors. Let $\mathbf{B} \in \mathrm{R}^{N_c N_s \times N_b}$ be a matrix whose N_b columns are the first N_b PCA basis vectors of length $N_c N_s$ samples. The first PCA basis vector is the mean ERP signal: $\bar{\mathbf{E}}$. Projecting the measurement vector $\mathbf{E}_k$ onto the subspace spanned by the PCA basis vectors to get a vector of PCA basis weights $\mathrm{X}_{\boldsymbol{k}} \in \mathrm{R}^{N_b}$ can be written in matrix notation as:

$$\mathbf{X}_{\boldsymbol{k}} = \mathbf{B}^{\mathbf{t}}\mathbf{E}_{\boldsymbol{k}} \tag{5.18}$$

and the projected signal is:

$$\mathbf{E}_{\boldsymbol{pca}} = \mathbf{B}\mathbf{X}_{\boldsymbol{k}} = \mathbf{B}\mathbf{B}^{\mathbf{t}}\mathbf{E}_{\boldsymbol{k}}. \tag{5.19}$$

Given a diagonal filter matrix $\in \mathrm{R}^{N_b \times N_b}$, the PCA filtered ERP signal may be written:

$$\mathbf{E}^{\mathbf{f}}_{\mathbf{pca}} = \mathbf{B}\mathbf{F}\mathbf{X}_{\boldsymbol{k}} = \mathbf{B}\mathbf{F}\mathbf{B}^{\mathbf{t}}\mathbf{E}_{\boldsymbol{k}}. \tag{5.20}$$

As the expressions have the same form as previously, the weighted mean of the PCA filtered ERP response vectors is the same as the PCA filtered weighted mean ERP response.

Figure 5.7 illustrates the beginning of the first five PCA basis vectors. Only the part of each basis vector spanning the first two measurement channels is shown. These basis vectors continue to span all 19 simulated channels.

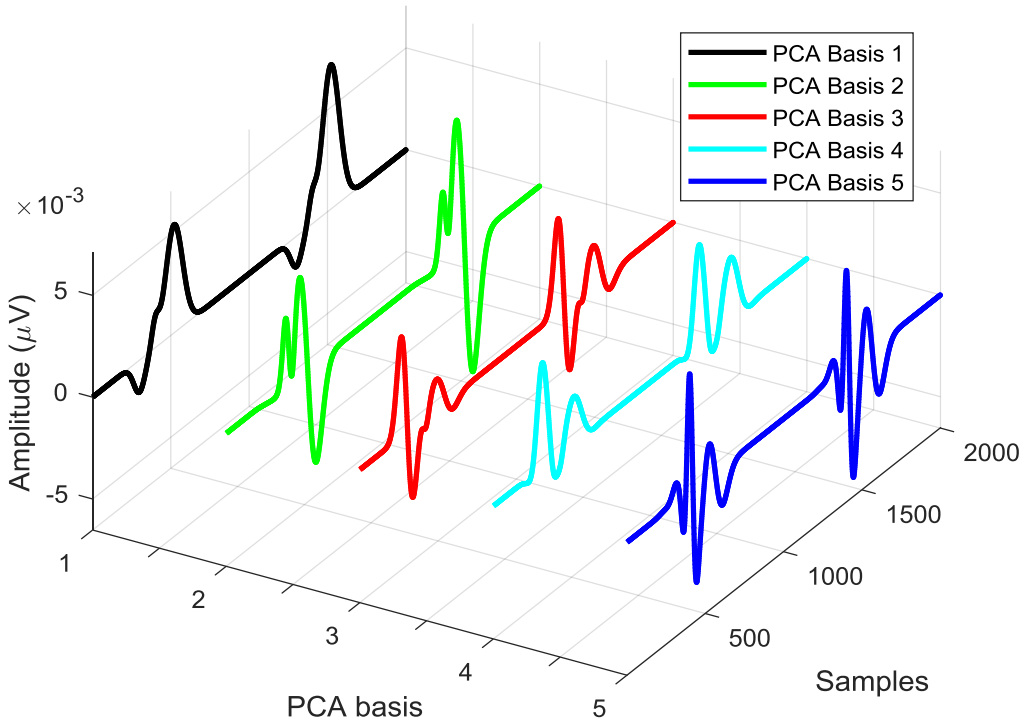

Figure 5.7 Sections of Principal Component Basis for first two channels of five PCA basis vectors. These basis vectors continue to span all 19 simulated channels.

5.4.1.1 Multi-Channel Information

As in 5.3.1.1, cross channel information is captured in the covariance of the filtered PCA weights. For a given trial *k*, the filtered PCA projection weights can be calculated using:

$$\mathbf{X}_k = \mathbf{F}\mathbf{B}^{\mathbf{t}}\mathbf{E}_k \tag{5.22}$$

Given a set of N_t ERP PCA projected and filtered weights, then a mean vector $\bar{\mathbf{X}} \in \mathrm{R}^{N_b \times 1}$ and uncentred covariance matrix $\mathrm{C_X} \in \mathrm{R}^{N_b \times N_b}$ may be estimated:

$$\bar{\mathbf{X}} = \mathrm{mean}(\{\mathbf{X}_k\}, \boldsymbol{k} = \mathbf{1}, \cdots \boldsymbol{N_t}) \tag{5.23}$$

$$\mathbf{C_X} = \mathrm{cov}(\{\mathbf{X}_k\}, \boldsymbol{k} = \mathbf{1}, \cdots \boldsymbol{N_t}) \tag{5.24}$$

5.4.2 PCAKF Applied to Multichannel measurement Vectors

The mathematical expressions for PCA filtering and Kalman Filter estimation of the measured, multichannel ERP signal, are identical to those in the previous section 5.3.2. However, the projection weights vector is now of length N_b rather than $\mathrm{N}_c \times \mathrm{N}_b$, and the associated covariance and uncertainty matrices are of associated dimension.

5.4.2.1 Estimation of Measurement Uncertainty

We need to estimate the measurement uncertainty matrix $\mathbf{R}_k \in \mathrm{R}^{N_b \times N_b}$ such that the probability density function for the actual ERP PCA weight vector, given the measurement, is multi-variate Normal with mean $\mathbf{X}^{\mathbf{f}}_{\mathbf{pca}}$ and covariance $\mathbf{R}_k$. It will be assumed that the noise in the ERP measurement is uniformly distributed across the unfiltered PCA basis weights, and a full PCA basis of rank $N_c \times N_s$. Let n_i^2 be the noise power or variance in the *i*th PCA weight. Then, by Parseval's Theorem:

$$\boldsymbol{N^2} = \sum_{\boldsymbol{i=1}}^{\boldsymbol{N_s}} \boldsymbol{n_i^2} \tag{5.27}$$

where N^2 is the noise power in the measured ERP signal. This can be estimated by assuming the noise is close to the difference between the long vector measured ERP signal and the PCA filtered signal:

$$\boldsymbol{N^2} \approx \left\| \mathbf{E}^{\mathbf{f}}_{\mathbf{pca}} - \mathbf{E}_{\boldsymbol{k}} \right\|^{\mathbf{2}}. \tag{5.28}$$

Given (5.27) and (5.28) and the assumption of uniform distribution of noise, then for all *i*:

$$\boldsymbol{n_i^2 = \frac{N^2}{N_c \times N} \approx \frac{\|\mathbf{E}_{\mathbf{pca}}^{\mathbf{f}} - \mathbf{E}_k\|^2}{N_c \times N}}. \tag{5.29}$$

The covariance in the unfiltered PCA weights is then:

$$\mathbf{R}_k = \boldsymbol{n_i^2}\mathbf{I}_{N_b}. \tag{5.30}$$

where $\mathbf{I}_{N_b}$ is the identity matrix of rank N_b , and the covariance of the PCA filtered ERP is:

$$\mathbf{R}_k = \boldsymbol{n_i^2 diag}(\boldsymbol{F_i^2}). \tag{5.31}$$

5.4.3 SNR Performance for Multichannel State Vector

The same numerical experiments defined in Section 5.3.3. have been carried out to assess the multichannel vector form of the PCAKF algorithm. Simulated 20 channel AEEG data was used, with added white and pink Gaussian noise. Twenty PCA basis vectors were generated using simulated data and PCA filter weights were Gaussian.

Figure 5.8 illustrates multichannel ERP signals as generated with 0 dB AWGN and after PCA filtering and PCAKF. A single channel with band limited AWGN with an initial SNR=0 dB. The black curve is the synthetic ERP signal produced by the multi-channel simulator, the red curve is the measured signal including synthetic noise, and the green curve after PCAKF filtering. Channel 1 has been expanded in the inserted plot. Clearly there is significant improvement in SNR through noise rejection.

Figures 5.9 and 5.10 shows the SNR improvement with PCA and PCAKF filtering, starting from a range of initial SNRs, for AWGN and APGN respectively. The multichannel vector variant of the PCA filtering (solid lines) yields about a 17 dB SNR

improvement, significantly more than when a different basis is used for each channel. PCAKF (dashed lines) yields a further improvement of about 3 dB for relatively clean signals, less than for the previous method, and the improvement grows linearly for noisy signals where the measured signal is largely disregarded and the a priori expected signal is returned as the most likely response. AWGN and APGN yield very similar results.

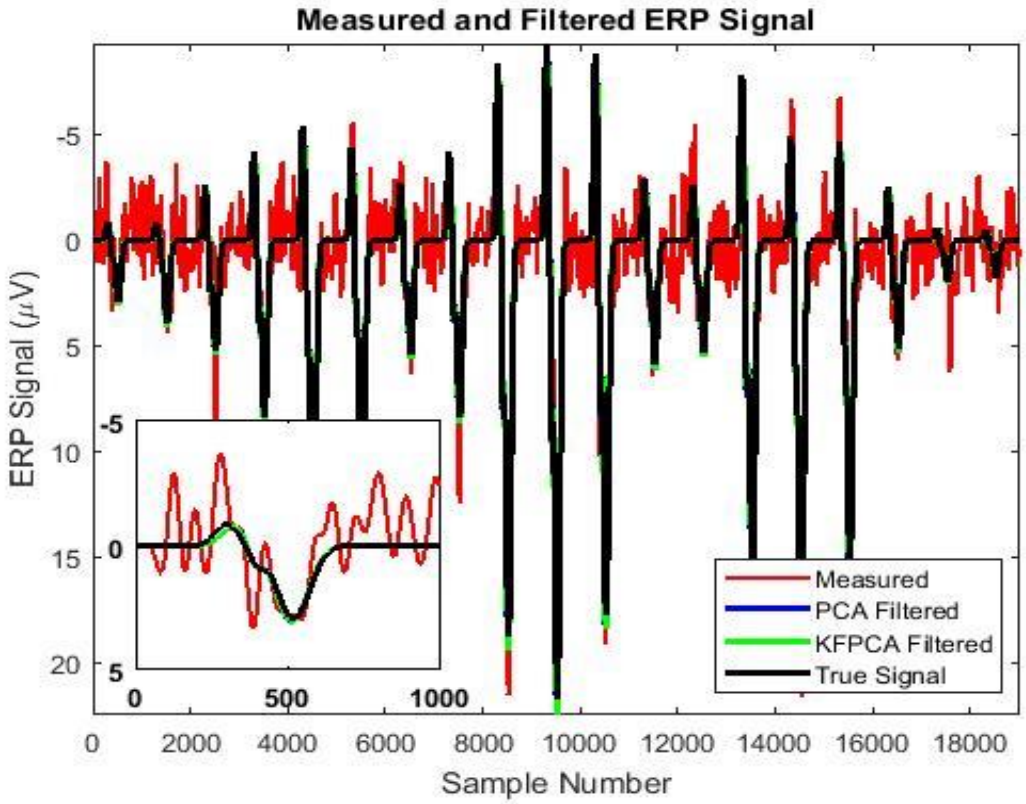

Figure 5.8 Measured, filtered and true channels 1&2 ERP signal for band limited AWGN, SNR=0 dB. The black curve is the synthetic ERP signal produced by the multi-channel simulator, and for these tests can be taken as the true, noise-free ERP signal. The red curve is the measured signal including synthetic white noise. PCA filtering reduces the noise in the signal by removing PCA components that are largely noise. This signal is further combined with the expected signal using a Kalman Factor to yield the green curve.

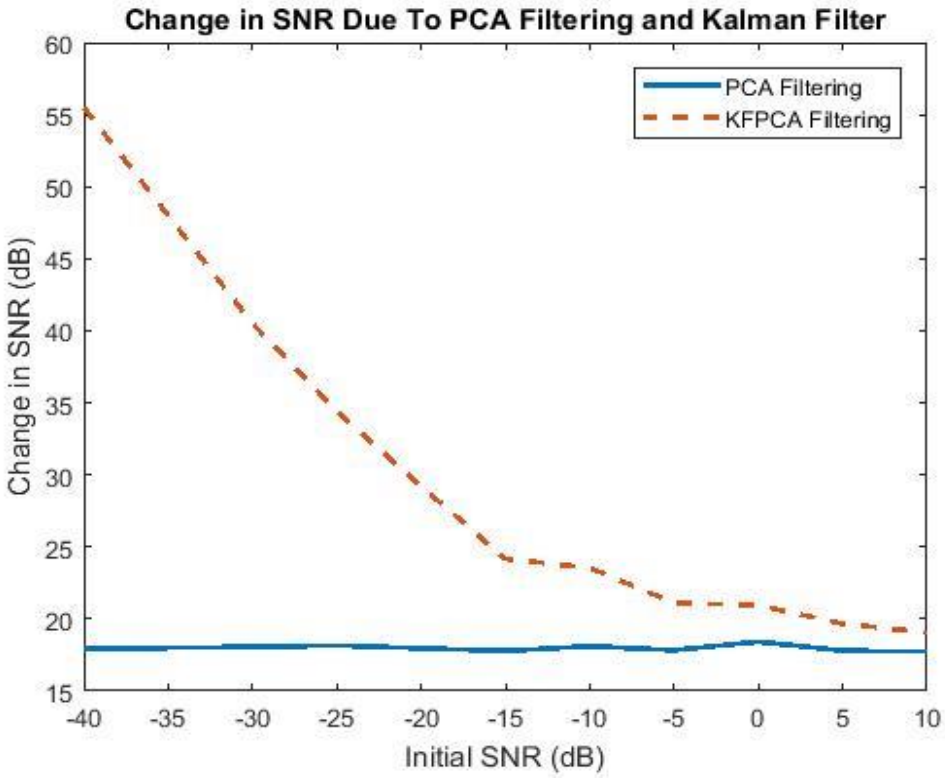

Figure 5.9 Change in SNR Due to PCA and Kalman Filtering for AWGN, for all channels. The SNR improvement with filtering, starting from a range of initial SNRs. PCA filtering (solid lines) yields about a 17 dB SNR improvement just by rejecting components that are predominantly noise. PCAKF (dashed lines) yields a further improvement of about 20 dB.

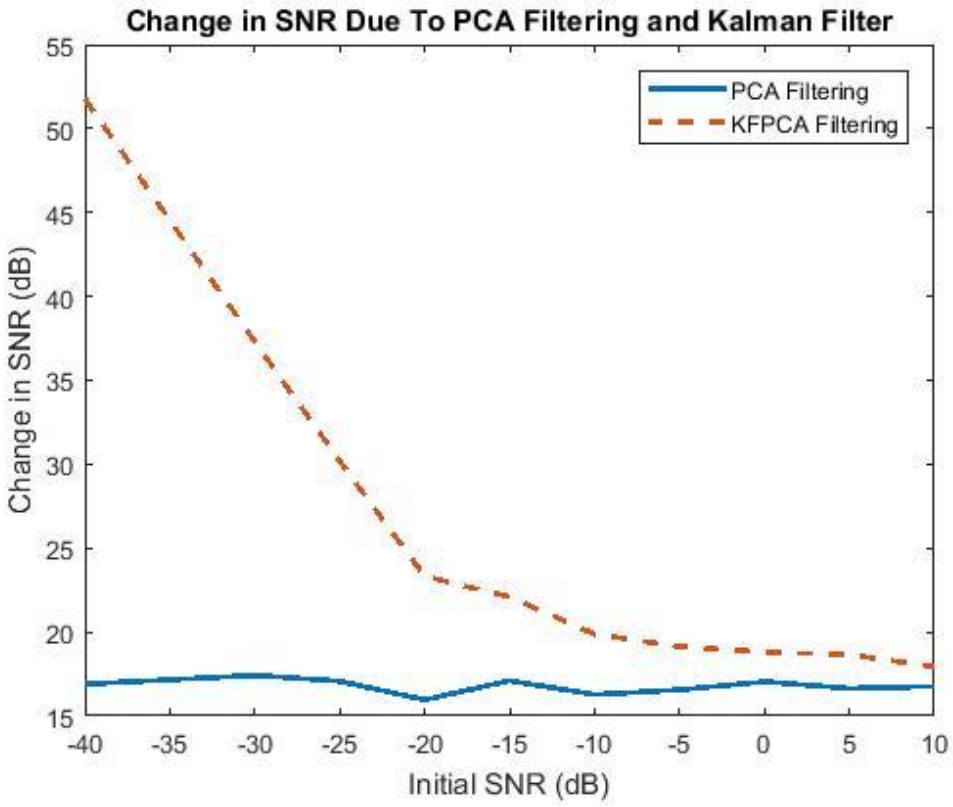

Figure 5.10 Change in SNR Due to PCA and Kalman Filtering for APGN. The SNR improvement with filtering, starting from a range of initial SNRs with APGN. PCA filtering and PCAKF (dashed lines) yields an improvement offer similar SNR improvements as with AWGN.

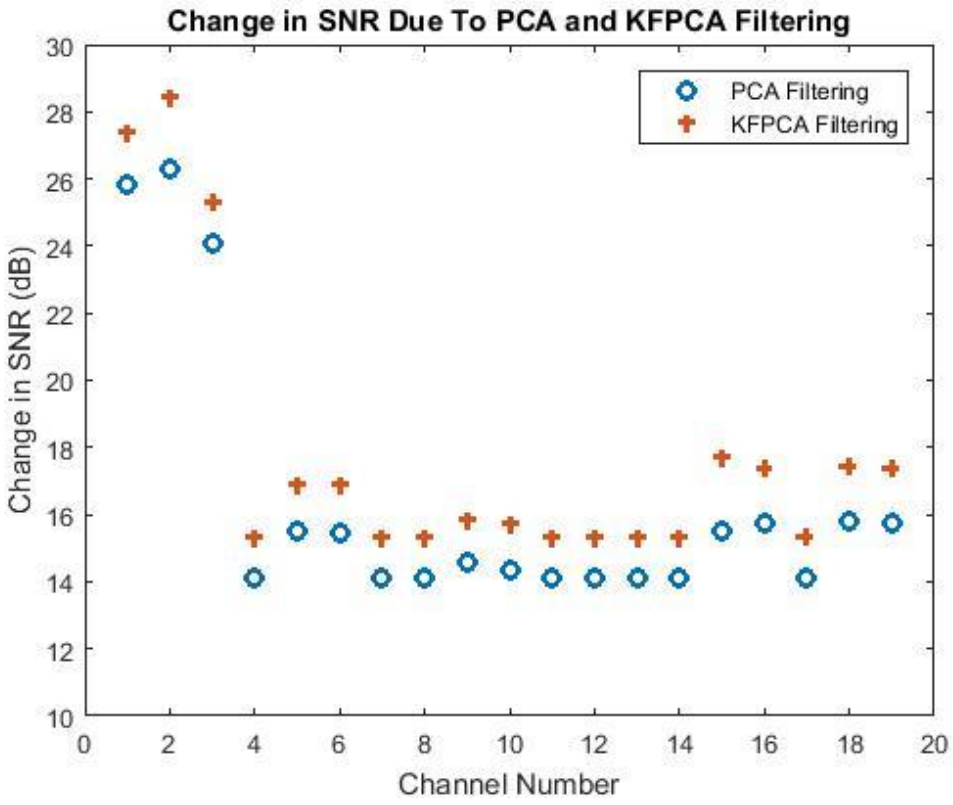

Figure 5.11 Change in SNR Due To PCA and Kalman Filtering where channels 1, 2 and 3 have an initial SNR=0 dB while the other channels have an SNR=10 dB. PCA filtering and Kalman Filtering use the cross-channel information and yields much higher SNR improvement in the three noisy channels. Kalman Filtering yields much better than PCA filter.

Finally, we consider the case where the initial SNR is not the same across all channels. This is illustrated in an example where channels 1, 2 and 3 (Fp1, Fp2 and F7) have initial SNR=0 dB while the other channels have SNR=10 dB. For this test, AWGN was used. Figure 5.11 shows the SNR improvement from filtering. PCA filtering yields the same SNR improvement on all channels as the same noise amplitude exists in all the PCA bases. However, Kalman Filtering uses the cross-channel information and yields much higher SNR improvement in the three noisy channels. In effect the algorithm reconstructs the signals on these channels from the more reliable information measured on the relatively clean channels.

5.4.4 Conclusion

The variant of the PCAKF method that uses long multichannel measurement vectors yields similar results to the previous method where each channel had its own PCA basis. The new method requires several orders of magnitude less computation.

5.5 SNR is required to estimate peak parameters

A numerical experiment has been performed to identify the SNR required for clinically useful features of an ERP to be observable. Synthetic ERPs have been generated and band limited (<30 Hz) additive pink Gaussian noise (APGN) has been added to yield a range of SNRs. Figure 5.12 shows some of the time series used in the experiment. A sample of 15 academics and PhD students were asked to view the time series on paper to determine whether or not they could observe the N100, P200 and P300 amplitude and delays. Analysis of the results suggested that a SNR of 14 dB was required to observe P200 features and a SNR of 12 dB for P300 features. This sets a target SNR for filtering and combining to achieve.

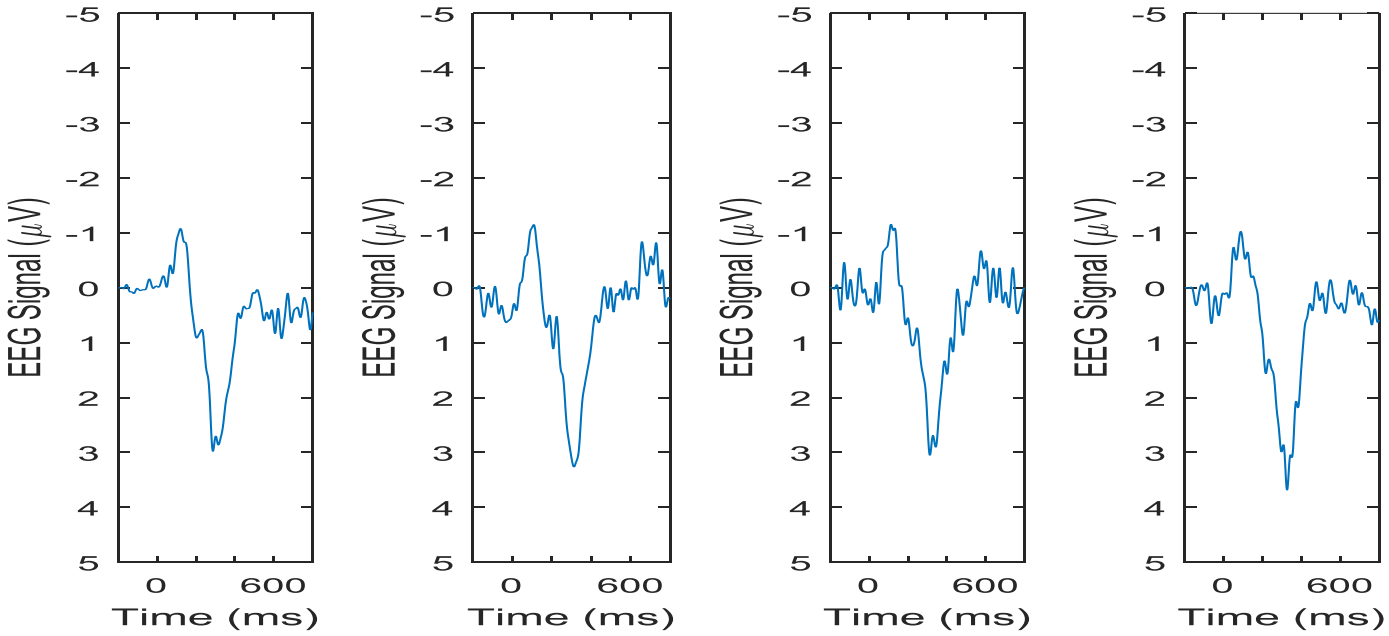

Fig 5.12 a).

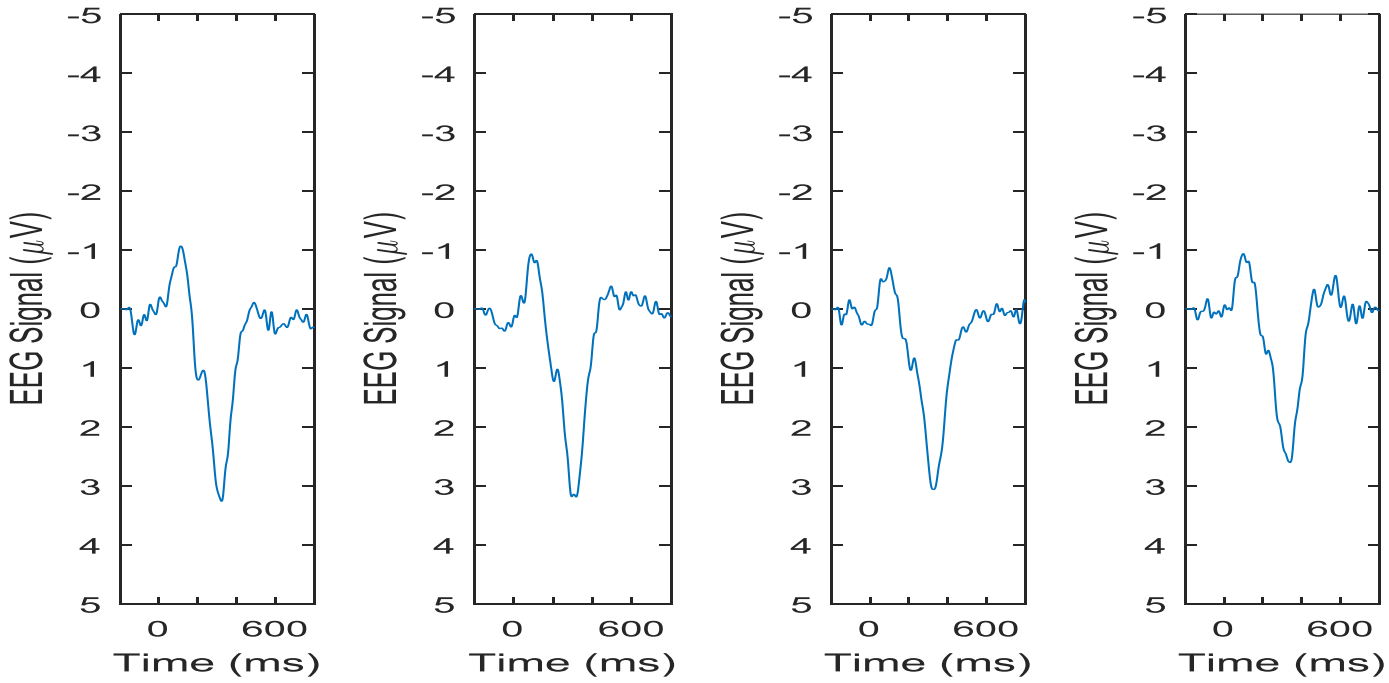

Fig 5.12 b).

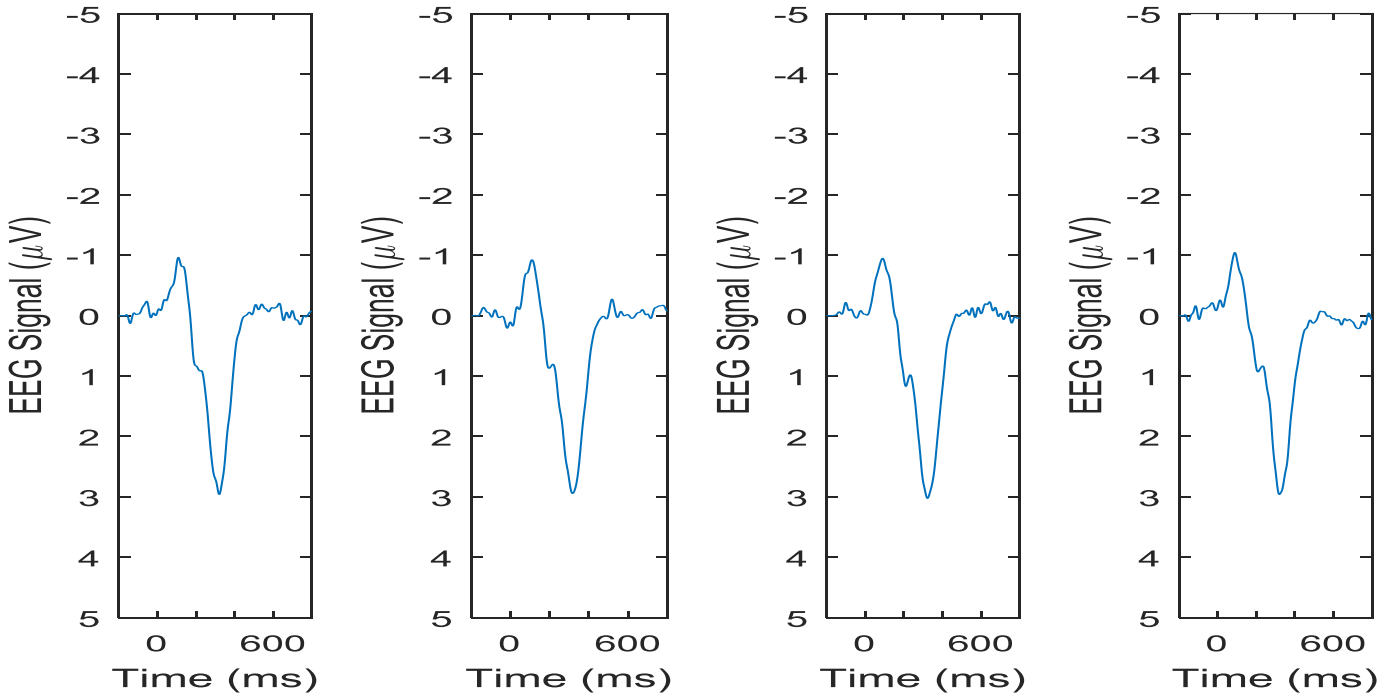

Fig 5.12 c).

Figure 5.12 Synthetic ERPs contaminated with band limited APGN to yield SNRs of a) 10 dB, b) 12 dB and c) 14 dB.

5.6 Conclusions

This Chapter has introduced the use of prior information to guide the rejection of noise in ERP measurements. Knowledge of the expected shape and variability of clean ERP measurements allows a PCA basis to be calculated that spans the expected ERPs while being orthogonal to a large proportion of the noise. A large SNR improvement can be achieved by projecting measured ERP time series onto the subspace spanned by the PCA basis signals. Further SNR improvement can be gained by combining the PCA projected measured signal with an aprioiri expected ERP response. Filtering yields the best estimate of the underlying ERP, for each trail measurement, given the measured time series. The next Chapter considers the combining of several filtered trail time series to estimate the mean underlying ERP.

Chapter 6 Estimating ERP Response by Combining Trials

The previous Chapter introduced PCA projection and Kalman Filtering to optimally estimate the ERP signal produced by each trial. Typically, each trial will yield an ECG signal with a different SNR, both before and after filtering, due to the time variation of noise processes. Within each trial recording, the SNR will also vary. As time progresses after the stimulus the brain can be distracted by other stimuli or thoughts, and so noise signals tend to increase over time. For this reason the N100 is likely to be more clearly imaged that P200 or P300.

This Chapter looks at the combining of trial ERP recordings. Clinically, ERP recording from many trials are averaged, sometimes combining trials from several individuals, to produce a clear ERP. The real variation in individual ERPs is unknown. When combining trials, it would make sense to give higher weight to recordings with higher SNR. The following subsections explore this idea further.

It is difficult to reliably estimate clinically important ERP parameters, such as P300 height and delay, from a single trial. Figure 6.1 illustrates some typical EEG measurements over oddball trials, illustrating typical noise levels. Although there is correlation in the positive and negative excursions related to P300 and N100, no reliable clinical parameters could be extracted from a single recording. The signal variation during the interval before the stimulus indicates the level of noise likely to exist after the stimulus. Before the stimulus the ERP signal is expected to be zero so all the measured signal is noise. Noise sources unrelated to the stimulus are expected to continue after the stimulus.

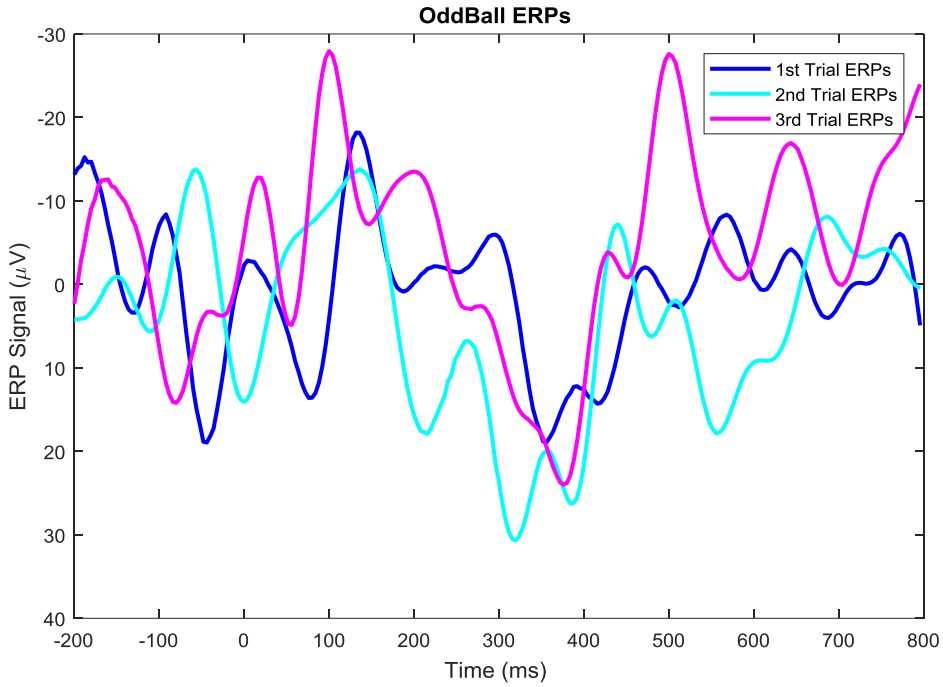

Figure 6.1 A selection of typical measured oddball ERP signals, illustrating typical noise levels. Although there is correlation in the positive and negative excursions related to P300 and N100, no reliable clinical parameters could be extracted from a single recording.

To reduce the noise, averaging across trials and averaging across subjects is commonly performed. Unweighted averages are a sub-optimal method of combining measurements and so more sophisticated methods are developed in this section.

6.1 Uniform Weighted Average

When an average is taken over many oddball trials then the uncorrelated signals are attenuated and the average approaches the pure oddball ERP signal. In situations where the non-ERP signals are of higher amplitude or more strongly correlated with the ERP signal, then larger numbers of trials need to be averaged before the ERP signal becomes apparent. In this section we estimate the signal-to-noise ratio (SNR) in averages of ERP signals and compare the approach of the average over increasing numbers of trials to the best estimate of the pure ERP signal. The SNR curves allow

us to estimate the number of repetitions required to identify an ERP signal from data acquired in different environments.

Let an oddball trial be $O_i(t)$ for index $i = 1, \cdots N^{odd}$. Each trial is a mixture of the pure oddball response $O(t)$ and noise $N_i(t)$:

$$O_i(t) = O(t) + N_i(t) \tag{6.1}$$

Let the unweighted average of *M* trials be:

$$\overline{O}_M(t) \equiv \underset{M}{mean}(O_i(t)) \tag{6.2}$$

Defining the power of a time-series to be the mean square value: $P(X) \equiv E[X^2]$, and assuming the pure oddball signal and the noise are uncorrelated, then the power of the measured oddball response can be written:

$$P(O_i) = P(O) + P(N_i) \tag{6.3}$$

Furthermore, assuming that the noise is uncorrelated across trials, averaging *M* trials reduces the noise power by a factor of *M:*

$$P(\overline{O}_M) = P(O) + \frac{1}{M} P(N) \tag{6.4}$$

The signal-to-noise ratio, SNR, is defined to be the signal power divided by the noise power:

$$SNR \equiv \frac{P(O)}{P(N)} \tag{6.5}$$

Individual trials often have low SNRs due to the large amplitude of other biological signals and artefacts. Averaging across trials reduces the noise power. Equation (6.4)

allows both $P(O)$ and $P(N)$ to be estimated by fitting equation (6.4) to the measured average trial power $P(\overline{O}_M)$. From equations (6.4) and (6.5), the SNR as a function of number of trials in average can be expressed:

$$SNR(M) = \frac{P(O)}{P(N_i)} \times M = SNR(1) \times M \tag{6.6}$$

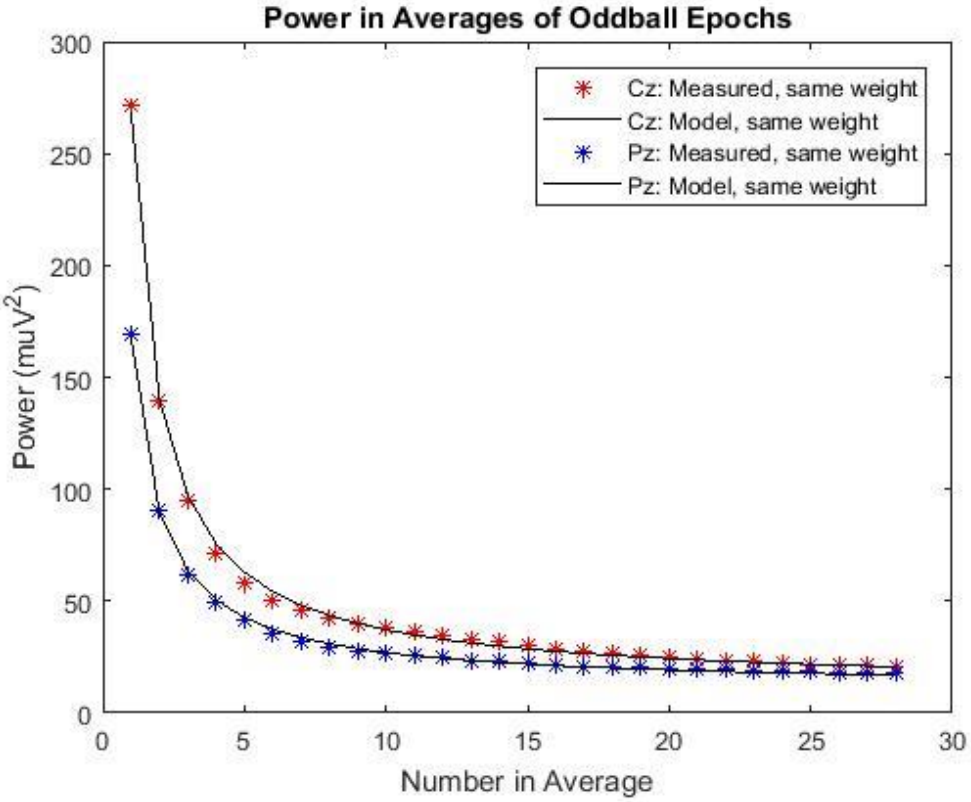

Figure 6.2 Reduction of noise by averaging over trials. The coloured symbols are the mean SNR over all subsets of trials of size while the black lines are the variation in SNR produced by extrapolation from the mean SNR of individual trials.

Figure 6.2 illustrates this for two EEG channels, showing the hyperbolic convergence to the oddball signal power. The coloured symbols are the mean SNR over all subsets of trials of size *M*. The black lines are the variation in SNR from equation (6.4), produced by extrapolation from the mean SNR of individual trials. The quality of these fits shows that the noise and artefacts may be treated as uncorrelated between trials.

It also suggests that the SNR was similar in all individual trials. This would not have been the case if trials contaminated by eye-blink artefacts had not been removed.

6.1.1 Discussion

Any recorded EEG contains brain's response to the stimulus plus other activity that is unrelated to the stimulus and the consistent response can be extracted by averaging across many trials (Luck, 2014). Most EEG recordings picked up many of artefacts which require special treatment such as filtering or averaging. Most common of artefacts arise from the eyes. When the eyes move or blink, a large voltage deflection is observed over much of the head, and this artefact is usually much larger than the ERP signals (Ochoa & Polich, 2000). Trials containing blinks, eye movements, or other artefacts are typically excluded from the averaged ERP waveforms. In luck study (2014), it is shown two controls and three patients have been excepted from the analysis because more than 50% of trials were rejected because of eye blinking whereas in remaining subjects around 20% of trials were rejected on average (Luck, 2014). There are deficiencies of this approach and most of trials possibly need to be rejected and reducing the number of trials contributing to the average ERP waveforms. Furthermore, brain effort involved in suppressing eye-blinks may weaken task performance (Ochoa & Polich, 2000). For that reason, it has been applied several of averaging in ERP signal.

Uniform averaging has been used for many activities and environments. Different EEG channels yield different SNRs in individual ERP measurements due to their location relative to signal generating parts of the brain and to major noise sources such as eyes. Typically, channels towards the posterior of the head measure progressively smaller ERP signals as they move away from the auditory processing areas of the

brain. However, eye blink and movement artefacts also decrease in amplitude faster than the ERP signal, as the electrodes move further from the eyes.

Table 6.1 presents the mean trial power in oddball ERP signals collected inside and outside the shielded room while the subjects either sat or walked for 70 trials and around 20 trials affected by eye blinks. The power is either calculated from all oddball ERP trials, or only those not contaminated by eye blink artefacts. Several observations can be made. Eye blink artefact power is 10 to 20 times larger than the ERP signal power for anterior channels but decreases quickly as channels move toward the posterior. Under ideal conditions, sitting inside, the ERP power only decreases slowly as the channel moves towards the posterior. When outside, the mean power after blink removal is always higher than when inside. This is due to other noise sources, such as brain activity processing other sensory inputs, e.g. visual processing; and movement artefacts such as electrode–scalp connection changes and muscle noise. If every measured trial for the same channel contains the same ERP signal but different noise, then the smallest power indicates the best estimate of the ERP power. For anterior channels, such as Fp1 and Fp2, the ERP signal power appears to be about $45\,\mu V^2$, suggesting that even after blink removal and averaging, the noise power in the walking outside scenario is ten times larger than the signal power.

Table 6.1 EEG signal power in μV^2 by channel, inside and outside the shield room, while sitting and walking, before and after eye blinks removal (filtered).

Channel Location	Sitting Inside		Sitting Outside		Walking Inside		Walking Outside	
	With Blinks	Blinks Filtered	With Blinks	Blinks Filtered	With Blinks	Blinks Filtered	With Blinks	Blinks Filtered
Fp1	1113	47	1387	157	2387	123	4259	320
Fp2	932	54	1381	234	2092	145	2746	541
F7	834	45	680	100	1327	112	2156	537
F3	480	61	463	188	535	67	792	248
Fz	441	76	465	216	490	86	771	393

F4	485	70	470	234	470	101	843	584
F8	459	59	714	384	799	204	1655	351
T7	172	30	200	137	160	39	283	158
C3	217	57	262	171	219	57	340	214
Cz	271	84	293	196	258	82	447	370
C4	215	67	308	205	267	92	555	421
T8	242	47	320	262	315	125	862	704
P7	107	32	156	137	85	40	164	152
P3	158	52	208	170	147	60	257	237
Pz	169	59	219	186	162	70	324	328
P4	164	63	228	191	182	78	415	418
P8	134	46	206	187	162	77	476	501
O1	230	42	185	139	115	70	282	296
O2	119	34	187	154	357	131	323	334

The average powers in Table 6.1 were calculated using a simple uniform average, i.e. the sum of M trials divided by M. This is the optimal method to combine trials when they all have the same SNR. However, even after averaging all the trials uncontaminated by eye blinks, the power while walking, or even sitting inside the shielded room, is many times that of the estimated pure ERP signal. Clearly removing eye-blink artefacts is essential if the goal is to observe the ERP response in as few repetitions as possible. However, it is observed that the SNR of individual trials still varies considerably. This suggests that a more sophisticated combining method may yield better estimates of the underlying ERP. Figures 6.3 and 6.4 show that the statistical model assumption of independent noise is accurate across all channels, with and without eye blink removal. This suggests that other major noise mechanisms can also be treated as independent. If noise is independent but not stationary then a different method of combining trials to yield an estimate of the underlying ERP signal is required.

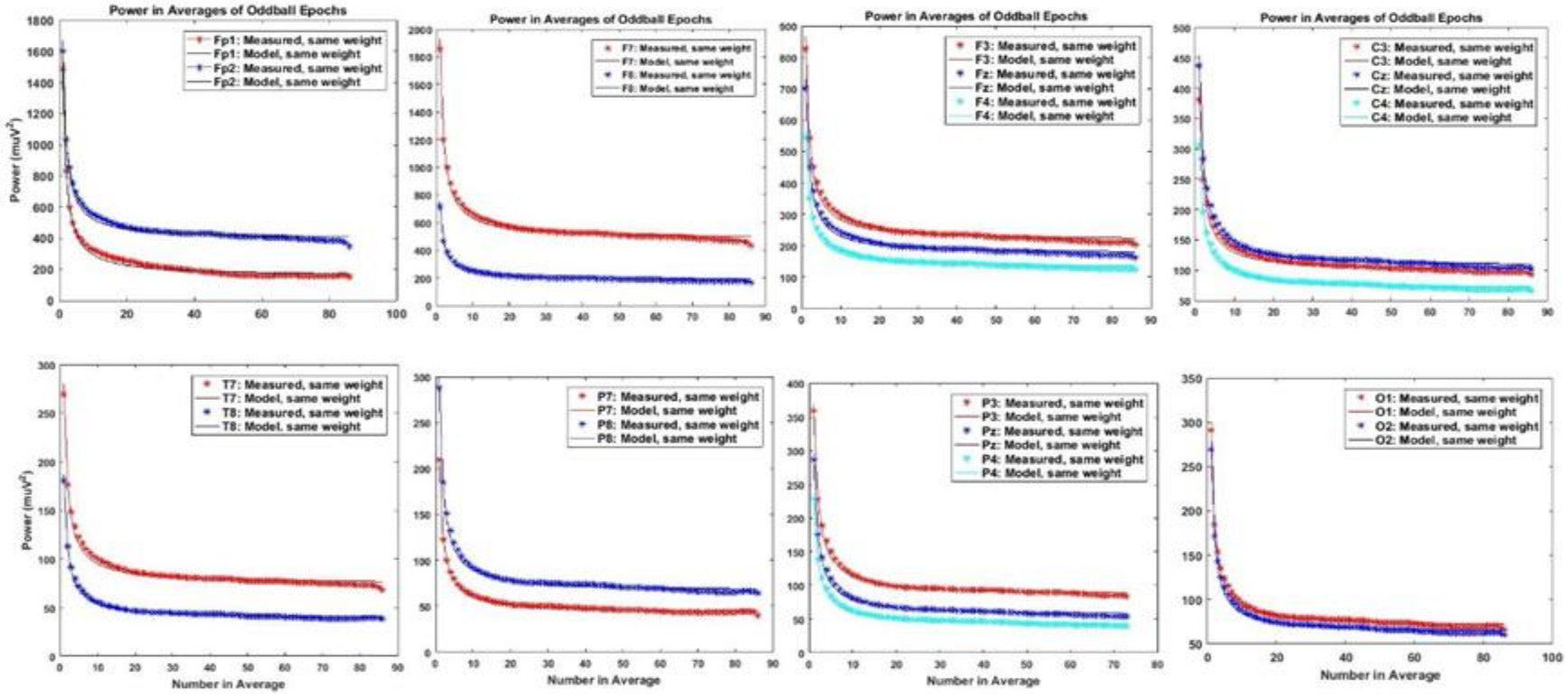

Figure 6.3 Reduction of noise by averaging over trials for 19 channels before eye blinks removal by using simple average.

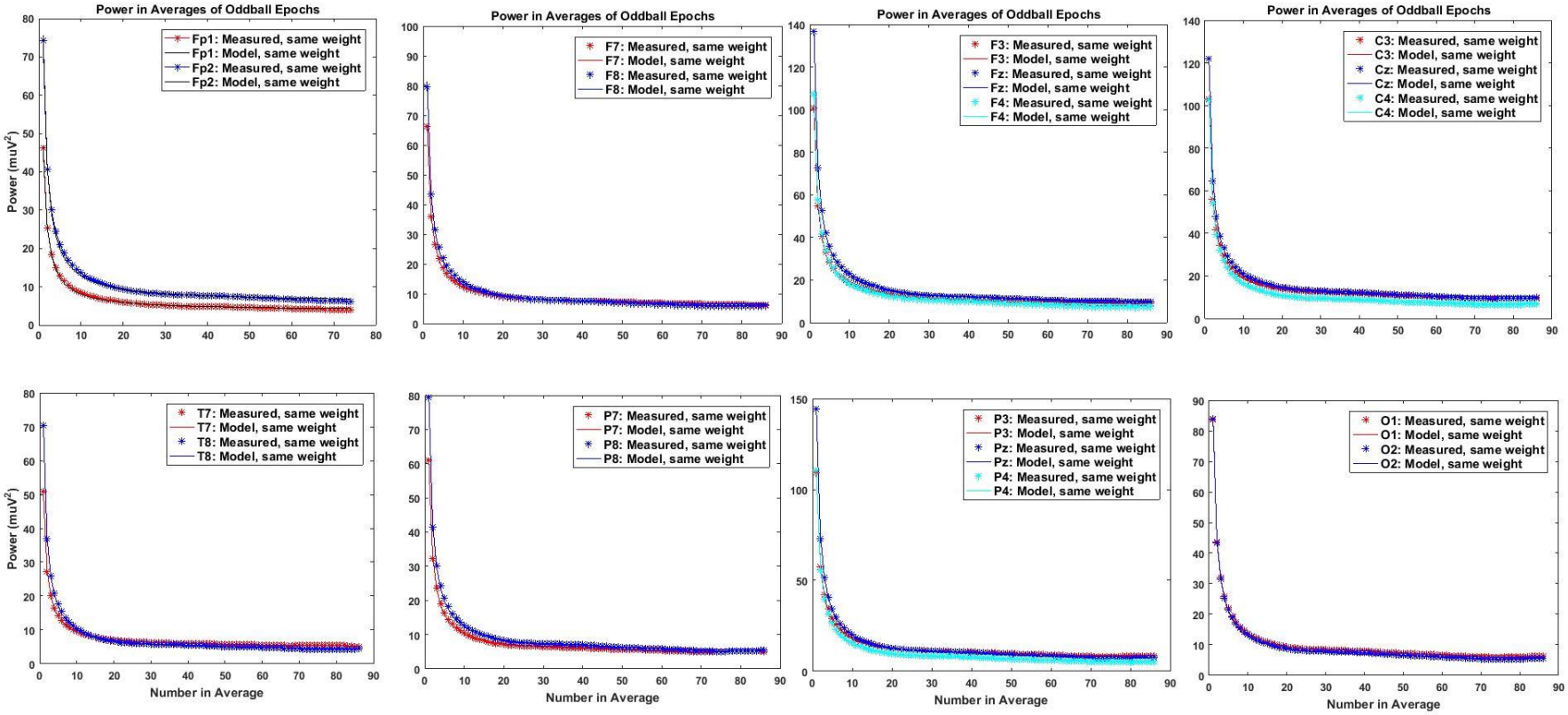

Figure 6.4 Reduction of noise by averaging over trials for 19 channels after eye blinks removal by using simple average.

6.2 Optimal Weighted Average

As in the previous section, consider M oddball trials:

$$O_i = O + N_i, \tag{6.7}$$

where $O(t)$ is the oddball response and $N_i(t)$ is the noise in the *i*th trial. If O and N are independent then $E\,[S \times N\,] = 0$, and the power in O_i is

$$P_i = E\,[O_i^2] = \;\; E\,[O^2] + \;E\,[N_i^2] \tag{6.8}$$

where $E\,[*\,]$ is the expected value. We want the weighted average oddball response:

$$\overline{\mathrm{O}} \; = \sum_i^N \mathrm{W_i} O_i \;\; : \sum \mathrm{w_i} = 1 \tag{6.9a}$$

$$\overline{\mathrm{O}} \; = \; \sum_i \mathrm{W_i} (O + N)_i \tag{6.9b}$$

$$\overline{\mathrm{O}} = O \sum_i \mathrm{W_i} + \; \sum_i \mathrm{W_i} N_i = \;\; O + \sum_i \mathrm{W_i} N_i \tag{6.9c}$$

Except for the unit norm constraint, the weights are arbitrary. Different choices of weights yield different noise powers in the weighted sum. Assuming the trial noises are independent then the SNR in $\overline{\mathrm{O}}$ is:

$$SNR \; = \frac{E[O^2]}{\sum W_i^2 \, E[N_i^2]} \tag{6.10}$$

and this is maximized when the denominator is minimized. This minimisation can be posed as a Lagrange multiplier:

$$\text{Min} \; (\; \sum \mathrm{W_i^2 E[N_i^2]} - \lambda (\sum \mathrm{W_i} - 1 \;))$$

And taking derivatives yield**:**

$$2 W_i E[N_i^2] - \lambda = 0 \tag{6.11a}$$

$$\sum W_i = 1 \tag{6.11b}$$

(6.11a) hold for all *i* trials and so:

$$W_i = \frac{\lambda}{2E[N_i^2]} \qquad \forall i \; . \tag{6.11c}$$

Combining with (6.11b) yields:

$$\frac{\lambda}{2}\sum\left(\frac{1}{E[N_i^2]}\right) = 1 \qquad (6.11d)$$

Eliminating λ from (7.11c) and (7.11d) yields the minimising weights:

$$W_i = \frac{\frac{1}{E(N_i^2)}}{\sum_i\left(\frac{1}{E(N_i^2)}\right)} \qquad (6.11e)$$

Equation (6.11e) provides the trial weights that maximize the SNR in the weighted sum. In the case where all trials have the same noise power then the weights are also the same. This is the assumption when uniform means are used. However, when the noise power varies between trials, the more reliable trials with the lowest noise powers are given a larger weight in the average.

The proposed ERP estimation method starts with a small number of trials. The average power in subsets of trials is calculated and the ERP power and average trial noise power, $P(O)$ and $P(N^1)$, are estimated by fitting equation (6.6) to these data. Further trials are then measured and combined using a weighted average with the weights estimated using equation (6.11e) and the weighted average SNR provided by equation (6.10). With each new trial, the ERP and noise powers may be re-estimated using equation (6.4).

Figures 6.5 and 6.6 compare the powers in uniform averages (all weights the same) and optimal weighted averages, for oddball trials acquired with the subject sitting in the shielded room. For this example, eye-blink artefacts have not been removed and so some trials contain large noise signals. The weighted average method automatically assigns these trials small weights and so they do not contaminate the average. It can be seen that the weighted average converges to the ERP signal power much faster than the uniform average.

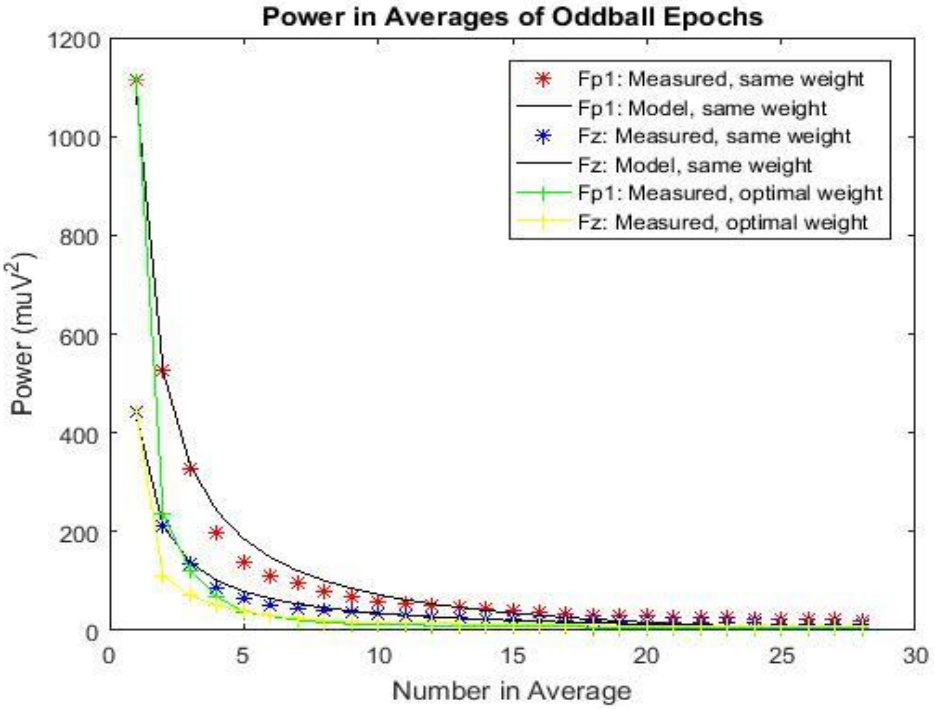

Figure 6.5 Power in uniform and weighted averages of oddball trials on electrodes Fp1 and Fz, for subject sitting in shielded room.

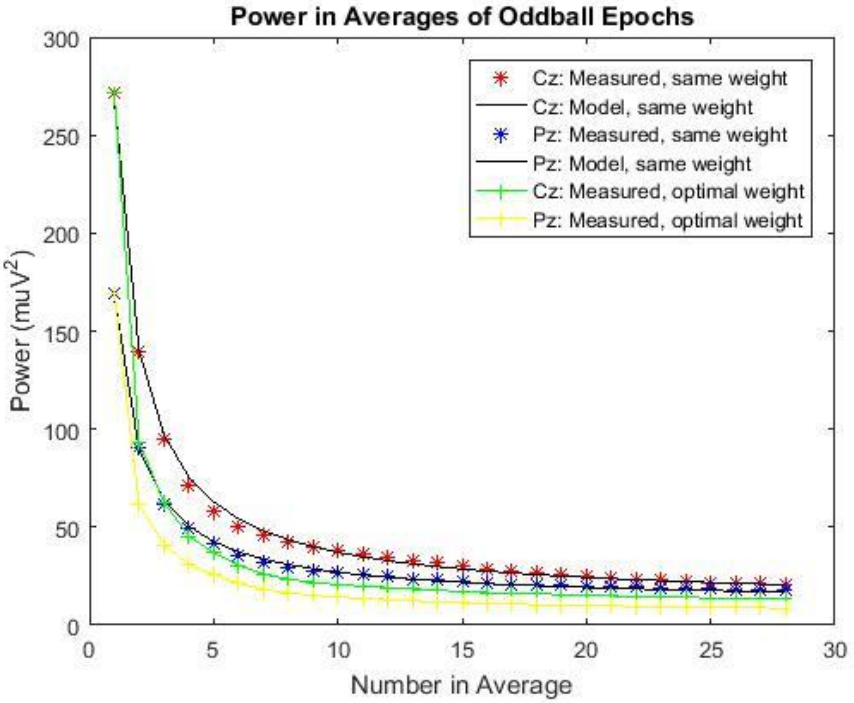

Figure 6.6 Power in uniform and weighted averages of oddball trials on electrodes Pz and Cz, for subject sitting in shielded room.

When eye-blink artefacts are removed the benefit of weighted averages is not as large but is still significant, see Figure 6.7.

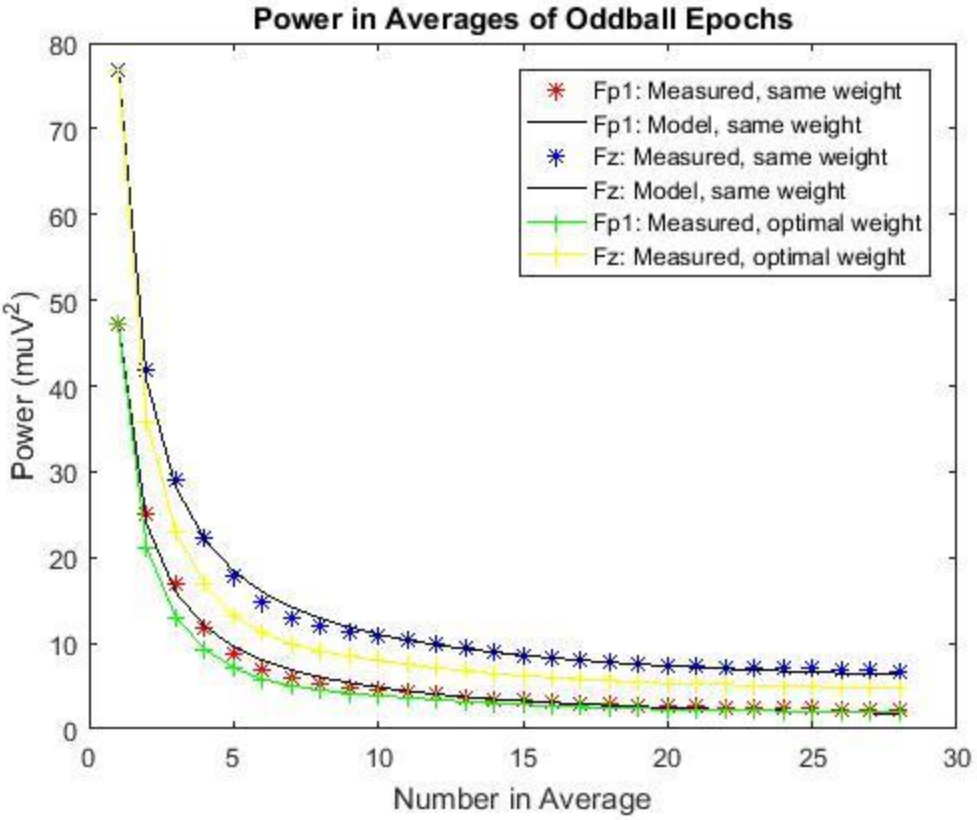

Figure 6.7 Power in simple and weighted averages of oddball trials on electrodes Fp1 and Fz, for subject sitting in shielded room, with eye-blink artefacts removal.

6.2.1 Extension of Optimal Weighted Mean

Simple and optimal weighted averaging were applied for same activities and environments. For optimal weighted averages, the power in the ERP estimate falls much faster than for simple uniform averages, suggesting it is much more effective at reducing the noise power. However, in some unusual cases the optimal weighting algorithm can be unstable. This is illustrated in Figure 6.8 below where channel P7

becomes unstable and the SNR increases dramatically with increasing numbers in the weighted average. This occurs when the estimate of the ERP signal power is poor, and so the noise power estimates are also poor, and so the SNR estimate is very poor. The estimate of the ERP signal power is derived by fitting the statistical model (7.6) to a simple average over small numbers of trials. This estimate can be poor if there is large variation in the individual trial SNRs. This problem can be addressed using an iterative method to estimate the ERP signal power i.e.

1. estimate signal power using uniform averages;
2. use this to estimate trial noise powers;
3. use weighted averaging to estimate the signal power;
4. iterate steps 2 and 3 until converged.

As seen in Figure 6.8 there were fluctuations in channel P7 when optimal weighted mean was used so the iterative algorithm above was employed to tackle this issue. It can be noticed in Figure 6.8 that the problem is resolved.

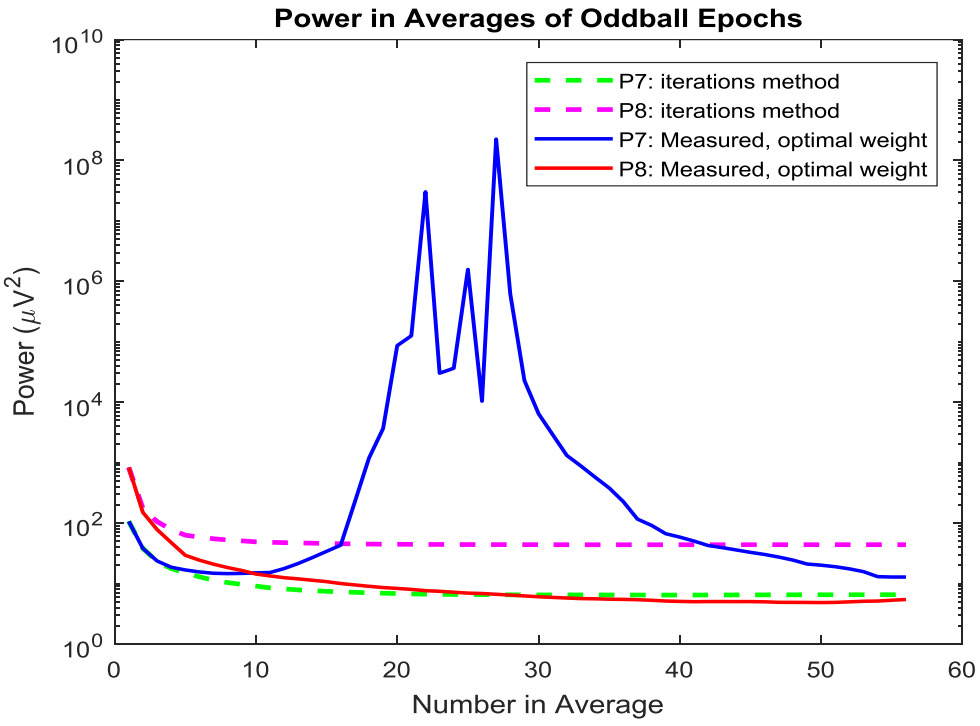

Figure 6.8 Iteration and Optimal Weight Methods to estimate ERPs power.

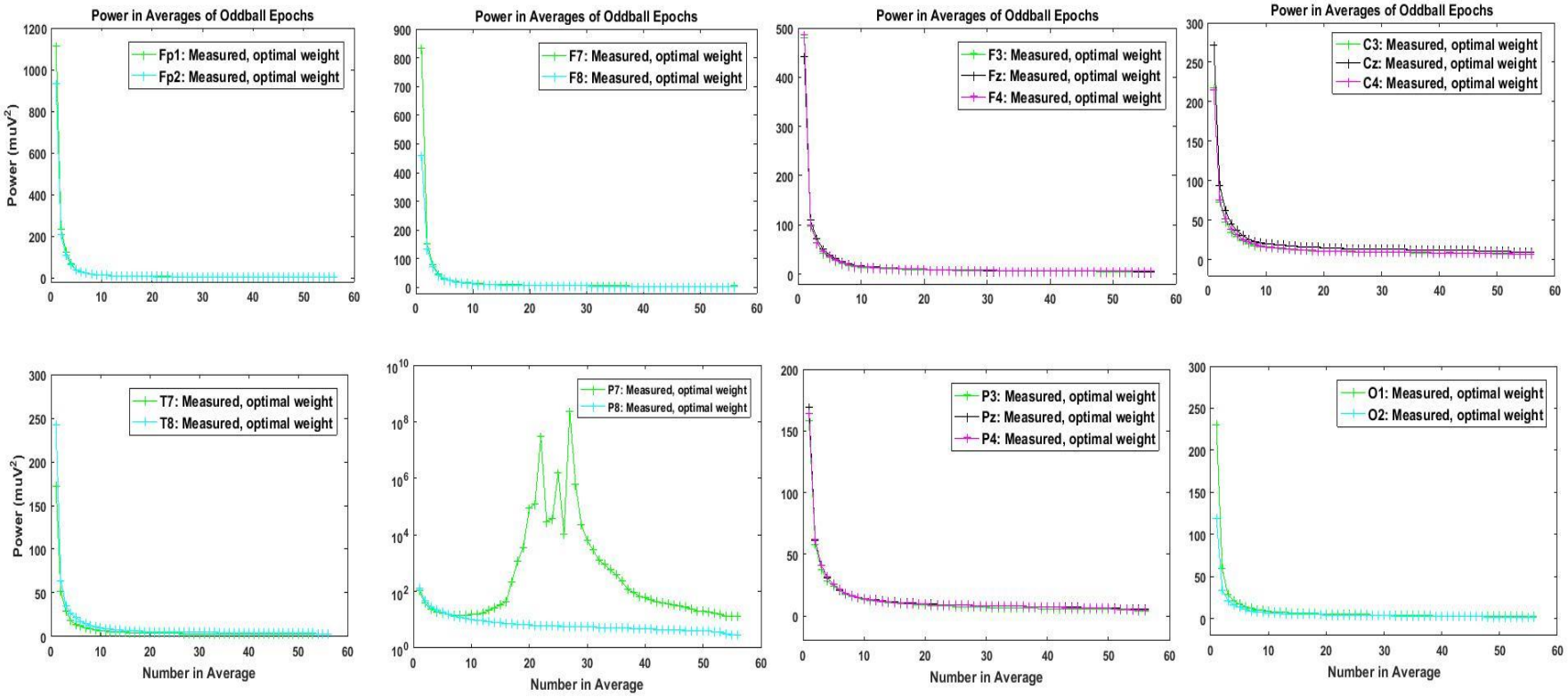

Figure 6.9 Reduction of noise by averaging over trials before eye blinks removal by using optimal average.

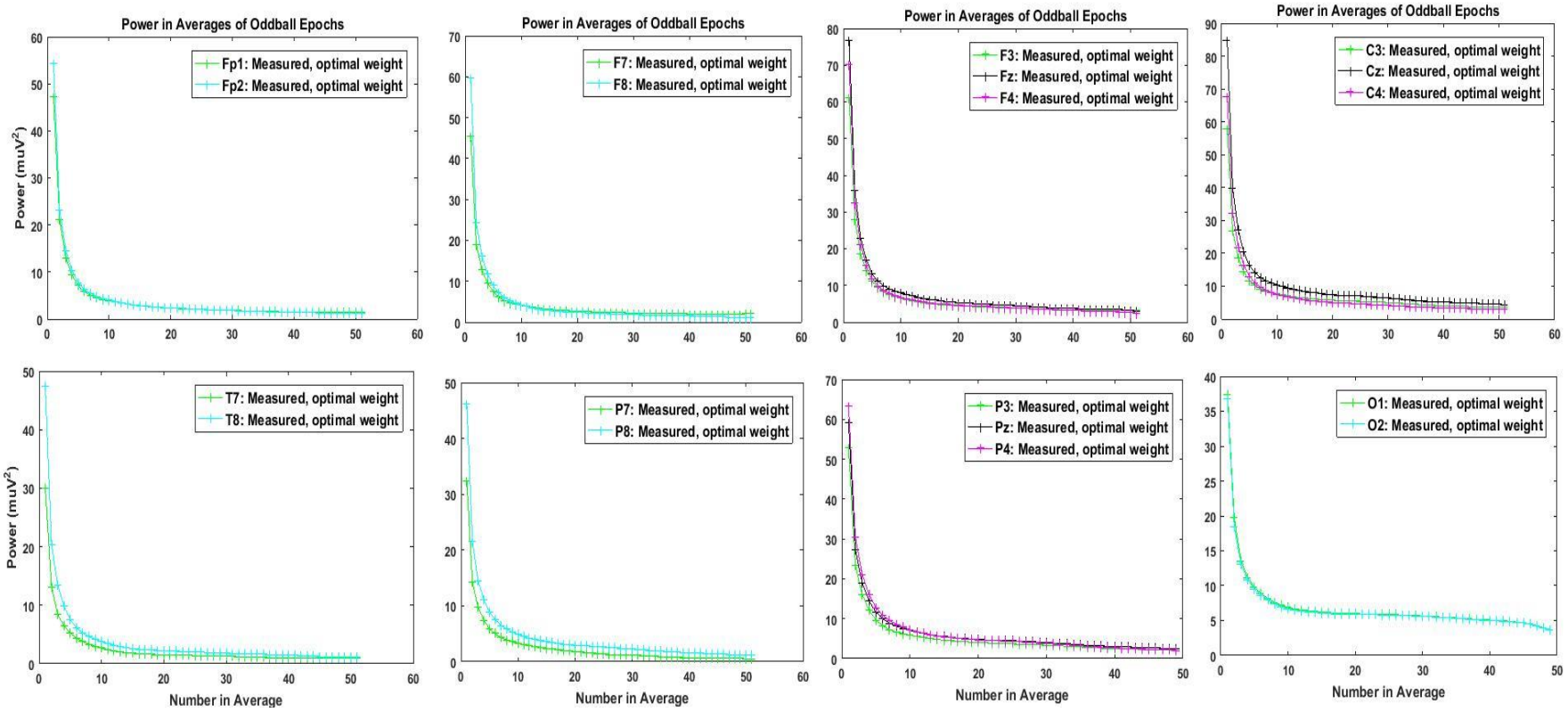

Figure 6.10 Reduction of noise by averaging over trials after eye blinks removal by using optimal average

6.2.2 Optimal Weighted Mean of Filtered Data

The OWM method uses a noise power estimate for each trial to calculate the weights that maximize the SNR in the weighted mean. In the case where all trials have the same noise power then the weights are also the same. This is the underlying assumption when uniform means are used. However, when the noise power varies between trials, the more reliable trials, with the lowest noise powers, are given a larger weight in the average.

Figure 6.11 illustrates a single measured oddball response and the OWM of 50 unfiltered trials. Evidence of the remaining noise can be seen in the interval before the stimulus and towards the end of the recording where the ERP is expected to be zero. Even after OWM of 50 trials the SNR is too low to reliably estimate clinically important parameters.

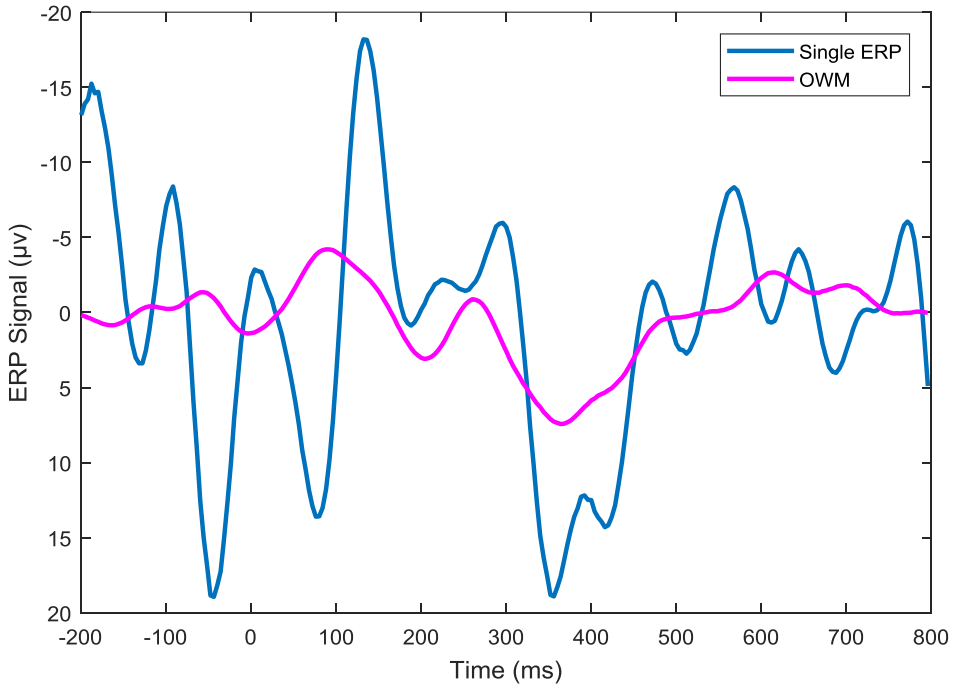

Figure 6.10 OWM of unfiltered ERP measurements. A single ERP measurement and the OWM of 50 unfiltered trials. Evidence of the remaining noise can be seen in the interval before the stimulus and towards the end of the recording where the ERP is expected to be zero.

In section 5.4, PCA and Kalman filtering were applied to synthetic EEG data. Figure 6.11 illustrates PCA projection and PCAKF applied to a measured EEG signal. PCA projection forces the noise to be zero before the stimulus and beyond 500 ms after the stimulus. Minor features such as the P200 become visible. This feature is developed even more by Kalman filtering. Filtering has removed much of the noise from the measured time series. Optimal combining of filtered measurements will yield an even better estimate of the underlying ERP.

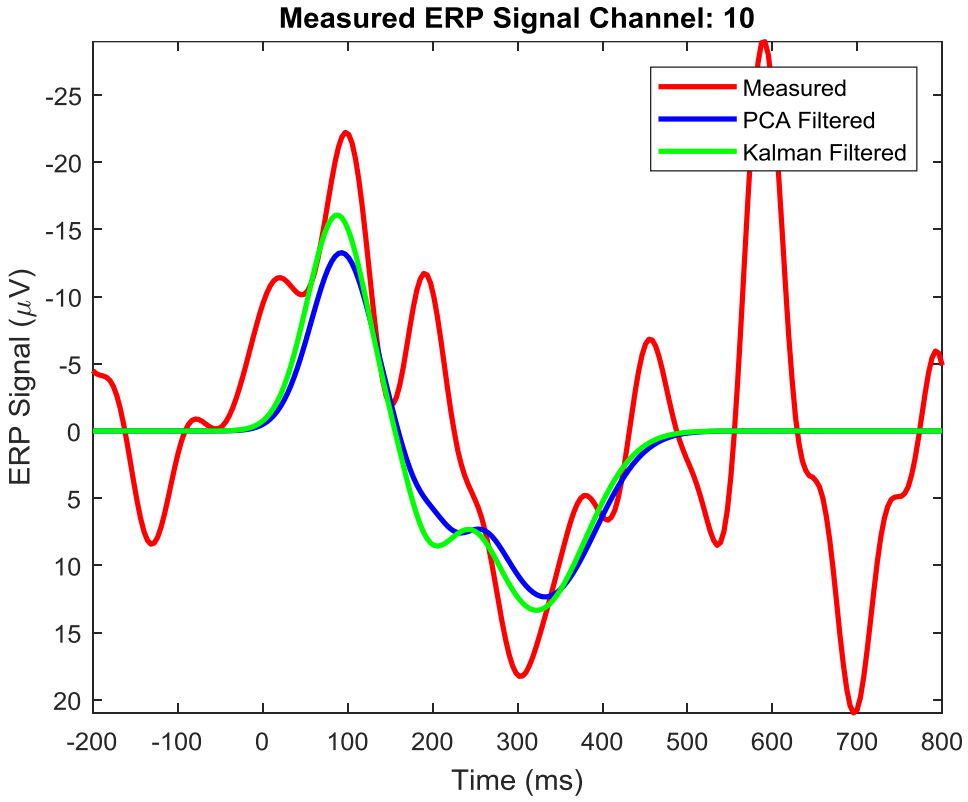

Figure 6.11 Measured, PCA and KF ERPs for Channel Cz. PCA projection forces the noise to be zero before the stimulus and beyond 500 ms after the stimulus. Minor features such as the P200 become visible.

Figure 6.12 illustrates the results of using OWM applied to signals after PCA projection and PCAKF. Estimates of time series noise power is the principal input

parameter to OWM. For unfiltered data, the noise power can be estimated from the interval before the stimulus where only noise was present. However, for filtered data the signal is forced to be zero over this period. In this example, noise power has been estimated as the difference between the power in the filtered time series and the power in a synthetic ERP for that channel. Both PCA projection and KF filtering greatly reduce the noise and both yield plausible ERPs for a single measurement. Combining 50 trials yields a result that should be closer to the mean ERP and, in this case, exhibits an even stronger and more reliable N200.

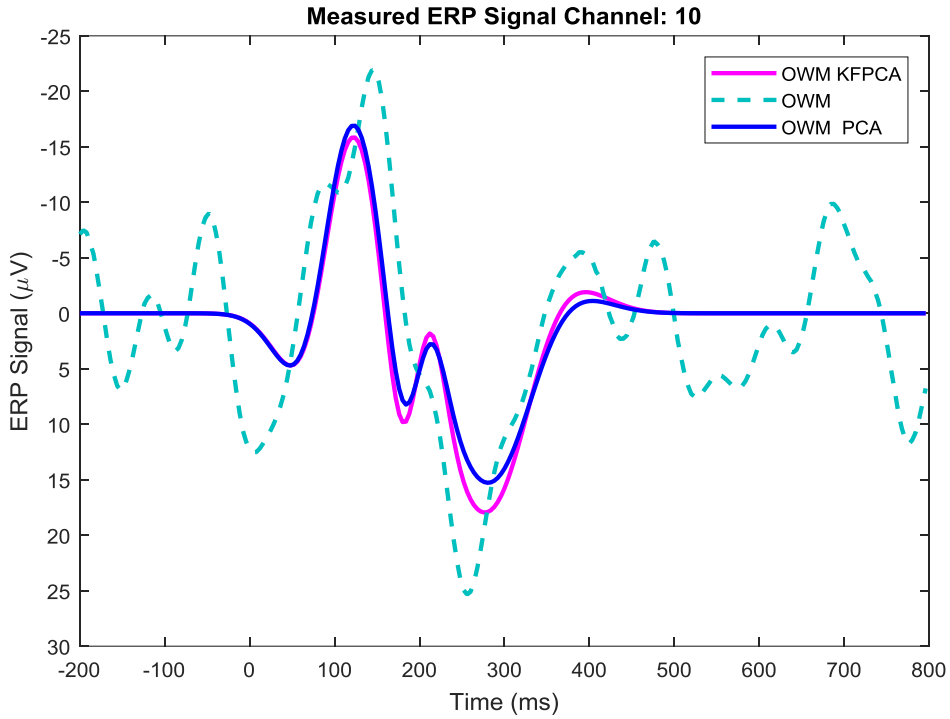

Figure 6.12 OWM of ERP measurements with PCA and PCAKF. Estimates of time series noise power is the principal input parameter to OWM. For unfiltered data, the noise power can be estimated from the interval before the stimulus where only noise was present while combining 50 filtered trials yields a result that should be closer to the mean ERP and, in this case, exhibits an even stronger and more reliable N200.

6.3 Bayesian Optimal Combining (BOC)

6.3.1 Optimal Combining of ERP Measurements for Uncertainty ERPs

The OWM method assumes that the noise is stationary across each trial recording. In some cases this is a valid assumption. However, for some noise sources, the noise signal is more impulsive. Eye-blink artefacts are an example, where the noise signal strongly affects only part of a trial time-series. Furthermore, as time passes after the audio stimulus, there is more chance of other stimuli generating a response. For example, the participant may notice a feature of the room or remember they left the gas on. Any brain activity unrelated to the audio stimulus will produce a response which is noise when the goal is to estimate ERPs. This section presents a Bayesian Optimal Combining (BOC) approach where the estimated error in each sample component can be used when combining trials. This means that information in trials that contain impulsive noise can still add to the confidence in the combined ERP. It is a more efficient use of the data.

The ERP response is a discretised Voltage time-series, or a vector of components in some basis, e.g. the PCA basis presented earlier. The current knowledge of the ERP is specified by a probability density function (pdf). Assuming this is a multivariate Normal then the ERP knowledge is specified by the mean and covariance: $\bar{\mathbf{x}}$ and $\mathbf{C}_x$. If an additional ERP measurement is performed, this provides a new estimate of the underlying ERP with its own pdf and uncertainty, specified by $\mathbf{x}_n$ and $\mathbf{C}_n$. This information can be used to refine our knowledge of the ERP by combining the two Normal distributions. The combined distribution is the product of the two multivariate Normal pdfs, is also multivariate Normal, and is known as the fused distribution. The fused distribution has mean and covariance:

$$\mathbf{X}_f = \mathbf{C}_n(\mathbf{C}_\mathbf{X} + \mathbf{C}_n)^{-1}\bar{\mathbf{X}} + \mathbf{C}_\mathbf{X}(\mathbf{C}_\mathbf{X} + \mathbf{C}_n)^{-1}\mathbf{X}_n \quad (6.12a)$$

$$\mathbf{C}_f = \mathbf{C}_\mathbf{X}(\mathbf{C}_\mathbf{X} + \mathbf{C}_n)^{-1}\mathbf{C}_n \quad (6.12b)$$

This result suggests an iterative approach to ERP estimation. Each new measurement yields a refined estimate of the underlying ERP. When the norm of the fused covariance matrix is small enough, the experiment can be terminated.

$$\bar{\mathbf{X}} \leftarrow \mathbf{X}_1 \quad (6.13)$$

$$\mathbf{C}_\mathbf{X} \leftarrow \mathbf{C}_1$$

For n = 2 to *NumberOfTrials*

$$\bar{\mathbf{X}} \leftarrow \mathbf{C}_n(\mathbf{C}_\mathbf{X} + \mathbf{C}_n)^{-1}\bar{\mathbf{X}} + \mathbf{C}_\mathbf{X}(\mathbf{C}_\mathbf{X} + \mathbf{C}_n)^{-1}\mathbf{X}_n$$

$$\mathbf{C}_\mathbf{X} \leftarrow \mathbf{C}_\mathbf{X}(\mathbf{C}_\mathbf{X} + \mathbf{C}_n)^{-1}\mathbf{C}_n$$

6.3.2 Validation for Synthetic Data

The method hinges on the estimation of the uncertainty in the measured ERP time series. The first test assumes that the uncertainty in each sample is independent and estimated by the variability present before the stimulus. During the ERP interval -200 ms to the stimulus, any variation is due to factors other than the brain response to the stimulus. Therefore, the total uncertainty in the samples can be estimated from the variability during this period, and assumed unchanged in the period after the stimulus. This yields a diagonal covariance matrix with uniform elements:

$$\sigma_n^2 = mean(ERP_n(t)^2, t < 0) \quad (6.14a)$$

$$\mathbf{C}_n = \sigma_n^2\mathbf{I}_n \quad (6.14b)$$

where $\mathbf{I}_n$ is the identity matrix of rank equal to the number of samples in an ERP trial. In this special case, the covariance matrices can be replaced by scalars.

This method has been tested using synthetic ERP signals and additive pink noise with a spectral range from DC to 30 Hz, to yield a measured SNR = 0 dB. Figure 6.13a

compares the best estimate ERP response using 1, 5, 10 and 15 measured ERP time series. This is compared to the unweighted mean of the 15 ERPs (green). The best estimate and unweighted average both yield final SNRs of 9.6 dB

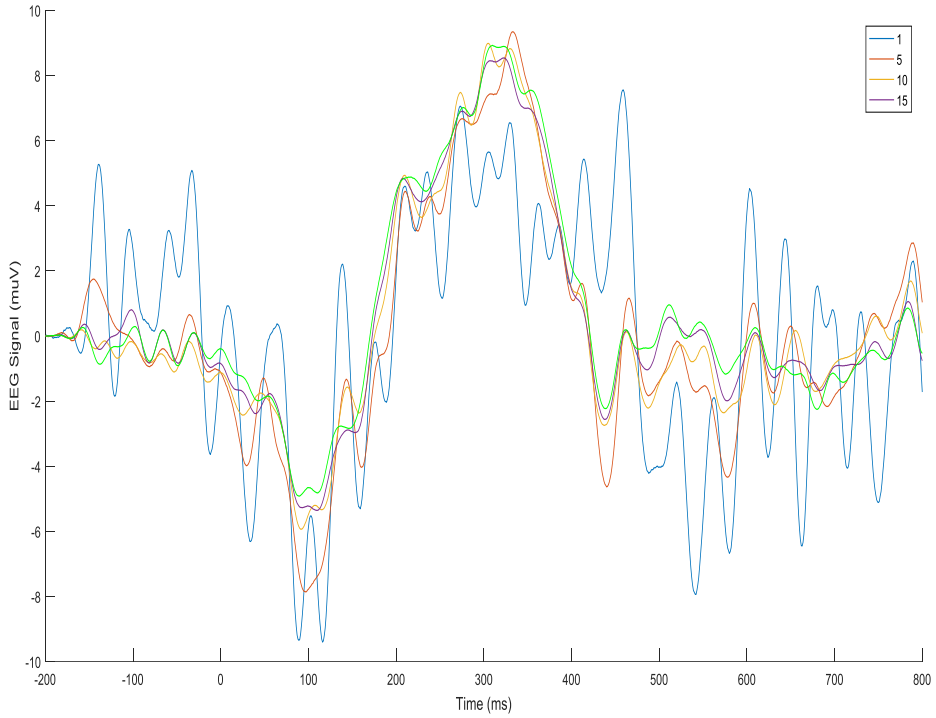

Fig 6.13a.

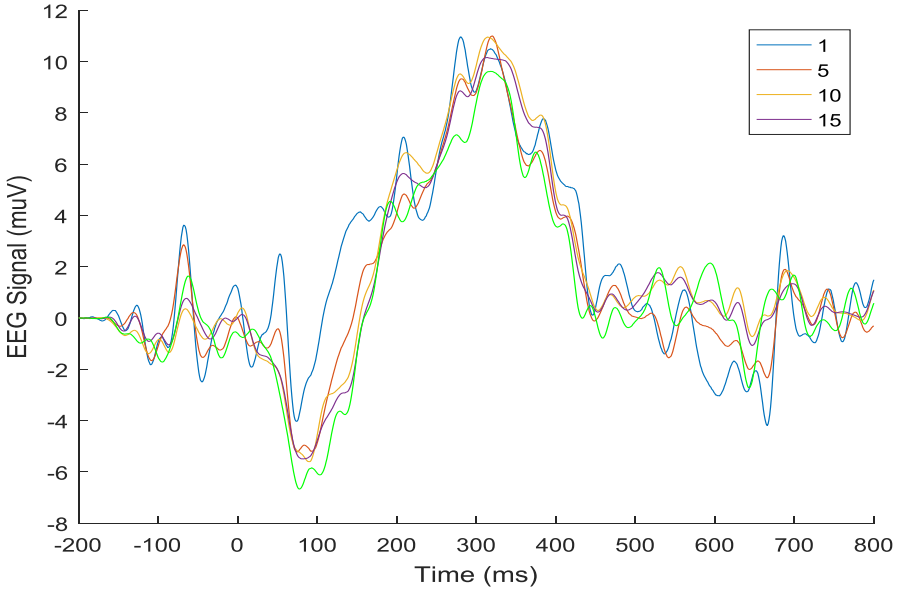

Fig 6.13b.

Figure 6.13 BOC ERP estimate using 1, 5, 10 and 15 trials; and the average of 15 trials (green). a) All trials have SNR=0 dB and b) odd trials have SNR = 5 dB while even trials have SNR = -5 dB.

A second test assumes measured ERP with SNR = 5 dB for odd numbered trials and SNR = -5 dB for even numbered trials, see Figure 6.13b. In this test the BOC method is significantly better than the unweighted average, yielding a final SNR of 12.5 dB compared to 10.10 dB for the unweighted average. BOC method effectively uses a lower weighting for the measured ERPs with lower SNR.

6.3.3 Optimal Combining of ERP PCA Projections.

The BOC method can also be applied to vectors of PCA projection weights. This reduces the rank of the matrices from 1000 to approximately 5, and so yields a considerable computational efficiency gain. However, the covariance between PCA projection weights needs to be estimated. To some extent, this removes the benefit of having a covariance linked to sample in the presence of impulsive noise. However, it has the large advantage that most of the impulsive noise will be eliminated by PCA projection, as the PCA basis signals are quite smooth. The covariance between the PCA weights is calculated from the difference between the measured signal and the PCA projected signal. The difference is assumed to be noise and equal across all PCA basis directions. Truncating the PCA projection leads to a proportionate reduction in the noise but is assumed to not affect the ERP signal.

Figure 6.14a illustrates the BOC-PCA process applied to synthetic data with APGN. The BOC method yields an uncertainty estimate for each PCA projection weight that can be translated into a standard error for each sample. Figure 6.14a shows error bars for each sample indicating the uncertainty. The uncertainty before the stimulus, and long after the stimulus, is zero as the PCA Basis signals are all zero in these regions. The uncertainty allows clinically significant parameters to be estimated, also with an uncertainty. This will be important when decision making based on ERP responses is automated.

Figure 6.14b presents the time-series of BOC PCA weights. These converge as the information from increasing numbers of trials is combined.

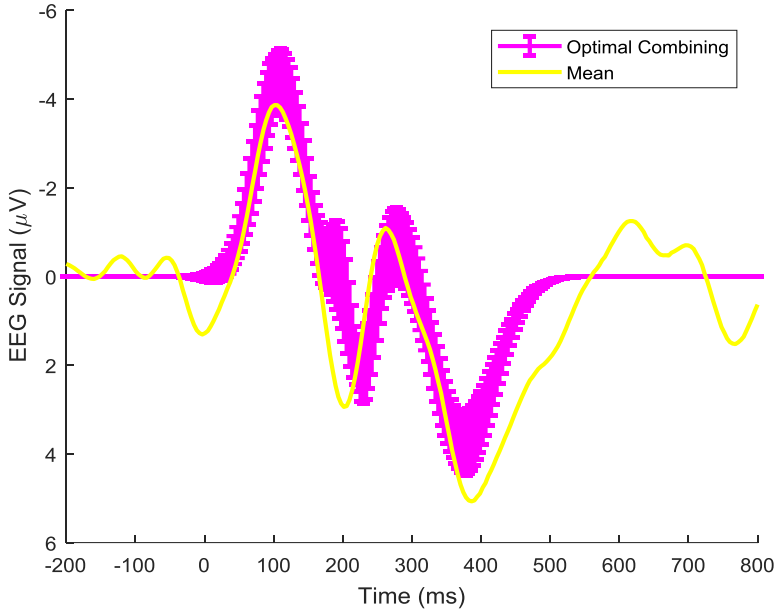

Fig 6.14a.

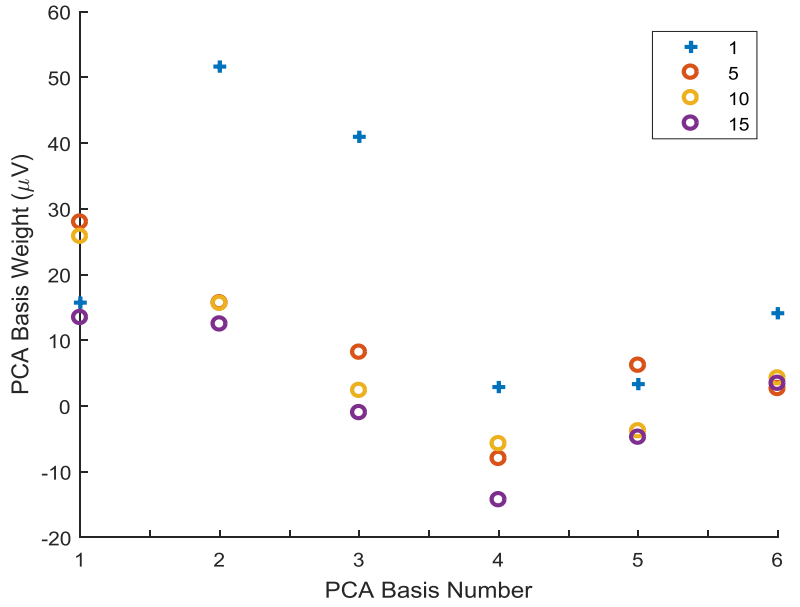

Fig 6.14b.

Figure 6.14 BOC of PCA weights to estimate the ERP: a) BOC-PCA process applied to synthetic data with APGN. and b) convergence of BOC PCA weights with increasing numbers of trials.

6.3.4 SNR Performance for different type of combining methods

A numerical experiment has been performed to compare the best estimate ERP produced by a variety of combining techniques. Synthetic multichannel data were generated for 50 trials and contaminated with band limited APGN. The SNR in dB of each trial and channel was selected randomly to be an i.i.d. sample from a Normal distribution with mean -4 dB and standard deviation of -4 dB. The unfiltered trial time series were combined using unweighted (or uniform) mean, OWM and BOC. For OWM, three techniques were used to estimate the time series noise power: the true noise power of the APGN, the power of the difference between an individual time series and the uniform mean, and the iterative method presented in Section 6.2.1. For BOC two methods were used to estimate the uncertainty: the true uncertainty from the APGN variance and the uncertainty estimated from the noise power during the period before the stimulus. Figure 6.15a illustrates the channel 1 ERPs estimated from combined trials, while Figure 6.15b presents the SNR of the combined ERP estimate, calculated by comparison with the mean of the clean synthetic data. For the majority of channels, OWM and BOC using the true noise power yielded the highest SNR. However, the true noise power is generally not available for measured data. In this case, OWM can estimate the noise by comparing with the uniform mean. This, more practical method, offered the next best results, typically less than 1 dB worse than using the true noise power. Iterative OWM tended to do slightly worse. These methods yield 1 dB to 3 dB improvement over unweighted means. BOC using a noise power estimate derived from the pre-stimulus period yielded the worst results. This 200 ms interval does not yield a good estimate of the power in band limited noise.

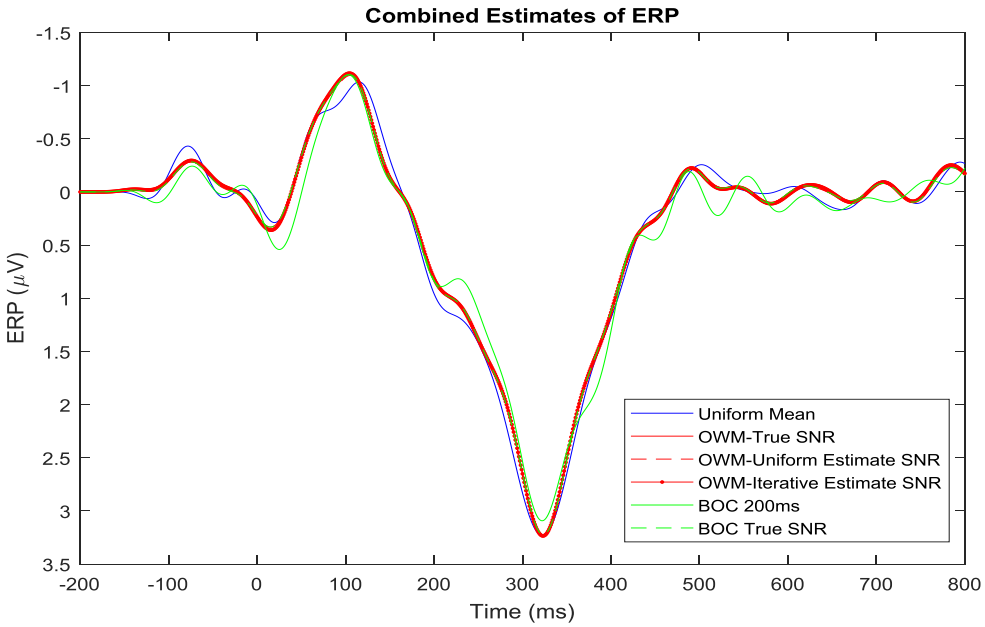

Fig 6.15a.

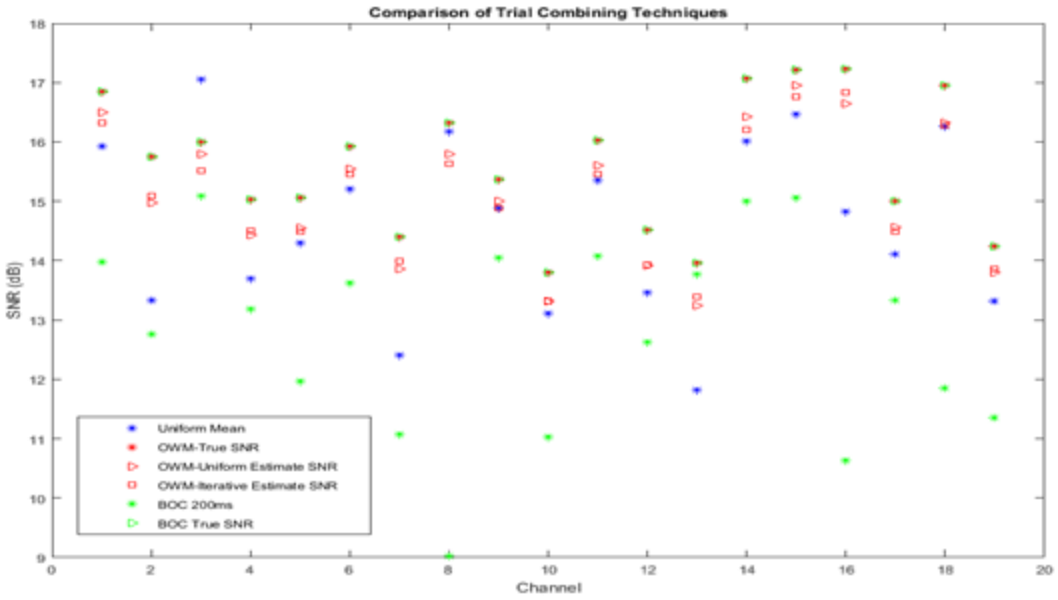

Fig 6.15b.

Figure 6.15 Comparison of Trial Combining Techniques: a) best estimate ERP and b) SNR achieved in different channels (UM is not accurate in most cases, BOC 200 ms is not good because of lots of noise before stimuli, OWM-True SNR and BOC True SNR are good but ERP signal and noise are unknown, OWM -Uniform Estimate SNR much better because of ERP signal and noise are known).

6.4 Conclusion

Two new methods for combining trial time series have been developed and tested. Both rely strongly on having a good estimate of the noise power or uncertainty in a time series. Where this is known accurately, and is uniform across a time series, then the results are very similar. For measured data, estimation of the noise power is difficult. Where the noise is not stationary across a time series, then BOC can still be used. The reliable parts of the measured signal will be used to improve the combined estimate. In the next chapter, the filtering and combining methods are applied to measured data.

Chapter 7 Estimation of Auditory ERPs from Measured Data

7.1 Introduction

Auditory event-related potentials (ERPs) are contaminated by a variety of artefacts and noise, making it difficult to separate ERPs from other brain signals, biological signals such as muscle and eye movements, artefacts due to electrode and equipment movement, and interference from other systems. In measurements from ambulatory EEG systems, the artefacts are often larger and more frequent than for a static system. However, there is increasing interest in the measurement of ERPs while individuals engage in the physical activities associated with normal living (Bateson et al., 2017).

In Chapter 5 a variety of filtering methods were developed to extract ERP signals from noisy measurements. Methods were also developed for combining ERP estimates from many trials to produce an estimate of the underlying ERP. In this Chapter, these filtering and combining methods are applied to real measured EEG data.

Measured data comes with new unknowns. In previous Chapters, the use of synthetic data meant that the correct answer was known, and so the effectiveness of methods could be quantified. With measured data this is not the case. Furthermore, KF and the combining methods require estimates of SNR or uncertainty. For synthetic data, these could be estimated accurately by comparison of signals with the correct answer, but this is not possible with measured data. New protocols need to be developed to address these problems.

The success of filtering methods often relies upon the effective use of apriori knowledge. Knowledge of the variation in ERPs informs the PCA basis that allows rejection of noise signals during PCA projection. Knowledge of the correlations of

PCA projection weights across channels allows further noise discrimination. Having an expected ERP response allows further noise rejection during KF, equivalent to Maximum A Posteriori estimation in this case as there is no tracking of parameters between trials. Processing of measured data requires careful use of apriori knowledge to reject noise but not to force the observations to have ERP characteristics when there is no measured evidence to support it.

The following Chapter proposes and tests a filtering and combining protocol for measured data. Starting with a set of trail ERP measurement time series, the steps are as follows:

1. Fit the N100, P200 and P300 amplitude and delay parameters of the synthetic ERP generator to the measured multichannel ERP averaged over trials;
2. Use the new synthetic ERP generator to produce a PCA basis for the multichannel data;
3. Use PCA projection, or PCAKF, to filter each measured trial time series;
4. Compare each filtered trial with the uniform average or synthetic ERPs to estimate the noise;
5. Use combining techniques to estimate the underlying ERP.

7.2 Fit Synthetic Model to Real ERP Data

The multi-channel ERP simulation presented in Chapter 5 has parameters chosen to match ERPs published in (Debener et al., 2012; Luck, 2005). However, ERPs measured using the Hull AEEG system yielded N100s and P300s with different amplitude and latency. In practise, we would expect these to vary between individuals. When analysing ERP time series from an individual, allowance needs to be made for the exact placement of electrodes on the scalp, head and brain morphology etc. Earlier chapters showed that measured ERP time series are too noisy for the estimation of PCA bases. Therefore, to produce PCA bases customised for an individual's set of measurements, it is necessary to adapt the synthetic ERP generator to their

particularities. The generator has 66 parameters describing the absolute and relative amplitudes of the three ERP peaks, their delays and widths, and the typical variability. Fitting all these parameters to data from an individual would yield unreliable results and so 60 of the parameters are assumed to be fixed. These parameters are the relative amplitudes, widths and variation of the peaks. They are estimated once from the cleanest data available i.e. the average of all trials and all participants. This process has been performed in several stages:

1. The typical channel variation of N100, P200 and P300 relative amplitudes has been estimated by fitting to multichannel ERPs calculated by averaging over data from 9 individuals and all oddball trials. The relative amplitudes are assumed to be consistent between individuals.
2. Typical variation in N100 and P300 absolute amplitudes and delays are estimated by fitting multichannel simulated data to averages over all oddball trials for all 9 individuals separately.
3. Finally, an individual's N100, P200 and P300 absolute amplitudes and delays are estimated by fitting multichannel simulated data to averages over all oddball trials for an individual.

Steps 1 and 2 need only be done once. Step 3 is repeated for each new set of data.

Figure 7.1 illustrates the step 1 process, identifying relative channel N100 and P300 amplitudes and delays. Data from the 9 participants while sitting in the shielded room, were averaged to yield the cleanest set of multichannel ERP responses available. The relative amplitudes N100, P200 and P300 were estimated by fitting synthetic ERPs to these multichannel data. The fit is not perfect due to noise on the channels and also because some parameters are assumed to be consistent across channels i.e. N100, P200 and P300 delay.

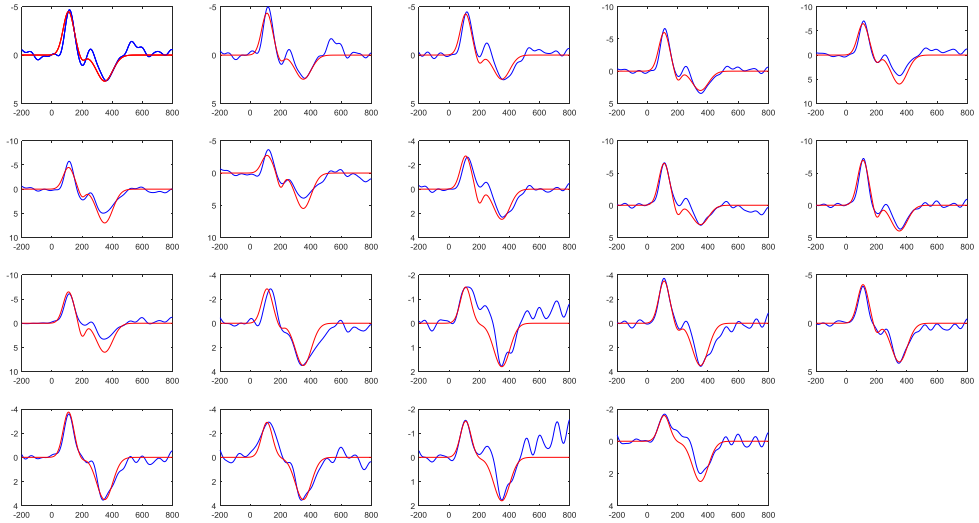

Figure 7.1 Synthetic ERP (red) amplitudes' and delays' fitted to the average ERP from 9 individuals and many oddball trials (blue), collected using an AEEG system while participants sat in a shielded room.

The estimated N100, P200 and P300 delays are: $\bar{t}_j = \{86,200,385\}\, ms$ and the peak widths, which were not fitted, are kept at the original estimates from published data: $\sigma_j = \{50,30,75\}\, ms$. For the 3 Gaussians representing N100, P200 and P300, the 19 channel relative amplitudes were:

$$\bar{A}_{ij} = \begin{bmatrix} 90 & 87 & 85 & 120 & 130 & 90 & 55 & 55 & 130 & 140 & 130 & 57 \\ 15 & 17 & 23 & 38 & 40 & 40 & 55 & 30 & 40 & 50 & 70 & 10 \\ 27 & 25 & 25 & 30 & 60 & 70 & 55 & 25 & 30 & 40 & 60 & 35 \end{bmatrix} \cdots$$

$$\begin{bmatrix} 30 & 70 & 80 & 75 & 58 & 30 & 32 \\ 01 & 15 & 25 & 05 & 01 & 01 & 01 \\ 18 & 35 & 40 & 35 & 35 & 18 & 25 \end{bmatrix} \times$$

$$10^{-2}\, \mu V \qquad [7.1]$$

Step 2 sets the variation in N100 and P300 absolute amplitudes and delays by fitting multichannel simulated data to averages over all oddball trials for each of the 9 individuals separately. Table 7.1 presents the delays estimated by fitting to individual's mean multichannel ERPs. The variation between individuals is expected to be representative of the variation between experiments. Note that fitting yielded

implausible results on some occasions i.e. N100 for participant 2 occurred before the stimulus. This is due to fitting to noise artefacts. The results from S3 and S7 were considered too unreliable for inclusion in the variance estimation as the average over all trials exhibited large noise variation before the stimulus.

Table 7.1 Delays in ms for the three Gaussians, fitted to the mean oddball response for 8 individuals.

Subjects	N100	P200	P300
S1	110	222	308
S2	-68	251	343
S4	106	202	354
S5	117	174	568
S6	105	205	376
S8	112	168	461
S9	124	180	316
S10	87	56	354
Mean	87	182	385
Standard deviation	59	54	82

The previous two steps fixed the majority of the parameters in the ERP generator. The final step fits the six parameters to data from and individual. These six parameters describe the grossest and most easily observed variation i.e. the absolute amplitude

and delay of the three major ERP peaks. These are estimated from to the mean ERP response from all channels for that individual. Figure 7.2 shows a single trial of synthetic multichannel ERP responses generated using this process for the participant labelled as S1. This process has been performed using the data expected to be cleanest i.e. while sitting in the shielded room. The same ERP variation is expected when the participant is active and in more stimulating environments, albeit measured with much larger amounts of noise. Data collected during activity was so noisy that including it in the mean increase uncertainty. The PCA bases calculated from data produced using the fitted synthetic generator and these are assumed to represent the possible ERPs present during activity.

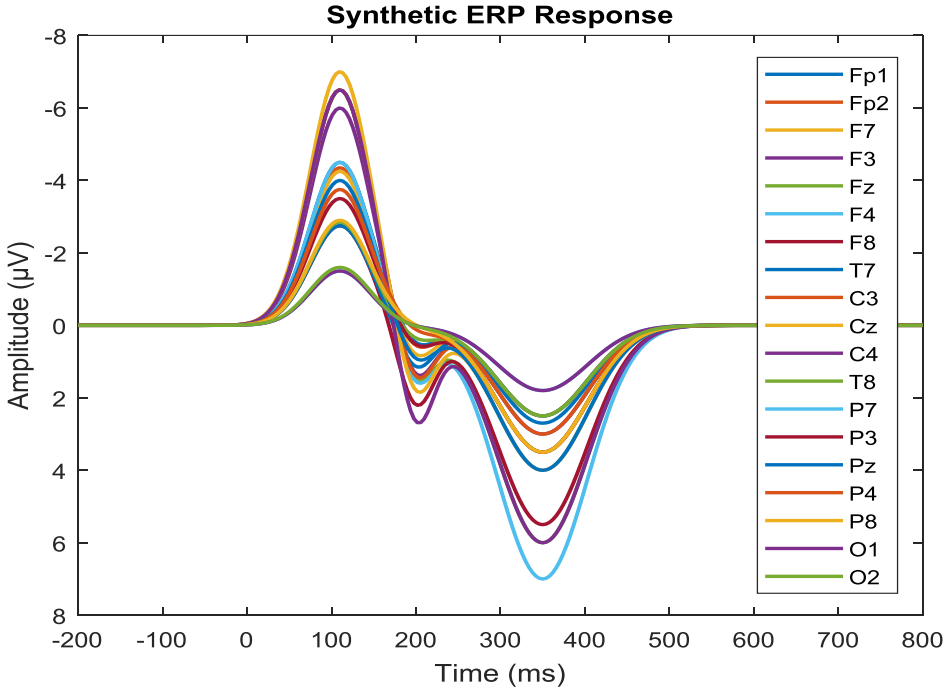

Figure 7.2 New synthetic ERPs using parameters fitted to measured ERP. Three parameters for N100, P200 and P300 specify the amplitude, centre time and width of each of the Gaussian pulses respectively for 19 channels across the head.

7.2.1 PCA Basis for each Channel of the ERP signal.

The PCA basis is calculated from the synthetic ERP data for each channel. Each channel ERP signal can then be expressed as a weighted sum of PCA basis signals.

Finally, the covariance of channel PCA basis weights is calculated. Each trial time series is projected onto the PCA basis and the weights formed into a vector. The covariance of these vectors is a constraint when estimating PCA weight vectors from measured data.

Once the PCA bases have been calculated, along with the mean and covariance of the vectors of PCA projection weights, it is possible to perform PCA and PCAKF filtering on measured data.

7.2.2 Estimation of ERP Response from measured data

Different filtered versions of the measured ERP trial data are possible. These are the outputs of ADJUST, PCA projection and PCAKF filtering. These data can then be combined using a range of methods and a range of noise estimation techniques. Unlike the results in Chapter 6, the true ERP response is not known for measured data, and so results are judged by their plausibility. Four classes of combining methods are tested:

1. Estimate the underlying ERP signal using uniformly weighted average from both the real and fitted-synthetic data.
2. Estimate the underlying signal using optimal weighted mean (OWM), using a noise power calculated from the difference between filtered trial signal and uniform mean of the measured data (OWM-UN). Alternatively, estimate the noise power from difference between the trial signal and uniform mean of the synthetic data (OWM-SN).
3. Estimate the signal using Bayesian optimal combining (BOC) using an uncertainty estimated from the uniform mean of measured trials as above (BOC-UN), or from the uniform mean of synthetic data (BOC-SN).

4. Estimate signal using Bayesian optimal combining (BOC) with an uncertainty estimated from the difference between the trail time series and the OWM-UN estimate (BOC-OWM-UN).

The combining methods in the protocol above were applied to the three filtered sets of measured ERP time series i.e. after ADJUST, PCA and PCAKF. The measured data came from S1 while sitting in the shielded room, as these are expected to be the cleanest data. Fifty oddball trials were recorded. When the best combination of filter and combining methods has been identified, data collected during activities will be analysed.

The clarity of the P300 will be used to judge the combined filtered ERP estimates. P300 is most visible on the channels inside the blue square in Figure 7.3, as this is over the part of the brain where the response is generated and far from major noise sources, such as the eyes, which particularly effect channels Fp1, Fp2. The response becomes weaker when measured at the back of the head on channels O1 and O2.

Figures 7.4 to 7.6 illustrate the estimated ERP signals for channels 10 and 15, corresponding to Cz and Pz. These are channels are expected to show clear P300 features. The gross features in Figures 7.4 and 7.5, using filters PCA and PCAKF respectively, are very similar for all combining methods. All combinations of filtering and combining methods yielded the same delays for N100, P200 and P300. The relative amplitudes of the three peaks were maintained by all the methods. Figure 7.6 uses the EEGLAB ADJUST filter and is the poorest result. PCA projection automatically zeros the ERP before the stimulus and produces an estimate where the signal decays to zero after the P300 peak. ADJUST does not do this and so large noise oscillations dominate before the stimulus and at times after 400 ms. This noise is also present during the response interval from time = 0 ms to 400 ms. All combining

methods have performed similarly, but the uniform mean exhibits the largest noise oscillations. This is due to large noise variation between trials. The OWM and BOC methods automatically reduce the impact of the noisiest trial time series, yielding superior ERP estimates.

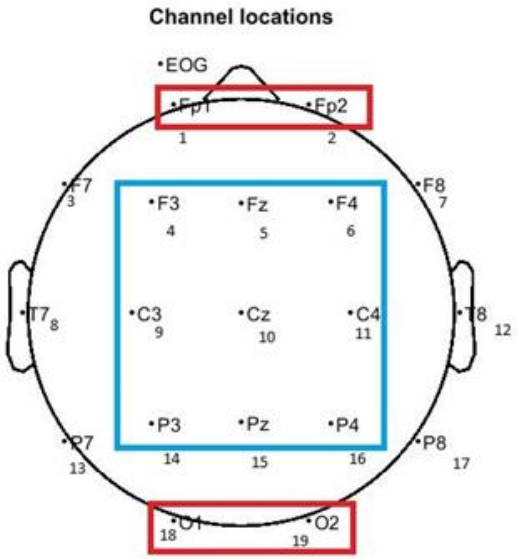

Figure 7.3 Electrode placement 10-20 system – in blue colour ERP signal appear clearer than red colours.

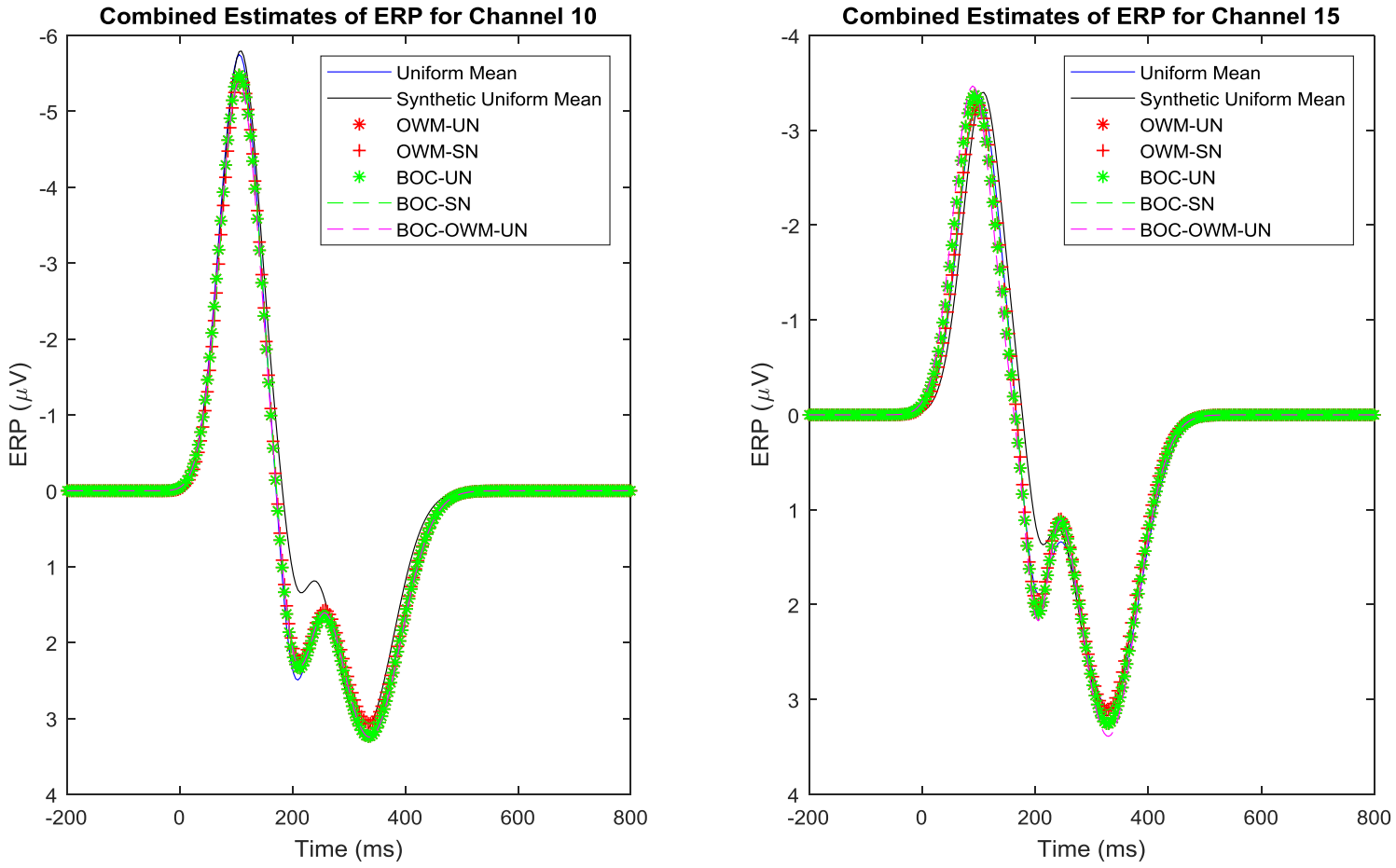

Figure 7.4 Different methods of ERP combined estimation for middle electrodes of the head after PCA filtering.

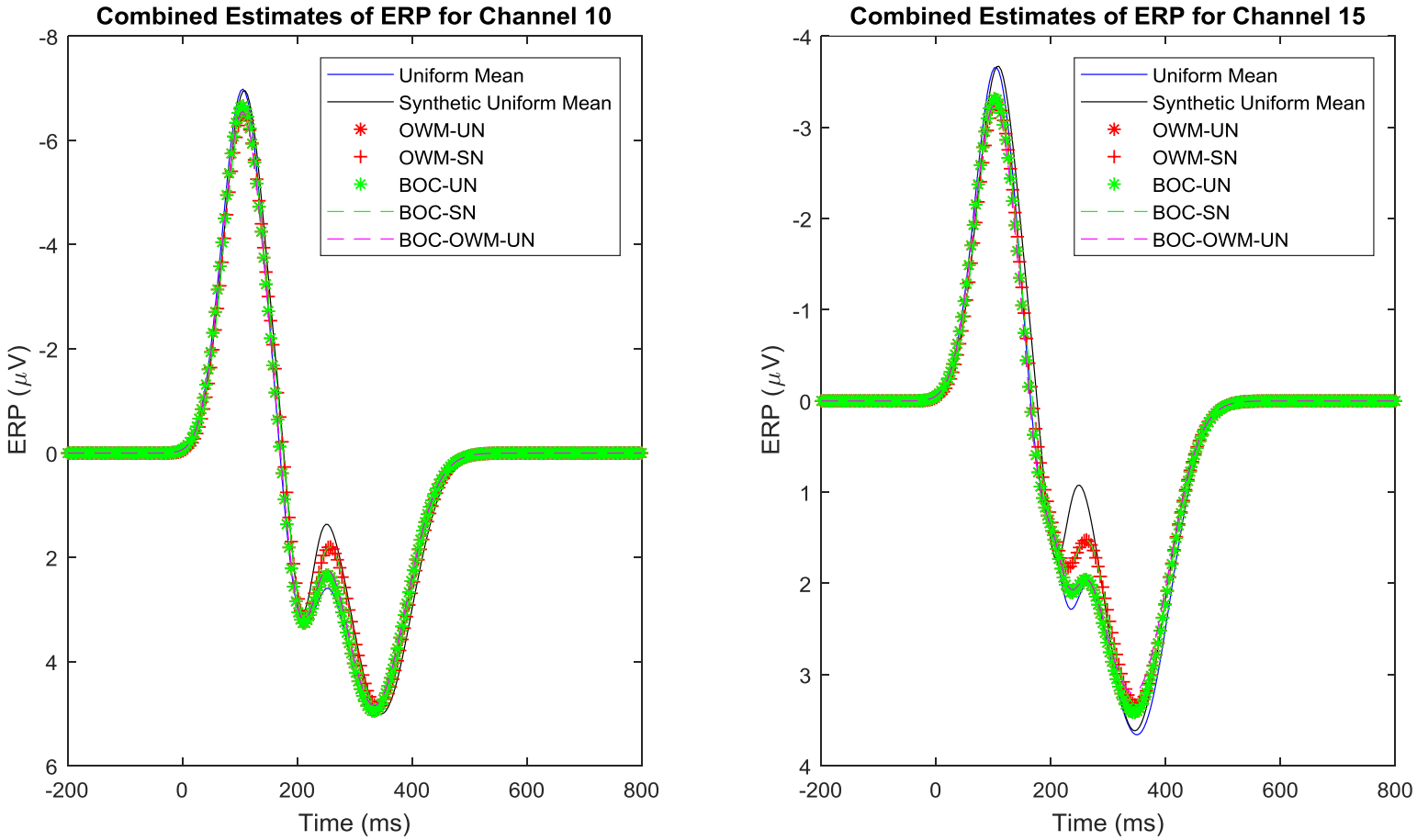

Figure 7.5 Different methods of ERP combined estimation for middle electrodes of the head after PCAKF filtering.

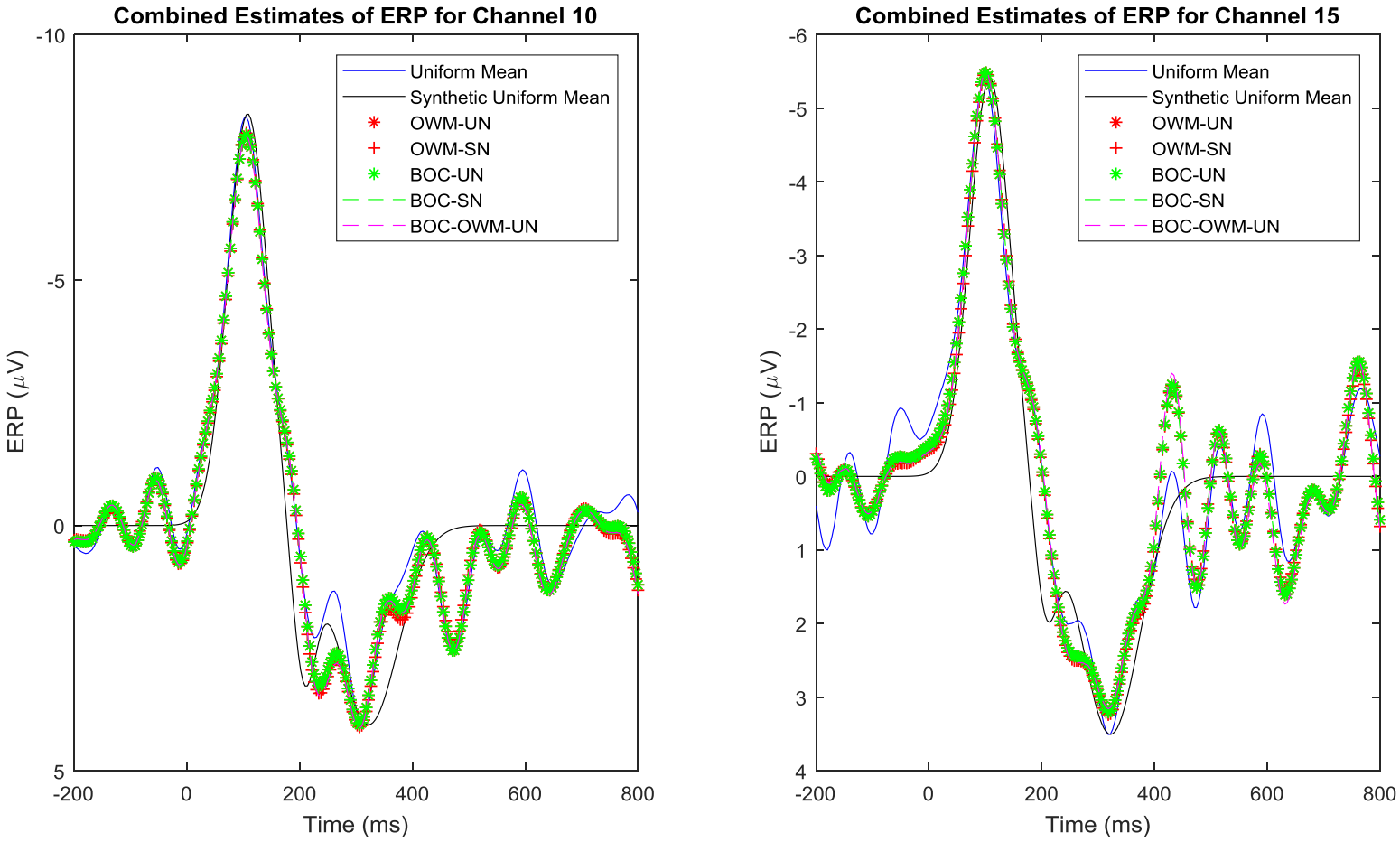

Figure 7.6 Different methods of ERP combined estimation for middle electrodes of the head after ADJUST filtering.

Figures 7.7 and 7.8 illustrate the estimated ERPs for channels 1 and 19, corresponding to FP1 and O2. These channels are expected to measure weak auditory ERPs and are strongly affected by noise. Fp1 experiences strong eye blink artefacts generated by the muscles around the eyes. O2 is over the optical processing part of the brain and so and visual stimuli leads to brain signals unrelated to the auditory stimulus. Figure 7.7 presents the combining results after PCA projection. Due to the variability in noise power across the trials, and the deviation of the synthetic signal from the measurements, there is more variation between combining results. The combining methods tend to agree very well on the time and amplitude of the N100 peak but vary more for the P200 and P300, where other stimuli are likely to have cause unrelated brain responses. The _SN methods yield a higher amplitude P300 as they follow the synthetic data more closely. The _SN results favour signals that match across channels. The positive peak at 300 ms in channel 1 is consistent with the strong peak identified by all methods in channel 19. The negative peak at 400 ms is present in all optimised combining techniques but not present in the uniform mean at all. The plausibility of the existence of this peak is strengthened by its presence in channel 19. That it is not present in channels 10 and 15 suggests it is a brain signal generated near the rear of the head. Figure 7.8 illustrates the ADJUST combined ERPs. As previously, these are far noisier than those after PCA filtering. For O2, all combining methods exhibit a clear P200 where there is none in the synthetic signals.

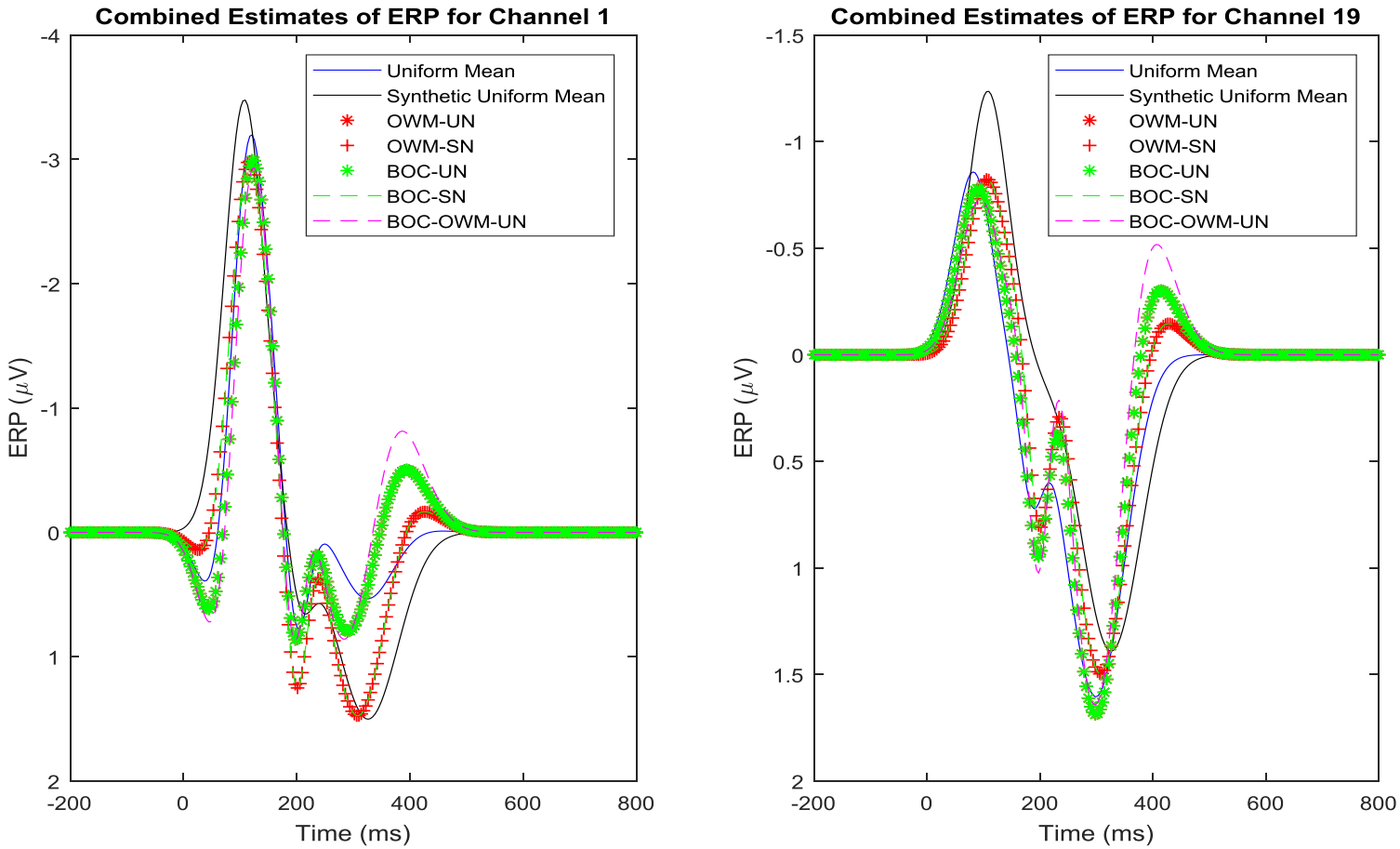

Figure 7.7 Different methods of ERP combined estimation for front and back electrodes of the head after PCA filtering.

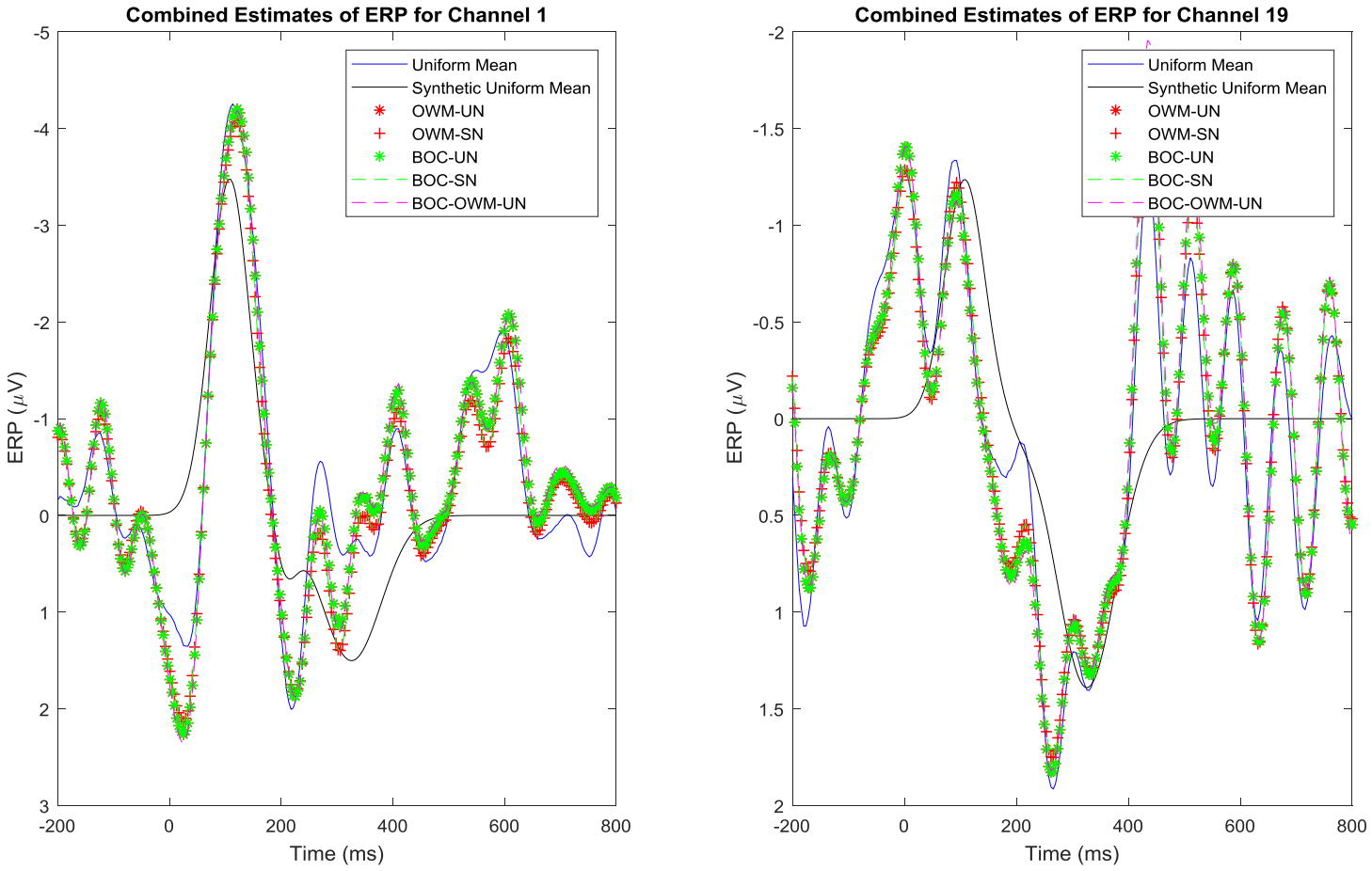

Figure 7.8 Different methods of ERP combined estimation for electrodes at the front of the head after ADJUST filtering.

7.3 Conclusion

The PCA and PCAKF filtering yields significant advantages over the EEGLAB standard ADJUST filtering. After PCA projection the ERP time series are much more plausible and have significantly less noise, due to the rejection of non-ERP signal components. All optimised combining methods perform better than uniform mean, sometimes allowing clinically important features to be seen where they could not be seen using the standard uniform mean. The methods that rely upon the synthetic generator can yield distorted outputs when the synthetic signal is very different from the measurements. For this reason, the BOC_OWM_UN method has been chosen for evaluating ERPs collected in more stimulating environments and during activities. In the next chapter, BOC_OWM_UN will be applied to real data collected during a range of activities and in different environments, to determine how many trials are need to observe clinically important features.

Chapter 8 Quantification of Trials Needed to Observe Clinically Important Features in ERPs

8.1 Introduction

A number of previous studies address the question: how many trials are required for the reliable observation of certain ERP components, under given conditions. Most reports are based on measurements made in ideal clinical conditions i.e. the participant reclined and immobile in a quiet and plain room. To reliably observe P300, a minimum of 36 usable trials (after artefact rejection or correction) in each stimulus category is recommended by (Luck, 2005). Eye-blink artefacts lead to trail rejection, and so the total number of trials could be significantly increased. However, (Polich, 1986) suggested that 20 trials were sufficient for observing the P300 in an oddball paradigm. He stated that 20 trials yielded reliable results and that no benefits were seen if the number of trials was increased (Cohen & Polich, 1997). Bruder et al said that after an average of 20 oddball ERPs trials P300 amplitude seemed to be statistically steady (Bruder et al., 1995). After applied and clinical examination of P300 amplitude and latency, (Humphrey & Kramer, 1994) concluded that there are only insignificant changes in P300 amplitude after 30 target trials or more. The results of Boudewyn's study demonstrate that there are several factors that should be considered in determining the number of trials needed in a given ERP experiment, and that there is no magic number of trials that can yield high statistical power across studies (Boudewyn et al., 2017).

Many parameters may affect the SNR in EEG signals, such as equipment, recording settings, paradigm, age and subject status, even control or individual participants (Luck

& Todd, 2004). It is not clear how these results translate into AEEG data from active participants in high sensory environments, and for features smaller than P300.

8.2 Aim of Chapter

The measurement of ERPs has clinical applications in the diagnosis and monitoring of psychiatric and neurological patients, see section 1.3. However in many circumstances it may be difficult to follow the standard measurement protocol, e.g. for subjects with mental health problems, for children, or for subjects that may not wish to cooperate. For measurements with ambulatory EEG, the ERP measurements exhibit intermittent and very large noise artefacts. In both these scenarios, it is important to be able to minimise the number of repetitions required to identify the important features in the processed ERP signals; or alternatively to produce the best estimate of the underlying ERP response from the set of measured ERP signals.

Historically, ERP signals have been pre-processed to reduce artefact noise. This may require whole trials to be discarded if too highly contaminated. Then the processed signals are combined to produce an estimate of the underlying ERP signals. Typically, this has been achieved using a simple average.

This chapter presents ERP measurements made following the protocol presented in Chapter 3. The data are analysed to produce estimates of the underlying ERP signal using PCA projection followed by BOC_OWM_UN combining. The convergence of ERP estimates to the best estimate formed using all the trial data, is examined to determine after how many trials the important clinical features could be reliably observed.

8.3 Estimating ERP Response from EEG Measurements

The aim of data processing was to identify features in the oddball ERP response from complex AEEG signals. AEEG signals contain large signals from sources other than the

brain, particularly EOG signals due to eye-movement. Participant brains are also engaged in activities other than listening for oddball responses, such as processing what the participant sees and hears, along with navigation and interaction with other people. Additionally, AEEG signals contain artefacts due to movement of the electrodes and interference with other systems.

Following the protocol presented in Chapter 3, subjects were exposed to a series of auditory stimuli in a range of environments. The stimuli were either a common or oddball tone, produced by the smartphone and presented through earphones worn by the participant. A time interval spanning each tone was recorded as a trial. Each trial started 200 ms before the start of the tone and ended 800 ms after. Typically, each trial recording contains the common or oddball response signal plus many other signals due to brain processes, other processes such as eye movements, and artefact noises.

For each individual subject, the synthetic ERP generator was fitted to the uniform mean of ERPs from the sitting inside dataset, as described in Section 7.2. The PCA bases were then generated, along with the PCA weight covariance matrix, specific to each individual. All ERP data is then PCAKF filtered using each individual's multichannel ERP variation. Finally BOC_OWM_UN combining is applied to subsets of trials collected in different activities and environments. Initially, all trials from an individual-activity-environment are combined to provide a reference set of ERP parameters. Then a sequence of smaller subsets are tested. Every subset size from 2 to 50 trials were tested, with 50 subsets of randomly chosen trials were tested for each subset size. Figures 8.1 and 8.2 show the convergence of the P300 amplitude and delay estimates to the results using all the trials, as a function of subset size. It can be seen that the delay estimates are more precise than amplitude estimates. The delay estimates have a 5% uncertainty for subsets of size 20 or more while the amplitudes have an uncertainty of 10% for the same number of trials. The increase in precision was very slow for increasing numbers of trials above 20. This

experiment has been repeated for all participants and each of the four scenarios, to determine the subset size to yield delay and amplitude uncertainties of 5% and 10% respectively.

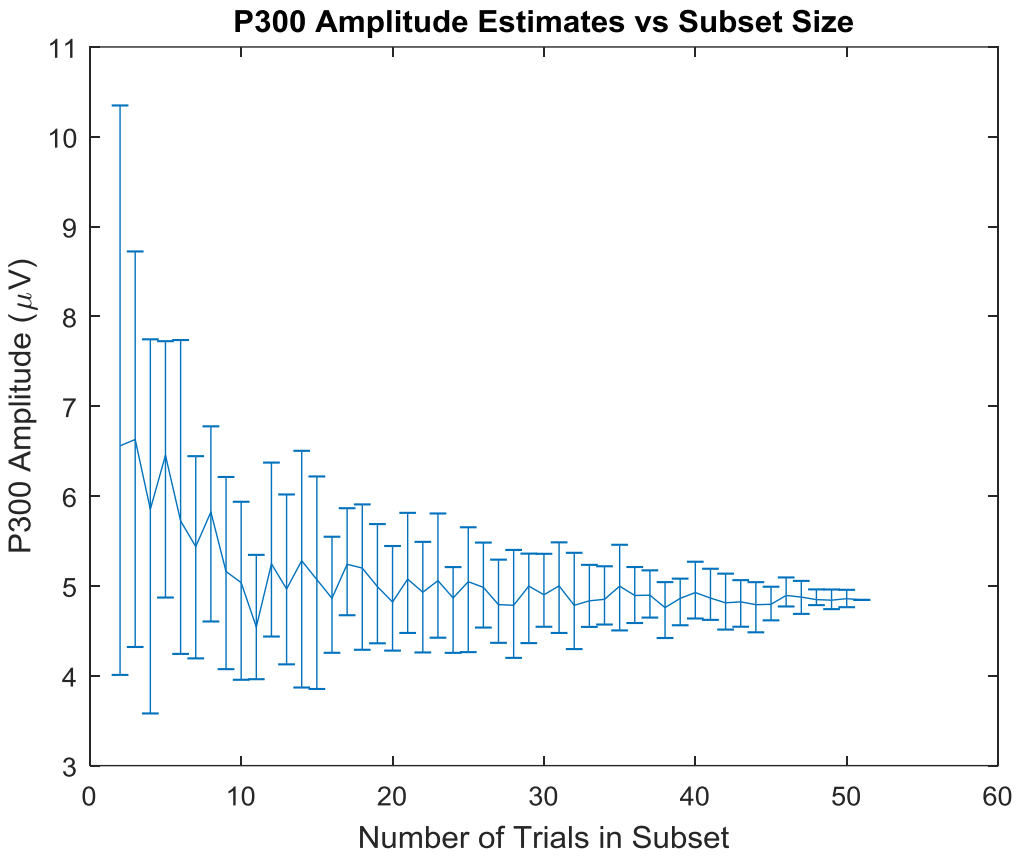

Figure 8.1 P300 amplitude estimates vs subset size. Error bars indicate mean and quartiles. It can be seen P300 amplitude from 4.5- 6.5 µV 15% error.

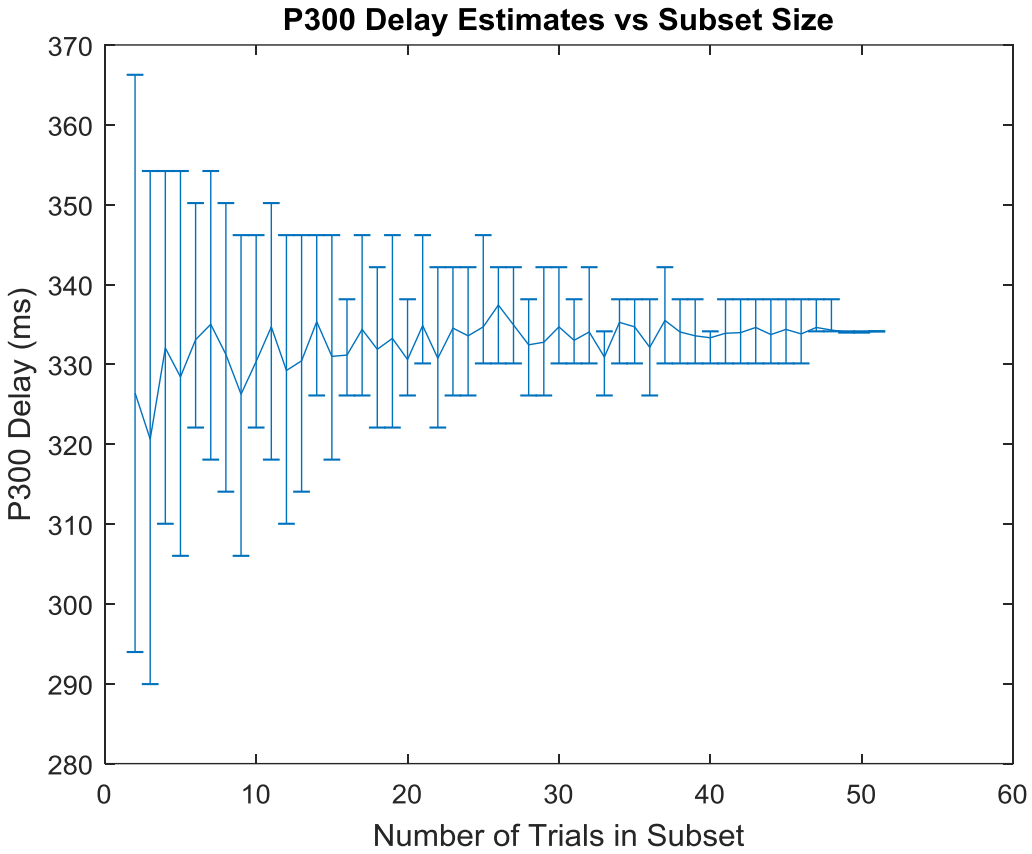

Figure 8.2 P300 delay estimates vs subset size. Error bars indicate mean and quartiles. It can be seen P300 delay from 320- 340 ms 15% error.

Figure 8.3 illustrates the combined ERP for participant S4 estimated while sitting in the shielded room from 12 trials after PCAKF with BOC_OWM_UN compared with 16 trials ADJUST with uniform mean. This is the smallest number of trials that yielded a consistent P300 amplitude and delay for this individual under these conditions.

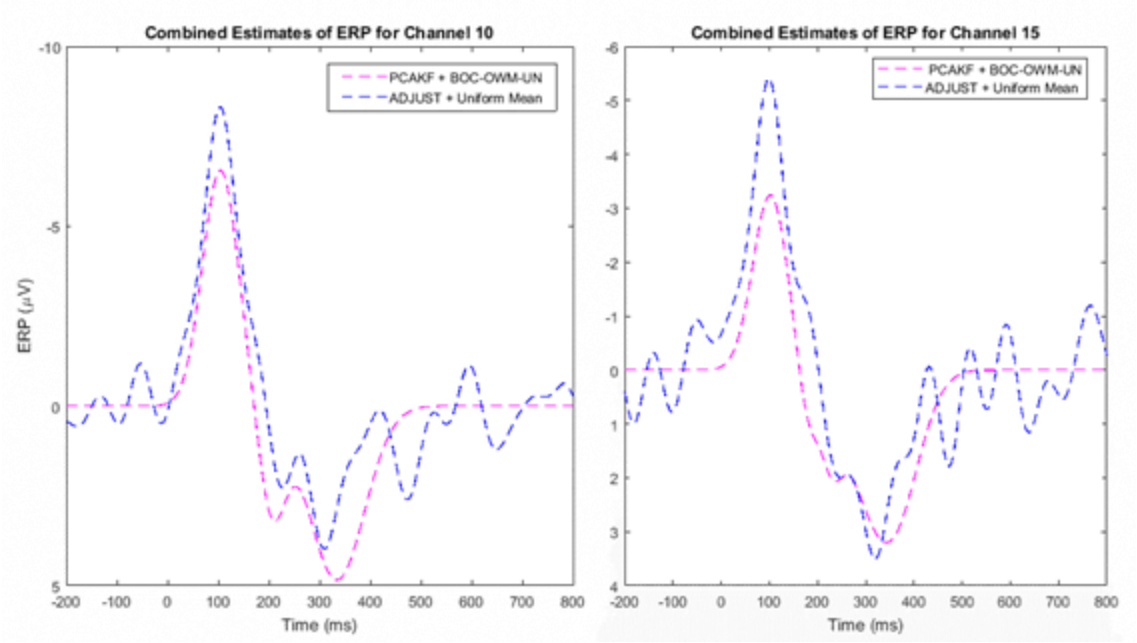

Figure 8.3 Comparison of estimated ERPs, after the standard and the proposed filtering and combining protocols. Combining protocols forcing the ERP signal to be zero before the stimulus and after the expected ERP response.

Table 8.1 lists the smallest number of trials, for the 8 individuals and the range of activities and environments, needed for a consistent P300 amplitude and delay estimate. It can be seen in table 8.1 that the number of repetitions needed to measure the P300 parameters in channels Cz and Pz varies from subject to subject, activity to activity (sitting or walking) and from environment to another environment inside shielded room or outside (in laboratory). In all but one case an increasing number of trials is required as the individual changes from sitting to walking and from inside to outside. Walking leads to movement of the electrodes, leads and equipment; and so more movement artefacts are present compared to sitting. Some muscle noise is also generated by the neck muscles maintaining the head position. Walking requires some brain control, leading to contaminating brain signals. Being in the more stimulating environment outside the shielded room causes more brain activity due to processing of other auditory and image stimuli.

Table 8.1 Number of trails need to be combined to observe P300 amplitude and delay using PCAKF with BOC_OWM_UN, compared with ADJUST and uniform mean in brackets ().

Subject	**Activities**			
	Sitting Inside	**Sitting Outside**	**Walking Inside**	**Walking Outside**
S1	17(23)	20(26)	30(37)	35(42)
S2	8(12)	10(17)	15(20)	23(26)
S4	12(16)	15(19)	18(22)	24(28)
S5	20(23)	23(30)	27(31)	32(36)
S6	6(12)	10(16)	13(20)	15(23)
S8	21(27)	19(25)	22(27)	27(31)
S9	5(14)	8(17)	11(15)	15(19)
S10	13(20)	15(24)	20(24)	25(31)
Mean	**12.8(16.3)**	**15(21.8)**	**19.5(24)**	**24.5(28.3)**
Range	**5 – 21 (12 – 27)**	**8 – 23 (16 – 26)**	**11 – 30 (15-37)**	**15 – 35 (19 – 42)**

Figures 8.2 compares the two processing protocols, for the 8 participants and the four scenarios. In all cases the proposed processing protocol reduces the number of trials required, typically by 20 to 30%. It can also be observed from the estimated ERPs in Figure 8.1, that even when the standard processing protocol yielded consistent P300 parameters, the uncertainty indicated by the noise before the stimulus and after 400 ms would suggest that a greater number of trials was necessary.

Single-tailed statistical hypothesis tests has been performed to determine whether PCAKF with BOC_OWM_UN yields estimates of P300 parameters in fewer trials than ADJUST. With a level of significance of α=0.05, there is statistically significant evidence that the proposed protocol requires fewer trials, in both sitting environments. The evidence of

superiority in the two more stimulating environments is not quite statistically significant. The table below provides the P-values which are the probability that the performance of the two protocols is purely due to chance. A low P-value is evidence that the performance of the protocols is systematic

Activities	Sitting Inside	Sitting Outside	Walking Inside	Walking Outside
P values	0.029	0.0053	0.071	0.082

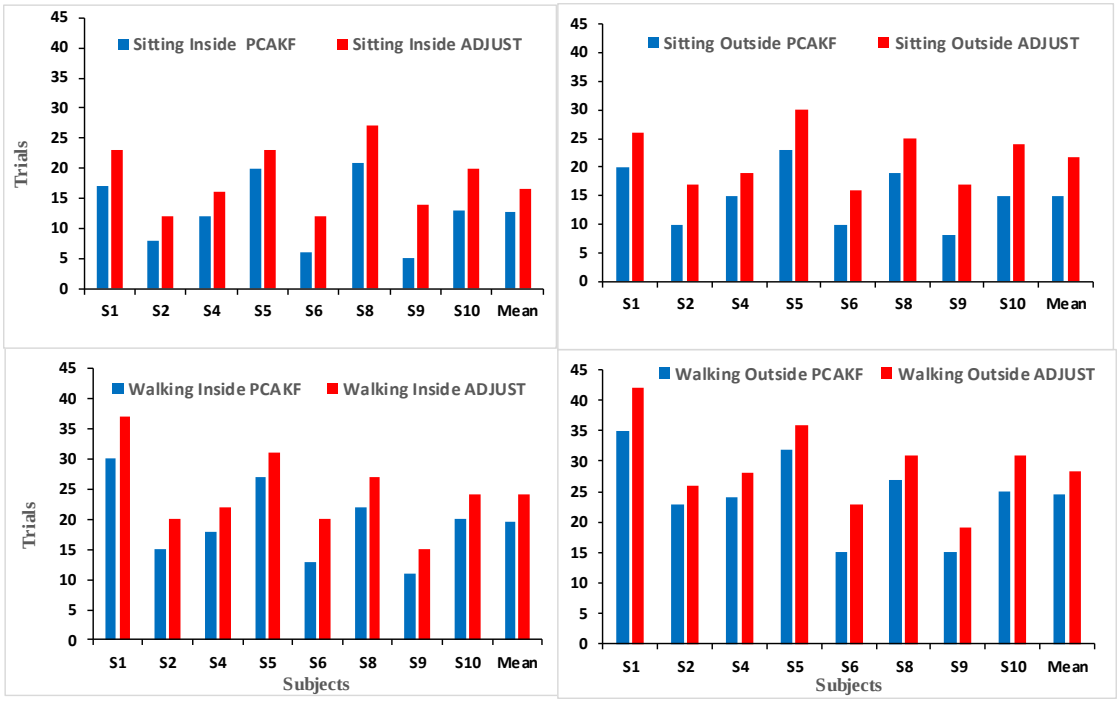

Figure 8.4 Number of Trials to observe P300 in different filters and environments.

8.4 Discussion

Usually some pre-processing, either manual or automatic, is needed to remove artefacts from measured ERP recordings. Linear filtering removes artefact components that are outside the ERP frequency band. However, more sophisticated filters are required to reduce the influence of artefacts so that ERP parameters can be identified in an acceptably low number of trials. If too many repetitions of the stimulus are required then the experiment becomes expensive, or impractical with some participant categories.

To reliably observe P300, a minimum of 36 usable trials (after artefact rejection or correction) in each stimulus category is recommended by (Luck, 2005). Eye-blink artefacts lead to trial rejection, and so the total number of trials could be significantly increased. However, (Polich, 1986) suggested that 20 trials were sufficient for observing the P300 in an oddball paradigm. He stated that 20 trials yielded reliable results and that no benefits were seen if the number of trials was increased (Cohen & Polich, 1997). Bruder et al said that after an average of 20 oddball ERPs trials P300 amplitude seemed to be statistically steady (Bruder et al., 1995). After applied and clinical examination of P300 amplitude and latency, (Humphrey & Kramer, 1994) concluded that there are only insignificant changes in P300 amplitude after 30 target trials or more. The results of Boudewyn's study demonstrate that there are several factors that should be considered in determining the number of trials needed in a given ERP experiment, and that there is no magic number of trials that can yield high statistical power across studies (Boudewyn et al., 2017).

Many parameters may affect the SNR in EEG signals, such as equipment, recording settings, paradigm, age and subject status, even control or individual participants (Luck & Todd, 2004). It is not clear how these results translate into AEEG data from active participants in high sensory environments, and for features smaller than P300.

8.5 Conclusions

Historically, ERP studies have used simple uniform means of trials to estimate ERP responses. Under ideal conditions, 20 to 30 trials are needed to estimate P300 parameters. The signal processing protocol developed in Chapters 5 and 6 has been applied to AEEG data collected while participants sit or walk, in a low or high stimulus environment. Even while walking in a high stimulus environment, the processing protocol allows P300 amplitude and delay to be accurately observed with as few as 15 trials and an average of

only 24.5. While inactive in a low stimulus environment the number of trails required is around 12 and can be as low as 5.

The processing protocol has two classes of applications. Firstly, if applied to clinical data collected in ideal conditions it greatly reduces the number of trials required to measure clinically important parameters. This represents a significant saving in time and money if applied to all ERP studies. Furthermore, it may make some ERP studies possible where the subjects are not cooperative. Secondly, it allows ERPs to be measured while participants engage in a wide range of activities in stimulating environments. This allows new science as meaningful EEG data can be acquired while participants engage in their normal daily activities, or in special activities designed to highly specific conditions.

Chapter 9 Discussion, Conclusions and Future Work

9.1 Discussion

Compared with other biomedical signals, EEG is extremely difficult for an untrained observer to understand, partially because of the spatial mapping of functions onto different regions of the brain and electrode placement. Data processing techniques can aim human interpretation by extracting clinically important parameters such as P300 delay and amplitude. Feature extraction followed by pattern recognition has also been used, as in automated spike detection during the monitoring for epileptic seizure activity. In early attempts to show a relationship between the EEG and behaviour, analogue frequency analysers were used to examine the EEG signals (D'Alessandro et al., 2003). Initially, only linear methods were applied to separate EEG signals from noise, and to identify artefacts. Principal component analysis (PCA), independent component analysis (ICA) and linear discriminant analysis (LDA) are well-known methods for feature extraction and data compression transforms the existing features into a lower-dimensional structures. This reduces the feature redundancy in measured signals (Cao et al., 2003; Widodo & Yang, 2007). These methods also allow the use of prior knowledge to distinguish signal from noise and artefacts. Independent Component Analysis (ICA) has been proven to be an effective data driven method for analysing EEG data, separating signals from temporally and functionally independent brain and non-brain source processes and thereby increasing their definition (Artoni et al., 2018).

Electroencephalography (EEG) is a widely used experimental technique to investigate human brain function by tracking the spatio-temporal neural dynamics correlated to experimentally manipulated events (Niedermeyer & da Silva, 2005). However, a major

problem common to all EEG studies is that the activity due to artefacts is typically much higher in amplitude than those generated by neural sources. Artefacts may have a physiological origin as eye movements or muscle contractions, or non-biological causes as electrode high-impedance or electric devices interference (Croft & Barry, 2000). In a typical event-related potential (ERP) paradigm, data are divided in epochs time-locked to the stimulus, and artefacts are removed by discarding epochs in which the EEG activity exceeds some predefined thresholds either in specific electrodes (e.g., electrooculogram (EOG) signals for ocular movements) or in all electrodes throughout the scalp. Artefact-reduced ERPs are then obtained by averaging the data over the remaining epochs, thereby increasing the signal-to-noise ratio. However, this procedure is problematic when only a few epochs are available, or when artefacts are very frequent, as in studies involving patients or children, or measurements taken in stimulating environements, or when the participants are physically active. Alternative procedures consist of modelling the signals generated by blinks or ocular movements and removing them from the data while preserving the remaining activity. Most of these methods are based on regressing out reference signals, usually recorded near the eyes, from the EEG signals with a model of artefact propagation. Regressing out eye artefacts inevitably involves subtracting relevant neural signals from each recording as well as ocular activity (Croft & Barry, 2002). Moreover, these methods do not work without reference signals, which are not always present for ocular movements, and very difficult to obtain for other types of artefacts (muscular, non-biological). Another approach to this problem is the use of independent component analysis (ICA), a statistical tool that decomposes EEG data in a set of sources with maximally independent time courses (Jung et al., 1998). ICA separates activity related to a large number of artefacts from neural activity by automatically segregating the former in specific independent components (ICs). Since the number of sources is potentially much higher than the number of ICs (Liu et al., 2002), this

separation will never be perfect (Groppe et al., 2009; Delorme et al., 2007). However, after removing non-physiological artefacts by an accurate pre-processing of the data, such that removing artefact ICs from the data by simple subtraction, generally leads to marginal distortion of the remaining EEG data (Joyce et al., 2004; Jung et al., 2000). Nevertheless, the practical usability of ICA as a tool for artefact rejection has an important limitation: the detection of the ICs associated with artefacts is time-consuming and involves subjective decision making (Delorme et al., 2007; Mantini et al., 2008). A single discriminative measure may already be very helpful in detecting specific artefacts blinks, lateral eye movements, heartbeat artefacts or even a wide variety of biological and non-biological artefacts (Mantini et al., 2008; Okada et al., 2007; Li et al., 2006; Viola et al., 2009). However, these algorithms are not completely automatic since they either require a training set (Delorme et al., 2007; Li et al., 2006; Mantini et al., 2008). ADJUST algorithms were found to detect EEG artefact automatically based on the joint use of Spatial and Temporal features (Mognon et al., 2011).

9.2 Conclusion

The EEG provides a clinically important measurement of brain activity and has applications in the diagnosis and treatment of brain diseases and abnormalities. It is also a research tool in the fundamental studies of brain function. To date, the use of EEGs has mostly been limited to measuring brain function of participants who are immobile and reclined in a low stimulus environment. Our knowledge of brain activity derived from EEG studies is mostly limited to this artificial scenario. It is assumed that similar activity would be measured if the participants were active or were exposed to other simultaneous stimuli. Ambulatory or mobile EEG devices have been developed to test this assumption and to measure brain activity under less artificial conditions. AEEG data is usually contaminated with various types of intermittent artefacts, often with large amplitudes.

This study, addressed first the pre-processing of continuous EEG data which were filtered and corrected by using an ADJUST algorithm. Further filtering methods based on PCA projection and Kalman Filtering developed and shown to be very effective in increasing signal to noise ratio. Usually, ERPs are detected by averaging over EEG measurements made with many repetitions of the stimulus. The average may require many tens of repetitions before the ERP signal can be observed with any confidence. This greatly limits the study and use of ERPs. This project explored more sophisticated methods of ERP estimation from measured EEGs. As the noise power varies considerably between trials, there is significant advantage in weighting any average formed so the emphasis is given to the cleanest data. A Bayesian Optimal Combining technique was developed allowed noisy trials to be incorporated in the best ERP estimate, even if the noise varied significantly during the trial measurement. The combination of these filtering and combining techniques yields a signal processing protocol that yields ERP estimates with significantly fewer trails than traditional methods. Furthermore, ERPs can be estimated from EEG data acquired during challenging conditions, where the participant is involved in activities or in stimulating environments.

9.3 Future Work

This work mainly focused on improving the quality and usability of EEG data by reducing the noise level via optimised use of the PCA, PCAKF, and introducing the OWM and BOC methods to improve ERP estimation. A ERP signal processing protocol: PCA projection filtering followed by BOC_OWM_UN, has been developed and tested. Further studies can extend the work presented, such as:

- Applying the protocol developed to other ERP measurements such as the use of visual stimuli.

- Combining the protocol with more robust artefact reduction methods to extend the range of activities in which ERPs can be measured, for example during participation in sport.
- Extend the algorithms to focus on observing the different ERPs from oddball and common stimuli.

The ultimate goal of this project was to make ERP measurement more research and clinically applicable, by cost reduction and extending the scenarios where it can be applied. An important element of future work will be the clinical use of the processing protocol developed in this project, to evaluate its effectiveness in practise, and to quantify the clinical and economic advantages of its use.

Reference

Acar, Z. A. & Makeig, S. (2013) Effects of forward model errors on EEG source localization. *Brain Topography*, 26 (3), 378-396.

Ahlfors, S. P., Ilmoniemi, R. J. & Portin, K. (1993) The effect of stimulation rate on the signal-to-noise ratio of evoked responses. *Electroencephalography and Clinical Neurophysiology/Evoked Potentials Section*, 88 (4), 339-342.

Akaishi, R., Ueda, N. & Sakai, K. (2013) Task-related modulation of effective connectivity during perceptual decision making: dissociation between dorsal and ventral prefrontal cortex. *Frontiers in Human Neuroscience*, 7 365.

Akay, A. (2012) *Evoked Potentials*. InTech. Available online: https://www.intechopen.com/books/electrophysiology-from-plants-to-heart/evoked-potentials [Accessed April 2017].

Anderer, P., Roberts, S., Schlogl, A., Gruber, G., Klosch, G., Herrmann, W., Rappelsberger, P., Filz, O., Barbanoj, M. J., Dorffner, G. & Saletu, B. (1999) Artifact processing in computerized analysis of sleep EEG - a review. *Neuropsychobiology*, 40 (3), 150-157.

Artoni, F., Delorme, A. & Makeig, S. (2018) Applying dimension reduction to EEG data by Principal Component Analysis reduces the quality of its subsequent Independent Component decomposition. *NeuroImage*, 175 176-187.

Ashwal, S. & Rust, R. (2003) Child neurology in the 20th century. *Pediatric Research*, 53 (2), 345-361.

Askamp, J. & van Putten, M. J. (2014) Mobile EEG in epilepsy. *International Journal of Psychophysiology*, 91 (1), 30-35.

Atwood, H. L. & MacKay, W. A. (1989) *Essentials in neurophysiology* Toronto: BC Decker.

Barbati, G., Porcaro, C., Zappasodi, F., Rossini, P. M. & Tecchio, F. (2004) Optimization of an independent component analysis approach for artifact identification and removal in magnetoencephalographic signals. *Clinical Neurophysiology: Official Journal of the International Federation of Clinical Neurophysiology*, 115 (5), 1220-1232.

Basar, E., Demiralp, T., Schürmann, M., Basar-Eroglu, C. & Ademoglu, A. (1999) Oscillatory brain dynamics, wavelet analysis, and cognition. *Brain and Language*, 66 (1), 146-183.

Bateson, A. D., Baseler, H. A., Paulson, K. S., Ahmed, F. & Asghar, A. U. (2017) Categorisation of mobile EEG: A researcher's perspective. *BioMed Research International*, 2017.

Bell, A. J. & Sejnowski, T. J. (1995) An information-maximization approach to blind separation and blind deconvolution. *Neural Computation*, 7 (6), 1129-1159.

Belouchrani, A., Abed-Meraim, K., Cardoso, J. & Moulines, E. (1997) A blind source separation technique using second-order statistics. *IEEE Transactions on Signal Processing*, 45 (2), 434-444.

Blackwood, D. & Muir, W. (1990) Cognitive brain potentials and their application. *The British Journal of Psychiatry*, 157 (9), 96-101.

Boudewyn, M. A., Luck, S. J., Farrens, J. L. & Kappenman, E. S. (2017) How many trials does it take to get a significant ERP effect? It depends. *Psychophysiology*, .

Bramon, E., Rabe-Hesketh, S., Sham, P., Murray, R. M. & Frangou, S. (2004) Meta-analysis of the P300 and P50 waveforms in schizophrenia. *Schizophrenia Research*, 70 (2-3), 315-329.

Bruder, G. E., Tenke, C. E., Stewart, J. W., Towey, J. P., Leite, P., Voglmaier, M. & Quitkin, F. M. (1995) Brain event- related potentials to complex tones in depressed patients: Relations to perceptual asymmetry and clinical features. *Psychophysiology*, 32 (4), 373-381.

Bruyneel, M., Van den Broecke, S., Libert, W. & Ninane, V. (2013) Real-time attended home-polysomnography with telematic data transmission. *International Journal of Medical Informatics*, 82 (8), 696-701.

Cao, L., Chua, K. S., Chong, W., Lee, H. & Gu, Q. (2003) A comparison of PCA, KPCA and ICA for dimensionality reduction in support vector machine. *Neurocomputing*, 55 (1-2), 321-336.

Casarotto, S., Bianchi, A. M., Cerutti, S. & Chiarenza, G. A. (2004) Principal component analysis for reduction of ocular artefacts in event-related potentials of normal and dyslexic children. *Clinical Neurophysiology: Official Journal of the International Federation of Clinical Neurophysiology*, 115 (3), 609-619.

Caspers, H., Speckmann, E. & Lehmenkühler, A. (1987) *Reviews of Physiology, Biochemistry and Pharmacology* Heidelberg: Springer.

Castells, F., Laguna, P., Sörnmo, L., Bollmann, A. & Roig, J. M. (2007) Principal component analysis in ECG signal processing. *EURASIP journal on advances in signal processing*, 2007 (1), 074580.

Chapman, R. M. (1999) Function and content words evoke different brain potentials. *Behavioral and Brain Sciences*, 22 (02), 282-284.

Chawla, M., Verma, H. & Kumar, V. (2006) ECG modeling and QRS detection using principal component analysis.

Clementz, B. A., Geyer, M. A. & Braff, D. L. (1997) P50 suppression among schizophrenia and normal comparison subjects: a methodological analysis. *Biological Psychiatry*, 41 (10), 1035-1044.

Clementz, B. A., Geyer, M. A. & Braff, D. L. (1998) Poor P50 suppression among schizophrenia patients and their first-degree biological relatives. *American Journal of Psychiatry*, 155 (12), 1691-1694.

Cohen, J. & Polich, J. (1997) On the number of trials needed for P300. *International Journal of Psychophysiology*, 25 (3), 249-255.

Costa, J. C., Da-Silva, P. J., Almeida, R. M. & Infantosi, A. F. (2014) Validation in principal components analysis applied to EEG data. *Computational and Mathematical Methods in Medicine,* 2014 413801.

Croft, R. & Barry, R. (2000) Removal of ocular artifact from the EEG: a review. *Neurophysiologie Clinique/Clinical Neurophysiology,* 30 (1), 5-19.

Croft, R. J., Chandler, J. S., Barry, R. J., Cooper, N. R. & Clarke, A. R. (2005) EOG correction: a comparison of four methods. *Psychophysiology,* 42 (1), 16-24.

Csibra, G., Kushnerenko, E. & Grossmann, T. (2008) 15 Electrophysiological Methods in Studying Infant Cognitive Development. *Handbook of Developmental Cognitive Neuroscience,* 247.

Dalal, S. S., Osipova, D., Bertrand, O. & Jerbi, K. (2013) Oscillatory activity of the human cerebellum: the intracranial electrocerebellogram revisited. *Neuroscience & Biobehavioral Reviews,* 37 (4), 585-593.

D'Alessandro, M., Esteller, R., Vachtsevanos, G., Hinson, A., Echauz, J. & Litt, B. (2003) Epileptic seizure prediction using hybrid feature selection over multiple intracranial EEG electrode contacts: a report of four patients. *IEEE transactions on biomedical engineering,* 50 (5), 603-615.

de Haan, M. (2013) *Infant EEG and event-related potentials* London: Psychology Press.

De Pascalis, V., Strippoli, E., Riccardi, P. & Vergari, F. (2004) Personality, event-related potential (ERP) and heart rate (HR) in emotional word processing. *Personality and Individual Differences,* 36 (4), 873-891.

Debener, S., Minow, F., Emkes, R., Gandras, K. & Vos, M. (2012) How about taking a low- cost, small, and wireless EEG for a walk? *Psychophysiology,* 49 (11), 1617-1621.

Delorme, A. & Makeig, S. (2004) EEGLAB: an open source toolbox for analysis of single-trial EEG dynamics including independent component analysis. *Journal of Neuroscience Methods,* 134 (1), 9-21.

Delorme, A., Palmer, J., Onton, J., Oostenveld, R. & Makeig, S. (2012) Independent EEG sources are dipolar. *PloS one,* 7 (2), e30135.

Delorme, A., Sejnowski, T. & Makeig, S. (2007) Enhanced detection of artifacts in EEG data using higher-order statistics and independent component analysis. *NeuroImage,* 34 (4), 1443-1449.

Delorme, A., Sejnowski, T. & Makeig, S. (2007) Enhanced detection of artifacts in EEG data using higher-order statistics and independent component analysis. *NeuroImage,* 34 (4), 1443-1449.

Djuwari, D., Kumar, D., Palaniswami, M. & Pota, H. (2005) Limitations of ica for artefact removal. *27th Annual International Conference of the Engineering in Medicine and Biology Society, 2005.* IEEE.

Doege, K., Bates, A., White, T., Das, D., Boks, M. & Liddle, P. (2009) Reduced event-related low frequency EEG activity in schizophrenia during an auditory oddball task. *Psychophysiology,* 46 (3), 566-577.

Dubey, R. & Pathak, A. (2010) Digital analysis off EEG brain signal. *WebmedCentral brain,* 1 (11), .

Farwell, L. A. & Donchin, E. (1988) Talking off the top of your head: toward a mental prosthesis utilizing event-related brain potentials. *Electroencephalography and Clinical Neurophysiology,* 70 (6), 510-523.

Fatourechi, M., Bashashati, A., Ward, R. K. & Birch, G. E. (2007) EMG and EOG artifacts in brain computer interface systems: A survey. *Clinical Neurophysiology,* 118 (3), 480-494.

Faulkner, H. J., Arima, H. & Mohamed, A. (2012) Latency to first interictal epileptiform discharge in epilepsy with outpatient ambulatory EEG. *Clinical Neurophysiology,* 123 (9), 1732-1735.

Fisch, B. J. & Spehlmann, R. (1999) *Fisch and Spehlmann's EEG primer: Basic principles of digital and analog EEG* Amsterdam: Elsevier Health Sciences.

Flemons, W. W., Douglas, N. J., Kuna, S. T., Rodenstein, D. O. & Wheatley, J. (2004) Access to diagnosis and treatment of patients with suspected sleep apnea. *American Journal of Respiratory And Critical Care Medicine,* 169 (6), 668-672.

Fridlyand, L. E., Jacobson, D. A. & Philipson, L. (2013) Ion channels and regulation of insulin secretion in human β-cells: a computational systems analysis. *Islets,* 5 (1), 1-15.

Goldenholz, D. M., Ahlfors, S. P., Hämäläinen, M. S., Sharon, D., Ishitobi, M., Vaina, L. M. & Stufflebeam, S. M. (2009) Mapping the signal- to- noise- ratios of cortical sources in magnetoencephalography and electroencephalography. *Human Brain Mapping,* 30 (4), 1077-1086.

Goncharova, I. I., McFarland, D. J., Vaughan, T. M. & Wolpaw, J. R. (2003) EMG contamination of EEG: spectral and topographical characteristics. *Clinical Neurophysiology,* 114 (9), 1580-1593.

Groppe, D. M., Makeig, S. & Kutas, M. (2009) Identifying reliable independent components via split-half comparisons. *NeuroImage,* 45 (4), 1199-1211.

Gouvea, A. C., Phillips, C., Kazanina, N. & Poeppel, D. (2010) The linguistic processes underlying the P600. *Language and Cognitive processes,* 25 (2), 149-188.

Hansenne, M., Pitchot, W., Moreno, A. G., Zaldua, I. U. & Ansseau, M. (1996) Suicidal behavior in depressive disorder: an event-related potential study. *Biological Psychiatry,* 40 (2), 116-122.

Heinrich, S. P. & Bach, M. (2008) Signal and noise in P300 recordings to visual stimuli. *Documenta Ophthalmologica,* 117 (1), 73-83.

Hoffmann, S. & Falkenstein, M. (2008) The correction of eye blink artefacts in the EEG: a comparison of two prominent methods. *PLoS one,* 3 (8), e3004.

Humphrey, D. G. & Kramer, A. F. (1994) Toward a psychophysiological assessment of dynamic changes in mental workload. *Human Factors,* 36 (1), 3-26.

Hyvarinen, A., Karhunen, J. & Oja, H. (2000) *Independent component analysis* New York: Wiley Online & Son, INC.

Hyvärinen, A., Karhunen, J. & Oja, E. (2001) *Independent component analysis* New York: John Wiley & Sons.

Javitt, D. C., Spencer, K. M., Thaker, G. K., Winterer, G. & Hajós, M. (2008) Neurophysiological biomarkers for drug development in schizophrenia. *Nature Reviews Drug Discovery,* 7 (1), 68-83.

Jeong, J. (2004) EEG dynamics in patients with Alzheimer's disease. *Clinical Neurophysiology,* 115 (7), 1490-1505.

Johnson, R. (1993) On the neural generators of the P300 component of the event- related potential. *Psychophysiology,* 30 (1), 90-97.

Joyce, C. A., Gorodnitsky, I. F. & Kutas, M. (2004) Automatic removal of eye movement and blink artifacts from EEG data using blind component separation. *Psychophysiology,* 41 (2), 313-325.

Jung, T., Humphries, C., Lee, T., Makeig, S., McKeown, M. J., Iragui, V. & Sejnowski, T. J. (1998) Extended ICA removes artifacts from electroencephalographic recordings. *Advances in Neural Information Processing Systems*, 10 894-900.

Jung, T., Makeig, S., Humphries, C., Lee, T., Mckeown, M. J., Iragui, V. & Sejnowski, T. J. (2000a) Removing electroencephalographic artifacts by blind source separation. *Psychophysiology,* 37 (2), 163-178.

Jung, T., Makeig, S., Lee, T., McKeown, M. J., Brown, G., Bell, A. J. & Sejnowski, T. J. (2000b) Independent component analysis of biomedical signals. *Proc. int. workshop on independent component analysis and signal separation.,* 633-644.

Kalman, R. E. (1960) A new approach to linear filtering and prediction problems. *Journal of Basic Engineering,* 82 (1), 35-45.

Kanda, P. A. M., Trambaiolli, L. R., Lorena, A. C., Fraga, F. J., Basile, L. F. I., Nitrini, R. & Anghinah, R. (2014) Clinician's road map to wavelet EEG as an Alzheimer's disease biomarker. *Clinical EEG and Neuroscience,* 45 (2), 104-112.

Kaplan, A. Y., Shishkin, S. L., Ganin, I. P., Basyul, I. A. & Zhigalov, A. Y. (2013) Adapting the P300-based brain–computer interface for gaming: a review. *IEEE Transactions on Computational Intelligence and AI in Games,* 5 (2), 141-149.

Karimi, F., Kofman, J., Mrachcz-Kersting, N., Farina, D. & Jiang, N. (2016) Comparison of EEG spatial filters for movement related cortical potential detection. *Engineering in Medicine and Biology Society (EMBC), 2016 IEEE 38th Annual International Conference of the*. IEEE.

Kim, J. H., Kushmerick, C. & von Gersdorff, H. (2010) Presynaptic resurgent Na+ currents sculpt the action potential waveform and increase firing reliability at a CNS nerve terminal. *The Journal of Neuroscience: The Official Journal of the Society for Neuroscience,* 30 (46), 15479-15490.

Kobayashi, T. & Kuriki, S. (1999) Principal component elimination method for the improvement of S/N in evoked neuromagnetic field measurements. *IEEE Transactions on Biomedical Engineering,* 46 (8), 951-958.

Kornmeier, J. & Bach, M. (2012) Ambiguous figures - what happens in the brain when perception changes but not the stimulus. *Frontiers in human neuroscience,* 6 51.

Kropotov, J. D. (2016) *Functional neuromarkers for psychiatry [eBook]* San Diego: Academic Press.

Lee, T. (1998) *Independent component analysis* Boston, MA: Springer.

Lee, T., Girolami, M. & Sejnowski, T. J. (1999) Independent component analysis using an extended infomax algorithm for mixed subgaussian and supergaussian sources. *Neural Computation,* 11 (2), 417-441.

Li, Y., Ma, Z., Lu, W. & Li, Y. (2006) Automatic removal of the eye blink artifact from EEG using an ICA-based template matching approach. *Physiological measurement,* 27 (4), 425.

Light, G. A. & Braff, D. L. (2003) Sensory gating deficits in schizophrenia: can we parse the effects of medication, nicotine use, and changes in clinical status? *Clinical Neuroscience Research,* 3 (1), 47-54.

Light, G. A., Williams, L. E., Minow, F., Sprock, J., Rissling, A., Sharp, R., Swerdlow, N. R. & Braff, D. L. (2010) Electroencephalography (EEG) and event- related potentials (ERPs) with human participants. *Current protocols in neuroscience,* 6.25. 1-6.25. 24.

Liu, A. K., Dale, A. M. & Belliveau, J. W. (2002) Monte Carlo simulation studies of EEG and MEG localization accuracy. *Human brain mapping,* 16 (1), 47-62.

Luck, S. J. & Todd, C. H. (eds) (2004) *Ten simple rules for designing and interpreting ERP experiments.[In:] Event-Related Potentials: A Methods Handbook*. USA: MIT Press.

Luck, S. J. (2005) An introduction to the event-related potential technique MIT press. *Cambridge, ma,* 45-64.

Luck, S. J. (2014) *An introduction to the event-related potential technique* USA: MIT press.

Makeig, S., Jung, T. P., Bell, A. J., Ghahremani, D. & Sejnowski, T. J. (1997) Blind separation of auditory event-related brain responses into independent components. *Proceedings of the national academy of sciences of the united states of america,* 94 (20), 10979-10984.

Makeig, S., Jung, T., Ghahremani, D., Bell, A. & Sejnowski, T. (1996) What (not where) are the sources of the EEG. *Proc. 18th Annual Meeting of The Cognitive Science Society*.

Mantini, D., Franciotti, R., Romani, G. L. & Pizzella, V. (2008) Improving MEG source localizations: an automated method for complete artifact removal based on independent component analysis. *NeuroImage,* 40 (1), 160-173.

Marella, S. (2012) *EEG Artifacts.* SlideShare. Available online: https://www.slideshare.net/SudhakarMarella/eeg-artifacts-15175461 [Accessed 04/05 2016].

Mathalon, D. H., Ford, J. M. & Pfefferbaum, A. (2000) Trait and state aspects of P300 amplitude reduction in schizophrenia: a retrospective longitudinal study. *Biological Psychiatry,* 47 (5), 434-449.

Mauguière, F. (1987) Monitoring cerebral function. Long-term monitoring of EEG and evoked potentials.: PF Prior and E. Maynard (Elsevier, Amsterdam, 1986, 458 p.). *Electroencephalography and Clinical Neurophysiology,* 67 (2), 194-195.

McMenamin, B. W., Shackman, A. J., Greischar, L. L. & Davidson, R. J. (2011) Electromyogenic artifacts and electroencephalographic inferences revisited. *NeuroImage,* 54 (1), 4-9.

Miltner, W., Krieschel, S. & Gutberlet, I. (2000) P300-a signature for threat processing in phobic subjects. *Psychophysiology,* 37 S71-S71.

Mognon, A., Jovicich, J., Bruzzone, L. & Buiatti, M. (2011) ADJUST: An automatic EEG artifact detector based on the joint use of spatial and temporal features. *Psychophysiology,* 48 (2), 229-240.

Moore, A. R., Zhou, W. L., Sirois, C. L., Belinsky, G. S., Zecevic, N. & Antic, S. D. (2014) Connexin hemichannels contribute to spontaneous electrical activity in the human fetal cortex. *Proceedings of the National Academy of Sciences of the United States of America,* 111 (37), E3919-28.

Nakayama, K. & Mackeben, M. (1982) Steady state visual evoked potentials in the alert primate. *Vision Research,* 22 (10), 1261-1271.

Nicolas-Alonso, L. F. & Gomez-Gil, J. (2012) Brain computer interfaces, a review. *Sensors,* 12 (2), 1211-1279.

Niedermeyer, E. (2005) The normal EEG of the waking adult. *Electroencephalography: Basic Principles, Clinical Applications, and Related Fields,* 167 155-164.

Nunez, P. L. & Cutillo, B. A. (1995) *Neocortical dynamics and human EEG rhythms* Oxford: Oxford University Press.

Nunez, P. L. & Srinivasan, R. (2006) *Electric fields of the brain: The neurophysics of EEG* Oxford: Oxford University Press.

Ochoa, C. J. & Polich, J. (2000) P300 and blink instructions. *Clinical neurophysiology,* 111 (1), 93-98.

Odom, J. V., Bach, M., Barber, C., Brigell, M., Marmor, M. F., Tormene, A. P. & Holder, G. E. (2004) Visual evoked potentials standard (2004). *Documenta Ophthalmologica,* 108 (2), 115-123.

O'Donnell, B., Vohs, J., Hetrick, W., Carroll, C. & Shekhar, A. (2004) Auditory event-related potential abnormalities in bipolar disorder and schizophrenia. *International Journal of Psychophysiology,* 53 (1), 45-55.

Oikonomou, V. P., Tzallas, A. T. & Fotiadis, D. I. (2007) A Kalman filter based methodology for EEG spike enhancement. *Computer Methods and Programs in Biomedicine,* 85 (2), 101-108.

Oikonomou, V. P., Tzallas, A. T., Tsalikakis, D. G., Fotiadis, D. I. & Konitsiotis, S. (2009) *The use of Kalman filter in biomedical signal processing* INTECH Open Access Publisher.

Okada, Y., Jung, J. & Kobayashi, T. (2007) An automatic identification and removal method for eye-blink artifacts in event-related magnetoencephalographic measurements. *Physiological measurement,* 28 (12), 1523.

Olincy, A. & Martin, L. (2005) Diminished suppression of the P50 auditory evoked potential in bipolar disorder subjects with a history of psychosis. *American Journal of Psychiatry,* 162 (1), 43-49.

Papadelis, C., Chen, Z., Kourtidou-Papadeli, C., Bamidis, P. D., Chouvarda, I., Bekiaris, E. & Maglaveras, N. (2007) Monitoring sleepiness with on-board electrophysiological recordings for preventing sleep-deprived traffic accidents. *Clinical Neurophysiology: Official Journal of the International Federation of Clinical Neurophysiology,* 118 (9), 1906-1922.

Park, J. L., Fairweather, M. M. & Donaldson, D. I. (2015) Making the case for mobile cognition: EEG and sports performance. *Neuroscience & biobehavioral reviews,* 52 117-130.

Patrick, C. J., Bernat, E. M., Malone, S. M., Iacono, W. G., Krueger, R. F. & McGue, M. (2006) P300 amplitude as an indicator of externalizing in adolescent males. *Psychophysiology,* 43 (1), 84-92.

Peterson, N. N., Schroeder, C. E. & Arezzo, J. C. (1995) Neural generators of early cortical somatosensory evoked potentials in the awake monkey. *Electroencephalography and clinical neurophysiology/evoked potentials section,* 96 (3), 248-260.

Pfurtscheller, G., Flotzinger, D. & Neuper, C. (1994) Differentiation between finger, toe and tongue movement in man based on 40 Hz EEG. *Electroencephalography and Clinical Neurophysiology,* 90 (6), 456-460.

Pham, T. T., Croft, R. J., Cadusch, P. J. & Barry, R. J. (2011) A test of four EOG correction methods using an improved validation technique. *International Journal of Psychophysiology,* 79 (2), 203-210.

Picton, T. W. (1992) The P300 wave of the human event-related potential. *Journal of Clinical Neurophysiology,* 9 456-456.

Polich, J. (2007) Updating P300: an integrative theory of P3a and P3b. *Clinical Neurophysiology,* 118 (10), 2128-2148.

Polich, J. (1986) P300 development from auditory stimuli. *Psychophysiology,* 23 (5), 590-597.

Polich, J. (2004) Clinical application of the P300 event-related brain potential. *Physical Medicine and Rehabilitation Clinics of North America,* 15 (1), 133-161.

Poulsen, T. B. & Jørgensen, K. A. (2008) Catalytic Asymmetric Friedel− Crafts Alkylation Reactions Copper Showed the Way. *Chemical Reviews,* 108 (8), 2903-2915.

Rager, G. & Singer, W. (1998) The response of cat visual cortex to flicker stimuli of variable frequency. *European Journal of Neuroscience,* 10 (5), 1856-1877.

Regan, M. & Regan, D. (1988) A frequency domain technique for characterizing nonlinearities in biological systems. *Journal of Theoretical Biology,* 133 (3), 293-317.

Reis, P. M., Hebenstreit, F., Gabsteiger, F., von Tscharner, V. & Lochmann, M. (2014) Methodological aspects of EEG and body dynamics measurements during motion. *Towards a new cognitive neuroscience: Modeling natural brain dynamics,* 8 156.

Romero, S., Mañanas, M. A. & Barbanoj, M. J. (2008) A comparative study of automatic techniques for ocular artifact reduction in spontaneous EEG signals based on clinical target variables: a simulation case. *Computers in Biology and Medicine,* 38 (3), 348-360.

Rossini, P., Burke, D., Chen, R., Cohen, L., Daskalakis, Z., Di Iorio, R., Di Lazzaro, V., Ferreri, F., Fitzgerald, P. & George, M. (2015) Non-invasive electrical and magnetic stimulation of the brain, spinal cord, roots and peripheral nerves: Basic principles and procedures for routine clinical and research application. An updated report from an IFCN Committee. *Clinical Neurophysiology,* 126 (6), 1071-1107.

Sadleir, R. & Argibay, A. (2007) Modeling skull electrical properties. *Annals of Biomedical Engineering,* 35 (10), 1699-1712.

Sahoo, S. (2016) The P300 Event Related Potentials and its Implications in Psychiatric Disorders. *EC Psychology and Psychia-try,* 1 76-84.

Salisbury, D. F., Shenton, M. E. & McCarley, R. W. (1999) P300 topography differs in schizophrenia and manic psychosis. *Biological Psychiatry,* 45 (1), 98-106.

Sanei, S. (2013) *Adaptive processing of brain signals* Chichester: John Wiley & Sons.

Sanei, S. & Chambers, J. (2007) Introduction to EEG. *EEG signal processing,* 1-34.

Sanei, S. & Chambers, J. A. (2013) *EEG signal processing* Chichester: John Wiley & Sons.

Schulze, K. K., Hall, M., McDonald, C., Marshall, N., Walshe, M., Murray, R. M. & Bramon, E. (2007) P50 auditory evoked potential suppression in bipolar disorder

patients with psychotic features and their unaffected relatives. *Biological psychiatry,* 62 (2), 121-128.

Shepherd, G. M. (2003) *The synaptic organization of the brain* Oxford: Oxford University Press.

Simlai, J. & Nizamie, S. (1998) *Event related potentials-P300, CNV, MRCP in drug naïve and drug free schizophrenia.* Doctor of Medicine Thesis. University of Ranchi.

Sörnmo, L. & Laguna, P. (2005) *Bioelectrical signal processing in cardiac and neurological applications* Oxford: Academic Press.

Speckmann, E. (1993) *Electroencephalography: Basic principles, clinical applications, and related fields* Philadelphia: Williams & Wilkins.

Stecker, M. M. (2000) Generalized averaging and noise levels in evoked responses. *Computers in Biology and Medicine,* 30 (5), 247-265.

Sterman, M., MacDonald, L. & Stone, R. K. (1974) Biofeedback training of the sensorimotor electroencephalogram rhythm in man: effects on epilepsy. *Epilepsia,* 15 (3), 395-416.

Sur, S. & Sinha, V. K. (2009) Event-related potential: An overview. *Industrial psychiatry journal,* 18 (1), 70-73.

Sutton, S., Braren, M., Zubin, J. & John, E. R. (1965) Evoked-potential correlates of stimulus uncertainty. *Science (new york, N.Y.),* 150 (3700), 1187-1188.

Teplan, M. (2002) Fundamentals of EEG measurement. *Measurement science review,* 2 (2), 1-11.

Testa-Silva, G., Verhoog, M. B., Linaro, D., De Kock, C. P., Baayen, J. C., Meredith, R. M., De Zeeuw, C. I., Giugliano, M. & Mansvelder, H. D. (2014) High bandwidth synaptic communication and frequency tracking in human neocortex. *PLoS biology,* 12 (11), e1002007.

Tortora, G. J. & Derrickson, B. H. (2011) *Principles of anatomy and physiology* New York: Wiley.

Turan, T., Esel, E., Karaaslan, F., Basturk, M., Oguz, A. & Yabanoglu, I. (2002) Auditory event-related potentials in panic and generalised anxiety disorders. *Progress in Neuro-Psychopharmacology and Biological psychiatry,* 26 (1), 123-126.

Urigüen, J. A. & Garcia-Zapirain, B. (2015) EEG artifact removal—state-of-the-art and guidelines. *Journal of Neural Engineering,* 12 (3), 031001.

Vialatte, F., Maurice, M., Dauwels, J. & Cichocki, A. (2010) Steady-state visually evoked potentials: Focus on essential paradigms and future perspectives. *Progress in Neurobiology,* 90 (4), 418-438.

Vigário, R. N. (1997) Extraction of ocular artefacts from EEG using independent component analysis. *Electroencephalography and clinical neurophysiology,* 103 (3), 395-404.

Viola, F. C., Thorne, J., Edmonds, B., Schneider, T., Eichele, T. & Debener, S. (2009) Semi-automatic identification of independent components representing EEG artifact. *Clinical neurophysiology,* 120 (5), 868-877.

Walsh, P., Kane, N. & Butler, S. (2005) The clinical role of evoked potentials. *Journal of Neurology, Neurosurgery, and Psychiatry,* 76 Suppl 2 ii16-22.

Wandell, B. A., Dumoulin, S. O. & Brewer, A. A. (2007) Visual field maps in human cortex. *Neuron,* 56 (2), 366-383.

Wang, L., Liu, Y., Wei, L. & Deng, Y. (2012) The characteristics and related influencing factors of ambulatory EEGs in patients seizure-free for 3–5 years. *Epilepsy Research,* 98 (2-3), 116-122.

Waryasz, S. A. (2017) *The Clinical utility of P300 evoked responses in post-sport-related concussion Evaluation.* Available online: https://hearinghealthmatters.org/pathways/2017/clinical-utility-p300-evoked-responses-post-sport-related-concussion-evaluation/ [Accessed 10/06 2018].

Widodo, A. & Yang, B. (2007) Application of nonlinear feature extraction and support vector machines for fault diagnosis of induction motors. *Expert systems with applications,* 33 (1), 241-250.

Woodman, G. F. (2010) A brief introduction to the use of event-related potentials in studies of perception and attention. *Attention, Perception, & Psychophysics,* 72 (8), 2031-2046.

Wu, L., Wu, L., Chen, Y. & Zhou, J. (2014) A promising method to distinguish vascular dementia from Alzheimer's disease with standardized low-resolution brain electromagnetic tomography and quantitative EEG. *Clinical EEG and Neuroscience,* 45 (3), 152-157.